Year : 2021

Ex-vivo human skin permeation of Bisphenol A and its alternatives in thermal paper

Reale Elena

UNIL | Université de Lausanne

Faculté de biologie et de médecine

Unisanté, Département de Santé au Travail et Environnement, Unité de Sciences de l'Exposition

Ex-vivo human skin permeation of Bisphenol A and its alternatives in thermal paper

Thèse de doctorat ès sciences de la vie (PhD)

présentée à la

Faculté de biologie et de médecine
de l'Université de Lausanne

par

Elena REALE

Master en Chimie de l'Université de Florence, Italie.

Jury

Prof. David Gatfield, Président
Dre Nancy B. Hopf, Directrice de thèse
Prof. Dr David Vernez, Co-directeur de thèse
Dre Sophie Ndaw, Experte
Prof. Dr Richard Guy, Expert

Lausanne
2021

Imprimatur

Vu le rapport présenté par le jury d'examen, composé de

Président·e	Monsieur	Prof.	David	**Gatfield**
Directeur·trice de thèse	Madame	Dre	Nancy B.	**Hopf**
Co-directeur·trice	Monsieur	Prof.	David	**Vernez**
Expert·e·s	Madame	Dre	Sophie	**Ndaw**
	Monsieur	Prof.	Richard	**Guy**

le Conseil de Faculté autorise l'impression de la thèse de

Madame Elena Reale

Master - Laurea In Chimica, Università degli Studi di Firenze, Italie

intitulée

Ex-vivo human skin permeation of Bisphenol A and its alternatives in thermal paper

Date de l'examen : 27 mai 2021

Date d'émission de l'imprimatur : Lausanne, le 15 juin 2021

pour le Doyen
de la Faculté de biologie et de médecine

Prof. Niko GELDNER
Directeur de l'Ecole Doctorale

Table of contents

Acknowledgments

Résumé

Le bisphénol A (BPA), reconnu comme perturbateur endocrinien, est un important composant des papiers thermiques. Dans ces papiers, le BPA se trouve sous forme libre (non polymérisée), ainsi lors de leur manipulation, il peut migrer sur la peau et être absorbé. Les concentrations urinaires de BPA sont significativement plus élevées pour les travailleurs exposés au BPA que pour la population générale. De ce fait, depuis 2020 le BPA a été interdit d'utilisation pour les papiers thermiques, et a été substitué par d'autres substances. Les substituts du BPA les plus utilisés en Suisse dans les papiers thermiques sont le bisphénol S (BPA), le wincon 8 (D-8) et le pergafast 201 (PF201). Peu d'études existent sur l'exposition à ces substances et sur leur toxicité, notamment à travers l'exposition par la peau humaine. Dans ce travail de thèse, j'ai donc étudié la perméation cutanée *in vitro* du BPS, D-8 et PF201, soit les données manquantes pour l'évaluation du risque de ces substances lors d'une exposition par voie cutanée. J'ai aussi étudié les effets de divers paramètres expérimentaux sur la cinétique de perméation du BPA afin de comprendre les différences observées dans les résultats publiés par diverses études.

J'ai développé une méthode analytique robuste et sensible pour quantifier simultanément le BPS, le D-8, le PF201, ainsi que le BPA et son principal métabolite, le BPA-glucuronide (BPA-G). Pour les expériences de perméation cutanée, j'ai utilisé de la peau humaine montée sur des cellules de diffusion de type « flow-through » contenant du liquide physiologique (liquide récepteur). Les résultats montrent que la cinétique de perméation du D-8 est similaire à celle du BPA, et que celle du BPS est beaucoup plus lente. Les doses administrées ont été considérées comme finies pour le BPA et le D-8, mais comme infinies pour le BPS, ce qui a permis de déterminer le coefficient de perméation seulement pour le BPS (K_p = 2.4 x 10^{-5} cm/h). Les résultats de balance de masse ont montré que les quantités de BPA, de D-8 et de BPS ayant pénétrées dans la peau étaient respectivement le 15%, 16% et 11% de la dose appliquée sur la peau, et les quantités retrouvées dans le liquide physiologique étaient respectivement le 25%, 17% et 0.4%. Le PF201 n'était pas quantifiable ni dans le liquide récepteur ni dans la peau. La concentration de BPA-G dans le liquide récepteur était négligeable. Finalement, l'étude sur l'influence de certains paramètres expérimentaux sur la perméation cutanée du BPA a permis de conclure que les valeurs du flux (J, $\mu g/cm^2/h$) de différentes études sont cohérentes, lorsque les différentes conditions expérimentales sont considérées.

Ces résultats apportent les données d'absorption cutanée nécessaires pour une évaluation de l'exposition au BPA et à ses substituts dans le papier thermique. Ils mettent en évidence l'importance de l'exposition cutanée et permettent de supporter le développement de stratégies préventives d'exposition au BPA et à ses substituts.

Summary

Bisphenol A (BPA), a well-known endocrine disruptor, is used as a colour developer in thermal paper products, such as cashiers' receipts where one side is coated with BPA powder. BPA can migrate from thermal papers onto the skin during handling and be absorbed. Occupationally exposed individuals consistently have higher urinary BPA concentrations than the general population. Therefore, BPA has been banned from thermal paper since 2020, and the interest of regulatory authorities in BPA-alternative colour developers (Bisphenol S (BPS), Wincon 8 (D-8), Pergafast 201 (PF201)) is increasing. Only a handful of studies have determined human exposures to these BPA-alternatives and their toxicity, and little is known about their skin absorption. We first needed to characterize the human skin permeation in vitro for each alternative separately as this was not yet known. Then, we characterized BPA skin permeation, as the literature data on BPA have shown inconsistent results. We then compared the *in vitro* skin absorption of BPS, D-8 and PF201 to BPA. These data are the missing pieces to complete the exposure assessments of these colour developers.

No chemical analytical method existed for these BPA alternatives in biological matrices. Consequently, we developed a robust and sensitive analytical method by liquid chromatography tandem mass spectrometry (LC-MS/MS) for simultaneous quantification of BPS, D-8, PF201, as well as of BPA and its main metabolite, BPA-glucuronide (BPA-G). We used human skin mounted on flow-through diffusion cells filled with saline to characterise *in vitro* skin absorption. Our results show that D-8 had skin absorption kinetics similar to BPA, while BPS was much slower. Dose conditions that were finite for BPA and D-8 were infinite for BPS, therefore we could determine the permeability coefficient only for BPS: $K_p = 2.4 \times 10^{-5}$ cm/h. The mass-balance showed that the percent amounts of the applied dose penetrated into the receptor fluid were 25%, 17%, and 0.4% for BPA, D-8, and BPS, respectively. In the skin, we found 15%, 16%, and 11% for BPA, D-8, and BPS, respectively. PF201 was not quantifiable in the receptor liquid or in the skin. We also found that the BPA-G concentration in the receptor liquid was negligible. Finally, we studied the effects that different experimental parameters had on BPA skin permeation kinetics in an attempt to understand why published studies on BPA skin absorption have reported inconsistent results. We concluded that permeation rate (J, $\mu g/cm^2/h$) values agree among some studies when accounting for experimental conditions. We achieved steady state conditions for BPA and determined K_p values in the range 1.6–5.2 x 10^{-3} cm/h depending on skin thickness (200, 400, or 800 μm).

Our results provide the scientific community with the necessary skin absorption data for an exposure assessment of BPA and its alternatives in thermal paper. This could help understand the importance of skin exposure and lead to the development of preventive exposure strategies to BPA and other colour developers.

1. Introduction

1.1 Background

Bisphenol A (BPA) is one of the world's highest production-volume chemicals, with more than 4.6 million tonnes produced worldwide in 2012 (Merchant and Research Consulting 2013). BPA is primarily used as plasticizer in the production of polycarbonate plastics (i.e. bottles and food containers) and epoxy resins (i.e. internal lacquer in cans). BPA migrates into beverages and foods in contact with these materials (Brotons et al. 1995; Kubwabo et al. 2009), partly explaining human exposure. However, exposures from food alone cannot explain BPA blood concentrations reported in the literature (Vandenberg et al. 2010).

The interest of researchers, risk assessors and regulators in exposures to BPA is due to its toxicity as an endocrine disruptor (Rubin 2011; Wetherill et al. 2007). In March 2015, the European Food Safety Authority (EFSA) Panel for Food Contact Materials, Enzymes, Flavourings and Processing Aids (CEF) gave a Scientific Opinion on public health risks related to the presence of BPA in foodstuff (EFSA 2015). They concluded that there is no health concern for any age group from dietary exposure, but noted considerable uncertainty in the exposure estimates for non-dietary sources. Non-dietary sources of exposure for the general population include, among others, polycarbonate toys, epoxy resin-based paints, surface coatings, thermal papers, dental materials, medical devices, printing inks, and flame retardants (Geens et al. 2012; EFSA 2015). During their use and end-of-life, these products can release BPA particles to the environment creating additional indirect sources of exposure such as dust, indoor and outdoor air, drinking and surface waters (ANSES 2013). Occupational exposures can occur during the handling, manufacturing and recycling of BPA-containing products. Exposure to BPA is well documented both in the general population (review by Colorado-Yohar et al. 2021) and in the workers (Ndaw et al. 2016; Thayer et al. 2016; Heinälä et al. 2017; Waldman et al. 2016).

The EFSA CEF report indicated that the second largest source of human BPA exposure after food and beverage packaging is thermal paper. Thermal paper is a special paper coated with thermochromic ink, a chemical that changes colour when exposed to heat. In 2018, the total thermal paper market in EU amounted to 491 x 10^3 metric tonnes of thermal paper (ECHA 2019). Thermal paper is often used as e.g. point-of-sale receipts, adhesive labels, and parking tickets. Upon handling these papers, BPA migrates from the paper onto the skin (Hormann et al. 2014; Biedermann, Tschudin, and Grob 2010) and is absorbed in the body (Hormann et al. 2014; Liu and Martin 2017).

In 2016, BPA was classified as a presumed human reproductive toxicant (category 1B), and the European Union published a regulation to restrict BPA in thermal paper to no more than 0.02% (w/w) by 2020 (EU 2016/2235). Hence, alternatives to BPA are increasingly used in thermal paper. The most commonly used BPA alternatives in thermal paper are BPS, Wincon 8 (D-8) and Pergafast 201 (PF201) (Vervliet et al. 2019). BPS is a bisphenol, D-8 is a phenol, and PF201 is phenol free (Figure 1). Exposure to BPS has been documented in the general population (Frederiksen et al. 2020; Ghayda et al. 2019; Lehmler et al. 2018) and in workers (Thayer et al. 2016; Ndaw et al. 2018). There are no studies on the dermal absorption of D-8 and PF201.

The aim of this dissertation was to study the human skin absorption of BPA, BPS, D-8 and PF201 *in vitro*.

BPA   BPS   D-8   PF201
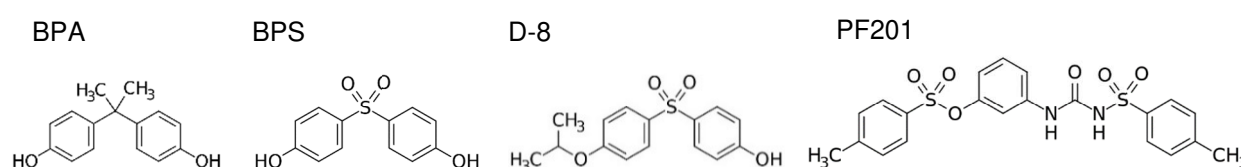
Figure 1 - Chemical structures of BPA and of its main alternatives used in thermal paper.

1.2 Toxicity

1.2.1 Endocrine activity

Endocrine disruptors act by interfering with the biosynthesis, secretion, action, or metabolism of naturally occurring hormones. BPA displays endocrine activity in *in vitro* assays, but has mixed results in *in vivo* (US EPA 2015a) studies. As reported by the US Environmental Protection Agency (US EPA 2015), *in vitro* studies show that BPA can bind to estrogenic receptors, elicit oestrogen-induced gene transcription, induce progesterone receptors, and induce cell proliferation in MCF7 cancer cells. BPA's affinity for binding to oestrogen receptors is approximately 100- to 10,000-fold weaker than 17β-estradiol (E2). Data from *in vivo* studies lead to a more complex picture, as oral BPA does not consistently produce robust estrogenic responses. The main concern is on developmental effects (US EPA 2015a) because BPA can cause neural and behavioural alterations related to disruptions in normal sex differences in rats and mice following developmental exposure at very low doses (0.01-0.2 mg/kg bw/day). Even though the human relevance is less certain, developmental effects at lower doses cannot be ruled out. The main concern is for populations who frequently handle this type of paper (e.g. cashiers, workers in industries producing and using BPA) and for particularly sensitive groups, such as pregnant women and young children.

As reported by the United States Environmental Protection Agency (US EPA 2015), there are considerably less studies on the toxicity of BPA alternatives used in thermal paper. Based on limited *in vitro* data, BPS exhibits some endocrine activity. BPS can bind to oestrogen receptors, elicit oestrogen-induced gene transcription, induce cell proliferation in MCF7 cancer cells, and inhibit the androgenic activity of dihydrotestosterone. *In vitro* data suggest that BPS acts as a weak oestrogen: endocrine activity is somewhat less than that of BPA, and approximately 5-7 orders of magnitude less than that of E2. One *in vivo* study suggests BPS potential for estrogenic activity (Yamasaki et al. (2004), as reported in US EPA (2015a)). D-8 was negative for estrogenicity in two ER binding assays and one competitive ER binding assay, and positive for anti-estrogenicity in a competitive binding assay in the presence of E2. Limited *in vitro* data show PF201 to be non-estrogenic with a relative potency substantially lower (10^{-7}-fold) than E2. In 2015, Goldinger et al. (2015) studied the potential of BPA and other colour developers to induce or inhibit the production of testosterone (T) and E2 *in vitro* using the H295R steroidogenesis assay. E2 production was induced by BPA, and T production was inhibited by BPA and BPS. D-8 and PF201 did not show any significant effects.

1.2.2 Toxicity endpoints other than endocrine activity

For repeated dose toxicity, the US EPA (2015) assigned a "high hazard" level to BPS and a "medium hazard" level to D-8 based on reproduction/developmental toxicity and repeated-dose oral studies on rats. In these studies, D-8 caused no significant effects, while BPS effects included, among others, decreased food consumption, hyperplasia and necrosis in cecal mucosal epithelium, increased kidney and liver weight in males. PG201 was designated "medium hazard" for reproductive, developmental and repeated dose. A summary of US EPA (2015)'s hazard assessment for these chemicals is shown in Table 1.

1.3 Toxicokinetics

Toxicokinetics is the study of how a substance gets into the body (absorption), how it is transported and transformed in the body (distribution, metabolism), and how the body gets rid of it (excretion).

1.3.2 BPA

After oral intake, BPA is very efficiently absorbed by the human gastrointestinal (GI) system (Thayer et al. 2015; Teeguarden et al. 2015). Then, BPA reaches the liver through the mesenteric blood vessels. In the liver BPA is rapidly metabolised (first pass metabolism) (Tominaga et al. 2006; Pottenger et al. 2000; Thayer et al. 2015) primarily to its glucuronide conjugate, and to a lesser extent to its sulphate conjugate (Völkel et al. 2002; Ye et al. 2005). Thayer et al. (2015) studied BPA toxicokinetics in humans following a single oral administration. In blood,

unconjugated BPA was < 1% of the total (unconjugated + conjugated) BPA; elimination of BPA conjugated metabolites into urine largely occurs within 24h post-ingestion; recovery of the administered BPA dose was 84-100% in urine. Therefore, total BPA urinary concentration is used to assess BPA exposure in human biomonitoring (Hines et al. 2017; Ndaw et al. 2016; Calafat et al. 2005).

Table 1 - BPA, BPS, D-8, and PF201 hazard summary for different endpoints, as established by US EPA (2015). Hazard levels in coloured text were assigned based on empirical data. Hazard levels in black italics were assigned using values from estimation software and professional judgment. The criteria for the assignment of these hazard levels is described in the report by US EPA (2015).

	Endpoints (*)														
	Human health effects											Aquatic toxicity		Environmental fate	
Chemical	Acute toxicity	Carcinogenicity	Genotoxicity	Reproductive	Developmental	Neurological	Repeated dose	Skin sensitisation	Respiratory sensitisation	Eye irritation	Dermal irritation	Acute	Chronic	Persistence	Bioaccumulation
BPA	L	M	L	M	H	*M*	M	M		M	M	H	H	VL	L
BPS	L	*M*	M	M	M	*M*	H	L		L	L	M	M	M	L
D-8	L	*M*	L	*M*	*M*	*M*	M	L		*L*	*L*	H	*H*	M	M
PF201	L	*M*	L	M	M	*L*	M	L		L	VL	H	H	VH	L

(*) **VL** = very low hazard, **L** = low hazard, **M** = moderate hazard, **H** = high hazard, **VH** = very high hazard.

BPA dermal absorption is less efficient than oral absorption (20-70% of the applied dose *in vitro*) (Demierre et al. 2012; Toner et al. 2018; Liu and Martin 2019; Champmartin et al. 2020). It is slow and leads to prolonged uptake. Animal studies have shown that, in contrast with oral absorption, dermally-absorbed BPA does not undergo first-pass metabolism, and it reaches the systemic circulation mostly in the unconjugated BPA form (Tominaga et al. 2006; Pottenger et al. 2000). In a human *in vivo* study by Liu and Martin (2017), cumulative BPA excretion in urine increased for two days after a single dermal contact with thermal paper.

These data suggest that the route of exposure can have a large influence on BPA toxicokinetics, and in particular on the concentration of unconjugated BPA circulating in the body (Gundert-Remy, Mielke, and Bernauer 2013; Vandenberg, Welshons, et al. 2014). This is important because BPA can bind to oestrogen receptors only in its unconjugated form, which suggests that only the unconjugated form may have endocrine activity (Matthews, Twomey, and Zacharewski 2001). Therefore, the dermal route of exposure may be particularly important for BPA (Figure 2).

1.3.3   BPS, D-8, PF201

Like BPA, BPS is efficiently absorbed and eliminated after oral intake in humans (Oh et al. 2018; Khmiri et al. 2020). A single oral dose of BPS reached peaks in plasma within 1 h, was rapidly conjugated by first-pass metabolism and had an elimination half-life of 8-9 h. As for BPA, glucuroconjugated BPS (BPS-G) in plasma was found in greater concentrations than unconjugated BPS (Khmiri et al., 2020). However, in Khmiri et al. (2020)'s study unconjugated (bioavailable) BPS showed larger peak plasma concentrations and areas under the plasma concentration-time curves (AUC) compared to BPA (Thayer et al. 2015), for a similar administered dose. In urine, unconjugated BPS was 1.7% of the administered dose, compared to 0.1% for BPA. These results suggest that unconjugated form is more prevalent for BPS than BPA, leading to a greater oral bioavailability of BPS than BPA. Mean total BPS in urine was 82% (n = 7, Oh et al. (2018)) and 56% (n = 6, Khmiri et al. (2020)) of the orally administered dose.

Two human studies showed that BPS skin absorption was slower than oral absorption (Liu and Martin 2019; Khmiri et al. 2020). No BPS was detected in serum up to 7.5 hours post-exposure in Liu and Martin (2019)'s study. No BPS was quantifiable in blood and urine of the participants in Khmiri et al. (2020)'s study at most time points, with some peaks detectable between 5-8 h in blood, and 5-11 h in urine. Conjugation was less efficient for BPS than for BPA (free/total urinary ratio was 6.9 % for BPS, and 2.7 % for BPA) (Liu and Martin 2019). Excretion was not complete 72 h after dosing. BPS and BPS-G recoveries in urine were 0.004 % and 0.09 % of the administered dose.

Skledar et al. (2016) observed that BPS is mainly metabolised into BPS-glucuronide *in vitro* using human liver and intestinal microsomes and recombinant human CYP450 enzymes. They studied also the endocrine activity of BPS and its metabolites, and observed that BPS-glucuronide has no activity on either estrogen, androgen or thyroid hormone receptors. Zhou et al. (2014) analysed 100 urine samples from male adults and found that 97% of total urinary BPS was unconjugated.

To our knowledge, there are no data on D-8 and PF201 toxicokinetics.
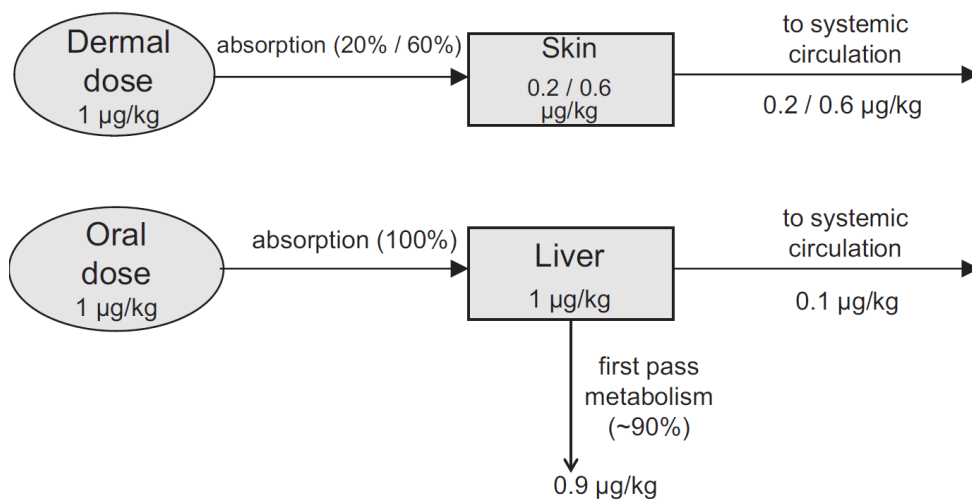
Figure 2 – Comparison of dermal and oral routes of exposure to BPA (Gundert-Remy, Mielke, and Bernauer 2013)

1.4 Thermal paper

BPA, BPS, D-8, and PF201 are used as colour developers in thermal paper (US EPA 2015a). Thermal paper is a base of paper covered by a thermally reactive layer (Figure 3). This layer contains a binder, a thermochromic ink, and a colour developer (van Es 2014).

The thermochromic ink is a halochromic chemical that changes colour depending on the pH. When thermal paper is not heated, the thermochromic ink is in its non-ionised form, which is colourless. During the printing process, the paper is heated above the binder's melting point by the printer head. Then, the binder melts allowing the protonation of the thermochromic ink by the weak-acidic colour developer. This protonation leads to the coloured form of the thermochromic ink, which becomes visible as the print on the paper. BPA, BPS, D-8 and PF201 are weak proton donors suitable to be used as colour developers.

Some thermal paper products contain one single major developer, while others contain a mixture of two or more developers with one main developer in higher amounts, and secondary developer(s) in lower amounts (Biedermann, Tschudin, and Grob 2010). A drawback of thermal paper is its susceptibility to external effects such as sunlight, heat, and oils that lead to printing discolouring. Discolouring is faster in thermal papers with less stable colour developers.

6
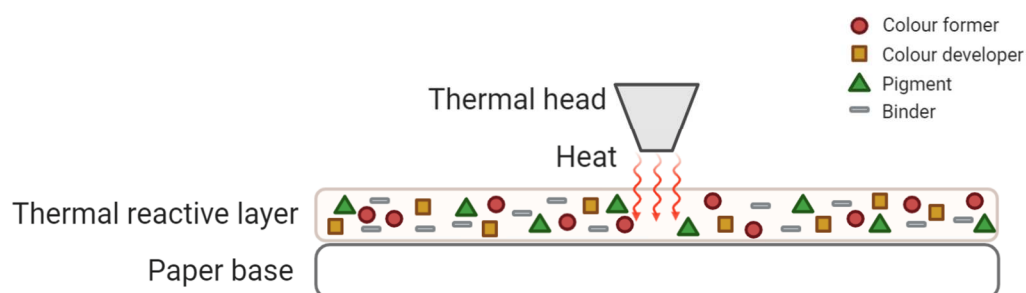
Figure 3 - Structure of thermal paper (adapted from van Es 2014). Figure created in Biorender.com

The lower the stability, the shorter the image will remain visible. According to the report of the Danish Environmental Protection Agency (Danish EPA, 2014), developer stability is from lower to higher: BPA < BPS < D-8 << PF201. The same order is followed when considering costs: paper containing BPA is the cheapest, and paper containing PF201 is the most expensive. PF201 has only a sole provider (BASF).

1.5 Exposure to BPA, BPS, D-8 and PG201 from thermal papers

Exposure to bisphenols can occur through ingestion, inhalation and dermal absorption. The primary route of exposure to BPA and BPS is dietary exposure from food and drink containers. When used as plasticizers in plastics and can lining, bisphenols are in a polymerised form; when used as colour developers in thermal papers, they are in their monomeric form as free solids. Therefore, relatively large exposures to colour developers may occur after handling these papers. Absorption from thermal paper may happen by the dermal route and by ingestion after hand-to-mouth contact. Skin contact with BPA from thermal paper contributes to the overall body burden among occupationally exposed populations, such as cashiers (Braun et al. 2011; Ndaw et al. 2016; Thayer et al. 2016), and workers in thermal paper industries (Heinälä et al. 2017).

1.5.2   Occurrence and amount of developers in thermal papers

BPA was the most used colour developer between 2015 and 2019. BPA was found in in 100/124, 78/100, and 195/308 thermal paper products tested by Goldinger et al. (2015), Björnsdotter et al. (2017), Vervliet et al. (2019), respectively. The most used alternatives to BPA in thermal papers were BPS, D-8 and PF201 (Björnsdotter et al. 2017; Eckardt and Simat 2017; Goldinger et al. 2015; Vervliet et al. 2019). The detection frequencies of these

colour developers are shown in detail in Table 1 of Annex III. These frequencies may be different now that BPA has been restricted from thermal paper since 2020. The European Chemicals Agency (ECHA) reported that BPA was still the dominant colour developer used in thermal paper in the EU in 2018, but that the market share of BPA-based thermal paper decreased to below 50%. From 2017 to 2018, the share of BPS-based thermal paper had increased from 19% to 21%, and the share of thermal paper based on other developers increased from 30 % to 31 % (ECHA 2019).

The amount of colour developers in thermal paper is around 1% (w/w), i.e. 10 mg/g paper. BPA has the highest concentration, followed by BPS, D-8 and PF201 (Table 2). Thermal paper receipts weigh 58 g/m^2 paper on average (US EPA 2015a). The amount of colour developer is then approximately 0.58 g/m^2.

Table 2 - Mean concentrations (mg/g) of developers in thermal paper

	CAS #	Eckardt and Simat (2017)		Danish EPA (2014)		Goldinger et al. (2015)	Yang et al. (2019)
		mg/g [a]	µg/cm^2 [b]	mg/g [c]	µg/cm^2 [c]	mg/g [d]	mg/g[e]
BPA	80-05-7	15.9/15.7/15.0[f]	80.0/79.3	10.8	61.0	13.5/14.5 (5.6 – 30.4)	3.61 (ND – 18.7)
BPS	80-09-1	13.1/14.7/13.7	67.5/68.2	11.6	64.9	10.2/10.0 (8.3 – 12.6)	1.15 (ND – 16.8)
Pergafast 201	232938-43-1	10.5/9.5/9.7	57.6/52.8	10.4	56.8	5.4/4.6 (3.3 – 8.2)	NA
D-8	95235-30-6	10.0/2.5/10.0[fg]	75.6/53.7	NA	NA	11.2/12.0 (3.4 – 13.2)	0.209 (ND – 25.0)
D-90	191680-83-8	NA	NA	NA	NA	NA	NA (ND – 4.18)
TGSA	41481-66-7	NA	NA	NA	NA	NA	0.380 (ND – 26.0)
BPS-MAE	97042-18-7	NA	NA	NA	NA	NA	0.416 (ND – 8.56)
UU	321860-75-7	13.9	68.8/71.6	NA	NA	NA	NA
DD-70	93589-69-6	NA	NA	NA	NA	NA	NA

[a] data are medians
[b] mean/median
[c] mean
[d] mean/median (range)
[e] mean (range)
[f] numbers listed by collection years 2015/2016/2017
[g] the last value (10.0) is not a median (n= 1)
NA, not available

1.5.3 Thermal paper handling

When considering thermal paper handling for exposure assessment purposes, at least several factors must be considered: handling duration, skin area in contact with thermal paper, number of handling events daily. The European Food Safety Authority (EFSA) modelled the exposure of the general population to BPA (EFSA 2015). In this model, the EFSA considered 10 seconds handling duration by three fingertips on one hand (typical exposure) and three fingertips on both hands (high exposure). The EFSA also estimated 1 and 4.6 handling events

per day as typical and high exposures, respectively, of the general population. However, these behavioural estimates are theoretical and have not been verified experimentally. Bernier and Vandenberg (2017) studied patterns of thermal paper handling by observing 700 individuals in a college-aged population purchasing food in a cafeteria. Only 11% of the observed individuals had a behaviour consistent with the EFSA model: participants handled receipts for an average of 11.5 min, using more than 3 fingertips (>30% of participants), and touching the paper with their palm (>60% of participants). Not all interactions with thermal paper are likely to be as long as those observed by Bernier and Vandenberg (2017), e.g. transactions at gas stations or visits to the ATM. However, the number of surfaces (fingers, palm) in contact with the paper may be similar.

The French Agency for Food, Environmental and Occupational Health & Safety (ANSES) modelled the exposure of the occupationally exposed population (cashiers) (ANSES 2013). In this model, the ANSES considered that cashiers handle thermal receipts for 3 to 10 h per day, with a skin contact area of 12 cm^2 that comprises all ten fingers.

1.5.4   Migration from thermal paper to human skin

Several studies have determined the amount of colour developers that migrates from thermal papers to the hands' skin in different handling conditions. The references to these studies and their results are shown in Table 3. In general, the amount of BPA that migrates on the skin after thermal paper contact is approximately 1 µg/finger. A similar or slightly less amount migrates for BPS, PF201 and D-8. Only one study determined PF201's migration and found the amount to be similar to BPA, BPS, and D-8. All studies reported that migration is approximately 20 times higher for sweaty or wet hands. One study reported approximately 200 times higher values for hands rubbed with hand sanitizer.

Table 3 – Amounts of developers migrated from thermal paper to hands (µg/finger).

Reference	Contact duration [s]	Dry skin [µg/finger][a][b]				Humid skin [µg/finger][b]				
		BPA	BPS	PF201	D-8	Substance to humidify skin	BPA	BPS	PF201	D-8
Biedermann et al. (2010)	5	1.1 (0.1-3)	NA	NA	NA	Saliva[c]	8.8 (3.5-14)	NA	NA	NA
						Water[c]	20.5 (18-23)	NA	NA	NA
						Vegetable oil[c]	5.8 (4.5-7)	NA	NA	NA
Lassen et al. (2011)[d]	10	1.9 (0.8-5.0)	NA	NA	NA	Sweat simulant	17.2 (3.5-40)	NA	NA	NA
						Hand lotion	4.7 (4.3-5.0)	NA	NA	NA
Danish EPA (2014)[d]	5	1.1 (1.08-1.13)	0.8 (0.7-0.9)	0.4 (0.3-0.5)	NA	Sweat simulant	17.8 (15.0-2.5)	3.2 (1.6-4.8)	17.1 (16.6-17.5)	NA
						Hand lotion	3.1 (2.3-3.8)	1.2 (0.9-1.5)	0.7 (0.5-0.9)	
Eckardt and Simat (2017)	5	0.8 (0.05–6.0) (median 0.3)[e]				Water[g]	35 (21–42)	mean range 9–14 (values range 2.3–24.6)[f]		
Liu and Martin (2019)	300	0.77 (0.07–3.0) µg/hand wipe	3.9 (0.71–10) µg/hand wipe	NA	NA	NA	NA	NA	NA	NA
Hormann et al. (2014)	60	3.0 (2.1-3.8) µg/hand wipe	NA	NA	NA	Hand sanitizer	550 (495-610) µg/hand wipe	NA	NA	NA

[a] All values are expressed in µg/finger as mean (values range) unless otherwise indicated.
[b] In some references data were reported in µg on two or more fingers. We have recalculated those data to report values in µg/finger.
[c] Skin was either humidified with saliva, as commonly applied to better grip paper, softened in warm water and shaken to remove excess water, or touching tissue paper containing vegetable oil.
[d] Data was recalculated based on the use of 6 fingers for migration, not 8 as stated in Lassen et al. (2011) (number of fingers used has been confirmed by Danish EPA (2014)).
[e] No significant difference in the amount transferred when comparing samples with different colour developers (BPA, BPS, PF201, and D8).
[f] No significant difference in the amount transferred when comparing BPS, PF201, and D-8.
[g] Skin was moistened by touching a water moistened tissue.
NA, not available

1.6 From the external to the internal dose: skin absorption

Coupling the exposure data, i.e. colour developer concentration in thermal paper, migration from thermal paper to the skin, and thermal paper handling, with data on skin absorption and metabolism allows the calculation of the colour developer biological effective dose (Figure 4). According to the US EPA (2015b), the potential dermal dose that could come into contact with the skin involves the contaminant and the matrix or vehicle in which it is embedded (i.e. the amount of developer in thermal paper). Only part of the potential dose will come into contact

with the skin, and is called applied dose (i.e. developer that migrates from thermal paper to the skin). The internal dermal dose is determined by the rate at which the contaminant is absorbed by the skin (skin absorption). Considering the amount of the internal dose that may be metabolised yields the biologically effective dose (e.g. unconjugated BPA) that interacts with the internal target tissue or organ (e.g. hormone receptors).
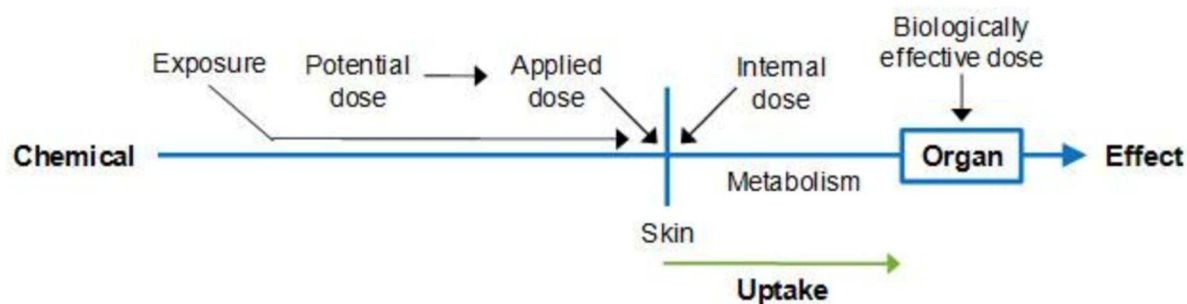
Figure 4 - Illustration of dermal route: exposure and dose (US EPA 2015b)

Typically, the internal dose is calculated using one of these equations (ANSES 2013), depending on the available data:

$$ID = \frac{J \times t \times A}{BW} \qquad \text{(eq. 1)}$$

$$ID = \frac{\%absorbed \times t \times M \times n}{BW} \qquad \text{(eq. 2)}$$

where ID is the internal dose, usually expressed in µg/kg/day, J is the flux of absorption in the skin (µg/cm^2/h), t is the exposure duration (h), A is the exposed skin area (cm^2), %absorbed is the percent of the permeant dose deposed on the skin that is absorbed (%), M is the mass of permeant deposed on the skin (µg/finger), n is the number of exposed fingers, and BW is the body weight (kg). J and %absorbed are determined by skin absorption studies.

Skin absorption, also called dermal or percutaneous absorption, is a permeation process where a permeant (i.e. a chemical from the environment) penetrates through a solid (i.e. the skin) and may get into the systemic circulation. In general, permeation can be modelled by equations such as Fick's laws of diffusion. Fick's first law of diffusion postulates that the flux (J) of molecules diffusing through a homogeneous membrane is proportional to the permeant's concentration gradient. Expressed in one dimension (x) and applied to skin absorption, the equation is:

$$J = -D\frac{dC}{dx} \qquad\qquad \text{(eq. 3)}$$

where C is the permeant's concentration, x is the distance from the skin surface, and D is the permeant's diffusion coefficient (cm^2/h). C and D are two of the many parameters that affect skin absorption. Skin absorption consists of a series of diffusion and partitioning steps between several compartments. When it comes in contact with the skin, a chemical must first partition between the matrix or vehicle where it is embedded and the skin surface; then from the skin surface into the outermost layer of the skin, the stratum corneum; then must partition and diffuse through the inner layers of the skin down to the capillaries. Therefore, several factors can affect skin absorption (WHO 2006):

1. the physicochemical nature, structural organisation, and metabolic activity of the skin;

2. the physicochemical properties of the diffusing substance (permeant) as well as of the vehicle in which the permeant is dissolved, especially if it changes the permeability of the stratum corneum.

3. experimental factors, that is the conditions of the test system used to measure skin absorption, e.g. dose and volume of the permeant, occlusion or non-occlusion of the test area, *in vitro* or *in vivo* test systems, and duration of the exposure.

The influence of these factors on skin absorption is discussed in Chapter 1.8.

1.7 Skin structure

The skin is the largest organ of the body. The main role of the skin is to protect the body against water loss and entry of exogenous substances. Skin barrier function is attributed to its layered structure (Figure 5), composed of hypodermis, dermis, epidermis (Hazel 2016).

The hypodermis (several millimetre thick) is composed of a network of fat cells, and plays an important role in energy storage and metabolism. The dermis (1-5 mm thick) lies above the hypodermis, and is composed of collagenous fibres and elastic connective tissue. The dermis determines the elasticity of the skin and provides the physical support needed for nerves and blood vessels.

The epidermis (60-150 μm thick, up to 800 μm thick in palms and soles) is composed of several layers above the dermis. The layers are, from the innermost to the uppermost: stratum basale, stratum spinosum, stratum granulosum, and stratum corneum (SC). The viable epidermis includes all layers of the epidermis except the SC, and is responsible for the formation of the SC: the epidermal cells at the basal layer proliferate and start to differentiate migrating towards the surface of the skin; the terminal differentiation occurs at the strum granulosum-

SC interface, during which viable keratinocytes are transformed into corneocytes. Corneocytes are flattened dead cells filled with keratin filaments and water. The keratinocytes also synthesize lipids and other structural proteins of the SC. The viable epidermis contains also melanocytes, which produce melanin for ultraviolet absorption, and Langerhans cells, which are responsible for the immune response of the skin.

The SC (10-30 μm thick) is made of physiological inactive cells (corneocytes), continually shedding and being replenished from the upward migration of cells from the underlying layers (Moss, Gullick, and Wilkinson 2015). The SC provides the majority of the skin's barrier function due to its "brick and mortar" structure: corneocytes can be imagined as bricks surrounded by mortar. The mortar is a lipid matrix made of lipid bilayers, and is more lipophilic and less hydrated than the other epidermal layers. SC water content depends on its anatomical location as well as on the environment: in presence of water, the SC may swell to many times its own thickness (Moss, Gullick, and Wilkinson 2015). The lipid bilayers are mainly made of ceramides, free fatty acids and cholesterol, and constitute the only continuous pathway across the SC.

1.7.2   Routes of permeation across the stratum corneum

Diffusion though the intact SC can occur via three main pathways: intercellular, transcellular and transappendageal (Figure 5). The permeant may follow a specific route or a combination of any of the three available routes. The intercellular pathway represents the diffusion through the SC's intercellular lipid matrix. The transcellular pathway is across the SC corneocytes. It is a shorter pathway compared to the intercellular one. Only amphiphilic permeants can follow the transcellular pathway because it contains both lipophilic and hydrophilic regions: the intercellular lipids, corneocyte membranes and hydrated keratin within the corneocytes. The transappendageal route of skin permeation occurs through pores associated with skin appendages, i.e. sweat glands, hair follicles and oil glands. These structures may offer low resistance to permeation compared to other routes because they lack the horny layer. However, this route is of limited significance in the overall absorption process because the appendages represent a very small percentage of the skin surface area (0.1% on average).
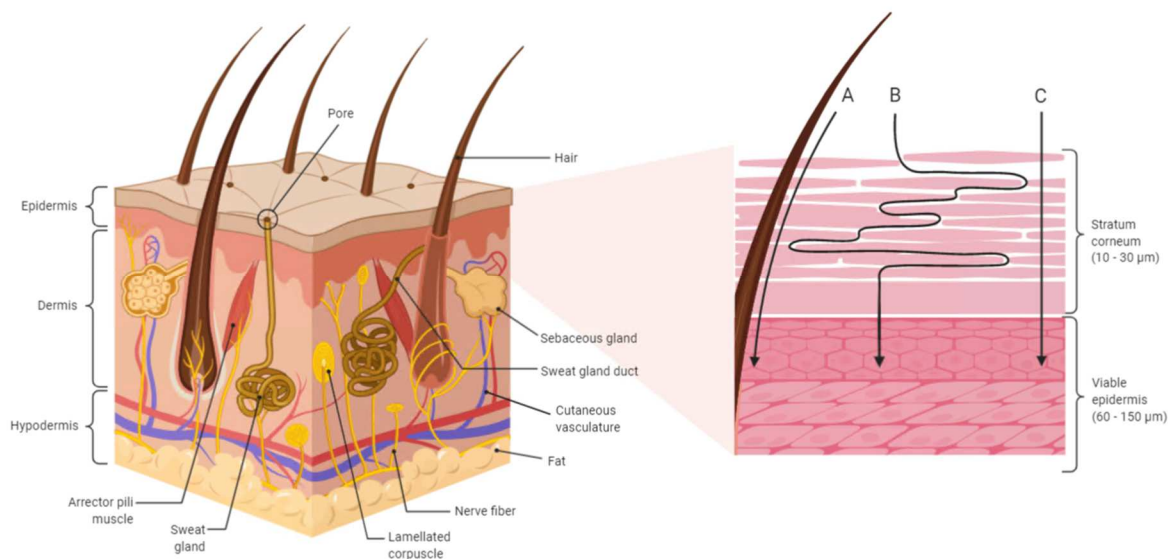
Figure 5 - Skin structure and permeation pathways: transappendageal (A), intercellular (B), and transcellular (C) routes. Figure created in BioRender.com.

1.8 Properties affecting absorption

1.8.2 Skin properties affecting absorption

The skin properties that affect dermal absorption include not only the skin's structure and physicochemical properties, but also external factors directly affecting the skin. The main factors are:

Skin damage, skin hydration, occlusion

Mechanical damage, such as cuts, abrasions or burns, and even just irritation and mild trauma may decrease the barrier properties of the skin and increase the absorption. Also, the depletion or disturbance of SC lipids, often related to skin diseases such as eczema or psoriasis, lead to a perturbation of the skin's barrier function (Sahle et al. 2015). When the skin barrier is disrupted, the absorption of hydrophilic solutes increases significantly more than hydrophobic molecules (Flynn 1985).

Also hydration, UV exposure, and contact with some chemicals can affect the SC's barrier function. An increase in skin hydration alters the structure of the SC and is widely associated with a decrease in the skin barrier function, and therefore an increase in the rate of absorption of most molecules (Moss, Gullick, and Wilkinson 2015). Skin occlusion by a material (e.g. a patch, a glove, a viscous ointment) placed on the skin increases the skin temperature and skin hydration, and in most cases leads to an increase in permeability.

Anatomical location

Great variations in skin permeability have been observed across different skin locations. These variations can generally be related to the thickness the SC at different body parts: posterior auricular skin < scrotum < head and neck < abdomen < forearm < thigh < instep < heel < planter (Moss, Gullick, and Wilkinson 2015).

Skin temperature

An increase in temperature increases the permeant's diffusion coefficient, which results in a higher flux. An increase in temperature will also affect blood flow and metabolism. Therefore, in general, it is accepted that an increase in temperature will increase the rate of absorption and that a decrease in temperature may lower the rate of absorption by up to one order of magnitude (Moss, Gullick, and Wilkinson 2015).

Skin metabolism

The skin has essential metabolic capability, due to the effects of enzymes that are mainly located in the epidermis. Skin metabolism is not rate-limiting in term of skin absorption, but may affect the nature of the chemical entering the body (WHO 2006; OECD 2004b), and therefore its toxicity.

Phase I and phase II enzymes are responsible of xenobiotic metabolism. Phase I enzymes modify xenobiotics, while phase II enzymes add polar groups to the phase I products to prepare them for the excretion. The skin contains both phase I and phase II enzymes (Zhang et al. 2009). Examples of phase I enzymes in the skin are cytochrome (CYP) P450 (CYP1, CYP2, and CYP3 families), cyclooxygenases (COX), aldehyde dehydrogenases (ALDHs), alcohol dehydrogenases (ADHs), esterases, flavin-containing monooxygenases (FMOs), proteases. Examples of phase II enzymes in the skin are glutathione S-transferases (GSTs), UDP-glucuronosyltransferases (UGTs), sulfotransferases (SULT), and N-acetyltransferases (NATs).

The expression and activity of these enzymes in the skin is relatively low compared to their equivalent hepatic forms (Wilhelm, Zhai, and Maibach 2012). Once excised from a donor, ex-vivo human skin for *in vitro* skin absorption and metabolism testing undergoes a rapid reduction in glutathione and phase I enzymes, and a slower reduction in energy metabolism (OECD 2004c). Some enzyme systems such as esterases remain active even after freezing (OECD 2004c).

Sex and race

Skin absorption is not significantly affected by neither sex nor race (WHO 2006).

1.8.3 Permeant properties affecting skin absorption

Partition coefficient and molecular weight

As pointed out in section 1.6, skin absorption consists of a series of diffusion and partitioning steps. The main physicochemical properties that affect SC permeability to a permeant are the permeant diffusivity (D) within the skin, and the partition coefficient between the stratum corneum and the vehicle (K_M). Potts and Guy (1992) considered that D is inversely proportional to the molecular volume (MV), and that octanol/water partition coefficient (K_{OW}) is often used instead of K_M because it is easier empirically determined. Therefore, they developed a simple model describing the dependence of the permeability coefficient (K_p, cm/sec) upon permeant molecular volume (MV) and octanol/water partition coefficient (K_{OW}). They fitted their model with experimental data, initially from (R. J. Scheuplein and Blank 1971), then with other datasets (Roberts, Anderson, and Swarbrick 1977; Ackermann, Flynn, and Smith 1987), with good results. Then, they fitted the Flynn (1990) data set of permeability data for about 90 chemicals using their model where MW was used as a reasonable approximation for MV. For compounds with MW ranging from 18 to >750 and logK_{OW} from -3 to +6, permeability through the skin can be predicted by this equation (Potts and Guy 1992):

$$\log K_p = -6.3 + 0.71 \times \log K_{OW} - 0.0061 \times MW \qquad \text{(eq. 4)}$$

This model is consistent with transport through the SC lipid lamellae, and suggests that lipid properties alone are sufficient to explain SC permeability. Therefore, the skin can be simply considered a lipidic layer (the SC) with predominately hydrophilic layers underneath (the epidermis and dermis) (Moss, Gullick, and Wilkinson 2015). Lipophilic substances will permeate the SC, but will permeate at a very slow rate in the epidermis or will remain in the SC (reservoir effect). In practice, the ideal permeant should be both lipophilic and hydrophilic. As a general rule (Moss, Gullick, and Wilkinson 2015), lipophilic substances with a logK_{ow} >3 will predominately permeate the SC via the intercellular pathway. Hydrophilic substances will have a comparatively higher tendency to permeate the SC via hydrophilic pathways, such as hydrated keratin-filled corneocytes. Permeants with intermediate partition coefficients (1 < logK_{OW} < 3) may traverse the skin barrier via both lipid and aqueous pathways, but the intercellular route is likely to predominate. Another general rule that is frequently adopted especially in pharmaceutical development is that permeants should have a MW < 500 Da to allow skin absorption (Bos and Meinardi 2000). The "500 Da rule" is based on the observation that most common contact allergens and topical drugs have a molecular weight < 500 Da.

Applied concentration

Increasing the concentration of a chemical within a topically applied vehicle generally increases the amount of chemical absorbed across the skin (Moss, Gullick, and Wilkinson 2015) due to the increased concentration gradient (chapter 1.6, eq.1).

Ionisation

Both non-ionised and ionised molecules can penetrate the SC. However, the SC lipophilic nature suggests that non-ionised molecules are more likely to penetrate the SC than ionised molecules. Non-ionised molecules may preferably permeate through the intercellular pathway. Ionised molecules may permeate the skin via the transappendageal route or by mechanisms of ion-pairing or ion-exchange. Therefore, the permeant pK_a and the vehicle pH may significantly affect the permeant skin absorption (Moss, Gullick, and Wilkinson 2015).

1.8.4 *Physicochemical properties of the vehicle*

The vehicle affects skin permeation mainly in two ways. One way is by altering the skin structure, hence the skin barrier integrity, e.g. aqueous vehicles may increase skin hydration, hence skin permeability. Another way to affect skin permeation is by influencing the permeant release from the vehicle to the skin, e.g. if the permeant has a low affinity for the vehicle (or a higher affinity for the SC), then it may partition into the skin more readily. The vehicle pH, as described above, affects the ionisation state of the permeant and its solubility in the vehicle, hence the permeant skin absorption.

1.9 Methods to estimate skin absorption

As already illustrated in figure 4, skin absorption is a necessary parameter to estimate a permeant internal dose. Several methods exist to estimate skin absorption: *in vivo* studies with human and animal skin, *in vitro* studies with human, animal and artificial skin, and *in silico* models.

In vivo studies are used to determine the penetration of a test substance in the skin as well as in the systemic circulation (blood). Urine can also be analysed, if excretion is studied. *In vivo* studies can be carried out on animals and on humans. *In vivo* studies have the advantage of using metabolically and physiologically intact skin, using a species common to many toxicity studies, and can be modified for use with other species (OECD 2004a). The disadvantages are the use of live animals, the need for radiolabelled material to facilitate reliable results, difficulties in determining the early absorption phase and the differences in permeability of the preferred species (rat) and

human skin (OECD 2004a). Studies on humans is the gold standard (WHO 2006) because animals have different skin permeability and metabolism compared to humans (OECD 2004c).

In vitro skin absorption methods measure the diffusion of chemicals through excised skin to a fluid reservoir. *In vitro* studies have less technical, ethical, and cost limitations, and help reduce the use of laboratory animals. Moreover, *in vitro* studies can utilise non-viable skin to measure diffusion only, or fresh, metabolically active skin to simultaneously measure diffusion and skin metabolism. Such methods have found particular use as a screening to compare chemicals' delivery into and through skin from different formulations, and can also provide useful models for the assessment of percutaneous absorption in humans.

There are sufficient data comparing *in vivo* and *in vitro* methods that support the use of skin *in vitro*. *In vitro* methods have been harmonised by the Organisation for Economic Co-operation and Development (OECD 2004b; 2004c; 2011). Skin from human or animal sources can be used, but studies on human skin should be given preference over studies on other species (OECD 2011). Rat, mouse and rabbit skin may be more permeable than human skin. Pig skin has been shown to be a good surrogate of human skin for *in vitro* testing in the cosmetic industry. For pesticides and biocides, the OECD (2011) supports the use of human or rat skin only. Reconstructed human skin models are also accepted for *in vitro* skin absorption assays (Kang-Sickel et al., 2010, as reported in OECD (2011)). Skin's permeability is maintained after excision from the body because the skin barrier function is carried out by the stratum corneum, which is non-viable. Therefore, frozen skin and cadaver skin can be used for *in vitro* studies. However, only viable skin (i.e. skin where the viable epidermis and dermis have metabolic capability) can be used to measure skin metabolism.

In silico methods, such as mathematical models and quantitative structure-activity relationships (QSARs), are used to predict dermal absorption. The advantage is that they avoid the ethical and cost limitations of the *in vivo* and *in vitro* methods. The disadvantage is that *in silico* models rely on data from *in vivo* and *in vitro* skin absorption assays, which are necessary for models development and the validation. Moreover, often no *in vitro* data are available on a studied chemical, and therefore *in vitro* data on analogues are used.

Our study on the skin absorption of BPA and its alternatives in thermal paper was conducted *in vitro*. The Exposure Science Unit at our institution (Unisanté) has the equipment and the know-how to conduct *in vitro* skin absorption assays. Results from these assays allow Unisanté Exposure Science Unit to assess exposures to industrial chemicals, and to understand the mechanisms behind the skin permeation. While most laboratories working on *in vitro* skin absorption use pig skin or human frozen skin from patients and cadavers, Unisanté has the rare

opportunity to receive viable (*ex-vivo*) human skin explants directly from plastic surgeries at the Centre Hospitalier Universitaire Vaudois (CHUV) in Lausanne. The general consent from the patients is obtained by the plastic surgeon according to an ethical protocol approved by the Ethics Committee of the Vaud Canton. Tissue distribution is organised by the Département de l'appareil locomoteur (DAL) at the CHUV. Our skin absorption assays with *ex-vivo* human skin generally start within two hours from the plastic surgery. The next chapter explains *in vitro* skin absorption methods in general. A detailed description of the *in vitro* skin absorption methods we used in our assays is given in Annex II and in Annex III.

1.10   In vitro skin absorption assays

1.10.2   Diffusion cells

Skin permeation studies are commonly carried out using diffusion cells. These cells consist of a donor chamber and a receptor chamber, divided by a flap of excised skin. The skin is clamped between the two chambers with the stratum corneum facing up. Diffusion cells usually have a water jacket connected to a water bath heater/circulator that keeps the skin and the cell content at a controlled temperature close to normal skin temperature (32 ℃). Once
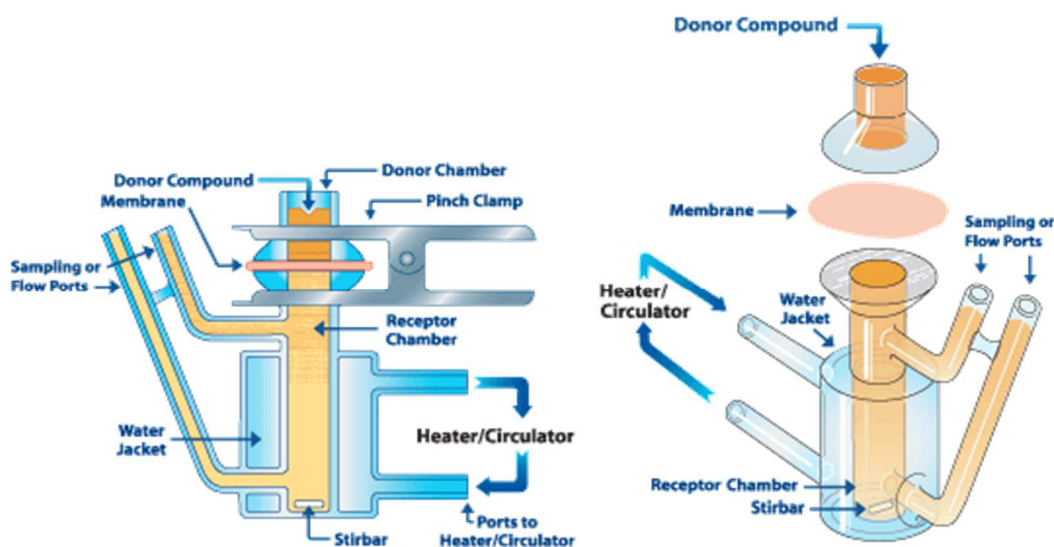
Figure 6 – A flow-through diffusion cell used in *in vitro* skin absorption assays (www.permegear.com)

applied on the stratum corneum in the donor chamber, the test substance diffuses through the skin and possibly into a fluid in the receptor chamber. The receptor fluid is then sampled at specific time points. A sampling period of 24 hours is typical, but could be shorter or longer for very fast or slow permeating chemicals (OECD 2004b). Manual sampling is required for static diffusion cells. For flow-through diffusion cells automatic sampling by a peristaltic pump and fraction collector is required (Figure 6). Sampling frequency should allow adequate

characterisation of the test substance's absorption profile, which is the cumulative mass of test substance in the receptor fluid per unit skin area ($\mu g/cm^2$), plotted against time.

Receptor fluid

The receptor fluid is most often isotonic to blood plasma, such as saline (NaCl 0.9% w/v in water). If skin metabolism is studied, cell culture media should be used to support cell metabolic activity. Most importantly, the receptor fluid should not hinder the diffusion of the test substance into the receptor chamber by exerting a counter-pressure. Therefore, the receptor fluid must be continuously stirred and should flow through the receptor chamber (or sampled regularly from static diffusion cells), and its composition should allow adequate solubility of the test substance.

Skin

Excised skin can be prepared in different ways for *in vitro* skin absorption testing: epidermal membranes thermally, chemically or enzymatically separated from the dermis; split-thickness skin, typically dermatomed at a 200-400 μm thickness; and full thickness, preferably of < 1 mm. Skin can be used freshly excised from the body or frozen. Frozen skin is usually stored at -20ºC for several months, with no changes in skin barrier properties. In any case, skin integrity must be verified before and after applying the test substance on the skin. This can be done by visual inspection and by checking that one of the following parameters is in its normal range: skin trans-epidermal water loss (TEWL), permeability to tritiated water, or electrical resistance to an alternating current. Skin must be allowed to equilibrate in contact with the receptor fluid for 10-30 minutes prior to the application of the test substance on the skin.

Test substance

Whenever possible, the test substance should be applied on the skin in the same form (neat, diluted or as part of a formulated material), concentration and duration as those of typical exposure scenarios. Doses applied on the skin can be finite or infinite.

Finite doses mimic human exposure. Indicatively, the OECD suggests 1-5 mg/cm² for solids and up to 10 $\mu l/cm^2$ for liquids (OECD 2004b). At the end of finite-dose experiments, the test substance should be analysed in all system components, i.e. receptor fluid, diffusion cell rinsing, skin surface rinsing, and skin. The SC may be tape-stripped several times and the tape analysed. The skin may also be divided into SC, epidermis and dermis, for separate analysis. The mean recovery (mass balance) should be 100±10 % of the applied dose for radio-labelled test compounds, and 100 ±20% for non-radio-labelled test compounds. The results of the analyses should allow to

calculate the distribution of test substance in the test system and the absorption profile (cumulative mass per unit exposed skin area) over time. The slope of the absorption profile is the absorption rate or flux, J ($\mu g/cm^2/h$):

$$J = \frac{1}{A}\frac{dM}{dt} \qquad \text{(eq. 5)}$$

where M is the cumulative mass of test substance in the receptor fluid, A is the exposed skin area, and t is time.

Infinite doses ensure a continuous excess of test substance in the donor cell, so that the concentration of the applied test substance does not significantly deplete during skin exposure (therefore it can be considerate "infinite"). When an infinite dose of a chemical is applied onto the skin, the chemical concentration can be considered constant. In this conditions, the chemical absorption rate increases until reaching and maintaining a maximum at the steady state (J_{SS}). J_{SS} can be calculated using Fick's first law of diffusion (equation 3 in section 1.6). At the steady state, Fick's first law applied to a permeant's diffusion through the skin becomes (Franz 1983):

$$J_{SS} = \left(\frac{D \cdot K_m}{L}\right) \cdot C_V = K_p \cdot C_V \qquad \text{(eq. 6)}$$

where K_m is the partition coefficient between the SC and the vehicle, L is the skin thickness, K_p is the permeability coefficient (cm/h), and C_V is the permeant's concentration in the vehicle. This equation is based on the assumptions of a homogeneous skin membrane, of a constant C_V, and of a perfect sink (the permeant's concentration in the receptor fluid is zero at all times). It is worth noting that the resistance to a permeant passive diffusion though the skin is generally attributed to the SC. Therefore, even though the epidermis and dermis have their own diffusion coefficient, they are normally treated together and represented by an average diffusion coefficient (Moss, Gullick, and Wilkinson 2015). When infinite dose conditions are used, the percentage absorbed is not relevant and the absorption profile is used to calculate J_{SS} and the permeability coefficient, K_p (OECD 2004b). Practically, J_{SS} can be estimated by calculating the slope of the steepest linear portion of the absorption profile, and K_p can be calculated using Fick's first law of diffusion at the steady state ($K_p = J_{SS} / C_V$). The time required to reach the steady state is called lag time (t_{lag}, h), and can be calculated as the time (x-axis) intercept of the linear portion of the absorption profile. The (OECD 2004c) indicates typical infinite doses of 100 $\mu l/cm^2$ (or > 10 mg/cm^2) and more. However, the vehicle volume is not always related to finite and infinite doses. While less than 100 $\mu l/cm^2$ may be enough for substances with low permeability to reach the stead-state, high permeable substances may need much more than 100 $\mu l/cm^2$ (Hopf et al. 2020). Maintaining infinite dose conditions may be difficult, especially for lipophilic substances (Selzer et al. 2013). This effect is described in Annex II, where 100 $\mu l/cm^2$ aq solutions

of BPA and alternative colour developers were applied on human skin, and in Annex III, where different experimental conditions are compared for BPA.

1.10.3 Test substance analysis

Once an *in vitro* assay has been completed, the test substance must be quantified in the different system components (for finite dose experiments) or in the receptor fluid only (for infinite dose experiments). Typically, test substances are radiolabelled. The quantification of radiolabelled test substances is relatively easy because it is not hindered by the matrix (e.g. receptor fluid, skin incubation media, tape stripping extraction solvents) and it does not require any or simple sample preparation. A liquid scintillation analyser is used for quantification. However, this type of analysis has several inconveniences. It requires special laboratory infrastructures and organisation to safely work with radioisotopes. Radiolabelled chemicals are very expensive compared to the non-radiolabelled ones. Often chemicals are tested for skin absorption not as a single compound but as commercially available mixtures (e.g. cleaning products, lubricants), and these mixtures are not radiolabelled. If metabolism is studied, then analytical separation (e.g. by chromatography) and other analytical techniques are necessary to distinguish the parent compound from the metabolite. Still, radiolabelled permeants should be used for skin absorption studies whenever possible (OECD 2004b). When the use of radioisotopes is not possible, other analytical method are used, such as liquid or gas chromatography coupled with an appropriate detector depending on the test compound's chemical and physicochemical properties.

Analytical methods for the quantification of BPA, BPS, D-8 and PF201

In the past twenty years, BPA and other bisphenols have been routinely analysed in different matrices by many laboratories: in sediments and in drinking, waste and ground water (Ballesteros et al. 2006; Gallart-Ayala, Moyano, and Galceran 2010; Chang, Chou, and Lee 2005; Laganà et al. 2004; Li, Wang, and Yuan 2009; Rodriguez-Mozaz, López de Alda, and Barceló 2004; Wang et al. 2017); in canned food (Alabi, Caballero-Casero, and Rubio 2014; Gallo et al. 2017; Sun et al. 2006); in animal tissues (Xiao et al. 2006); and in human biological fluids such as breast milk (Ye et al. 2006), serum and urine (García-Prieto et al. 2008; Kazemi et al. 2016; Mao et al. 2004; Ndaw et al. 2016; Vandenberg, Gerona, et al. 2014; Yang et al. 2014; Zhou et al. 2014; Ndaw et al. 2018).

Liquid chromatography tandem mass spectrometry (LC-MS/MS) is extensively used because of its high specificity and sensitivity (Ye et al. 2006; Zhou et al. 2014; Goldinger et al. 2015; Ndaw et al. 2018; Vandenberg, Gerona, et al. 2014; Yang et al. 2014). Sample preparation is in general necessary to avoid any matrix effects. Matrix effects are due to the presence of compounds in sample's matrix that may perturb analytes ionization, hence analytes

signals. Current most used techniques for sample preparation are solid-phase extraction (SPE), and solid-phase micro-extraction (SPME), and liquid/liquid extraction (LLE).

Even though LC-MS/MS is the gold standard for the analysis of bisphenols nowadays (Caballero-Casero, Lunar, and Rubio 2016), other analytical methods are suitable for the analysis of bisphenols. For BPA quantification, high-performance liquid chromatography (HPLC) has been used coupled with either fluorescence detection (FD), photodiode-array detection (DAD) (Li, Wang, and Yuan 2009; Mitani et al. 2003; Zarzycki, Włodarczyk, and Baran 2009), and ultraviolet (UV) and electrochemical detection (Peñalver et al. 2002). Gas chromatography coupled with mass spectrometry (GC-MS) with prior derivatisation has been used for BPA quantification mostly in water (Chang, Chou, and Lee 2005; Mol, Sunarto, and Steijger 2000; Sánchez-Avila et al. 2009; Zhao et al. 2009; Wang et al. 2017; Ballesteros et al. 2006), but also in other matrices such as canned food (Cunha et al. 2020).

BPS is mainly analysed by LC-MS/MS (Ndaw et al. 2018; Liu and Martin 2019; Gayrard et al. 2019; Oh et al. 2018; Rocha et al. 2015; Zhou et al. 2014; Goldinger et al. 2015; Yang et al. 2014). Other analytical techniques, such as LC-FL, LC-UV (Russo et al. 2018) and LC-DAD (Tuzimski et al. 2020) are also used for BPS.

D-8 and PF201 in thermal paper samples have been analysed by LC coupled with MS/MS (Goldinger et al. 2015) or time-of-flight MS (Vervliet et al. 2019) after extraction in methanol. A study carried out by the Danish Environmental Protection Agency (Danish EPA 2014) analysed PF201 in ethanol where participants had their fingers immersed for 30 seconds. Ethanol was analysed by HPLC coupled with UV and FL detection. We were not able to find in the literature any analytical methods to analyse D-8 and PF201 in more complex matrices.

Bisphenol metabolism is mainly conjugation with glucuronide, and in minor extent sulphate molecules (chapter 1, section 1.3 Toxicokinetics). The quantification of bisphenol metabolites is usually carried out by enzymatic hydrolysis of the conjugated (phase II) metabolites e.g. adding glucuronidase and sulfatase to the samples (Ndaw et al. 2016; 2018; Oh et al. 2018; Frederiksen et al. 2020; Thayer et al. 2016). The unconjugated parent compound is quantified before and after the enzymatic hydrolysis. Parent compound concentration after the hydrolysis represents the sum of the concentrations of the unconjugated and the enzymatically de-conjugated bisphenol (total concentration). Conjugated metabolite concentrations are indirectly determined by the difference in concentration of the parent compound before and after the hydrolysis (conjugated = total – unconjugated). Direct quantification of bisphenol metabolites has been seldom carried out, because it requires additional standards and analytical methods for the metabolites.

In our study, we developed and validated an LC-MS/MS method for the simultaneous quantification of BPA, BPS, D-8 and PF201 in *in vitro* skin absorption samples, and the direct quantification of BPA-G. This method is described in Annex I.

1.11 Skin absorption of BPA, BPS, D-8 and PF201

As introduced in section "1.3 Toxicokinetics", *in vivo* human studies have shown that BPA and BPS transferred on the skin during thermal paper receipts handling can be absorbed into systemic circulation and excreted in urine (Ehrlich et al. 2014; Liu and Martin 2017; 2019; Khmiri et al. 2020). Compared to oral absorption, dermal absorption of BPA and BPS led to prolonged exposure and could lead to higher proportions of the unconjugated form in systemic circulation. There are no *in vivo* studies on D-8 and PF201.

In vitro skin absorption studies of colour developers have focused mainly on BPA (Marquet et al. 2011; Demierre et al. 2012; Toner et al. 2018; Zalko et al. 2011; Mørck et al. 2010; Liu and Martin 2019; Kaddar et al. 2008; Champmartin et al. 2020). The *in vitro* studies on BPA have shown inconsistent results: percent of applied dose ranged from 1 to 46 % in the receptor fluid, from 13 to 42 % in the skin, and 3 to 72 % were unabsorbed; skin-metabolised BPA range from negligible to 27 % of the applied dose; permeation rate values for finite doses of BPA in water ranged from 3.0×10^{-5} µg/cm^2/h to 7.0×10^{-1} µg/cm^2/h. The wide range of BPA skin absorption results are due to the different experimental set ups used by different laboratories following the OECD guidelines on *in vitro* skin absorption (OECD 2004b). This is because the OECD guidelines allow some flexibility in the experimental parameters. In Annex III of this dissertation we studied the influence of some *in vitro* experimental parameters on BPA skin absorption, and used our findings to compare among some published *in vitro* studies. Champmartin et al. (2020) studied the *in vitro* skin absorption of BPA dissolved in water, acetone and artificial sebum. A BPA dose of 20 µg/cm^2 applied in 50 µl/cm^2 of vehicle led to steady state conditions when vehicle was acetone and artificial sebum. T_{lag} was long (10-12 h) and K_p was in the same order of magnitude (9.30×10^{-5} and 4.65×10^{-5} cm/h, for acetone and artificial sebum respectively). However, the same BPA dose did not lead to steady state when vehicle was ultra-purified water. Therefore, K_p values at steady state are unknown for BPA in water.

Only two *in vitro* studies on BPS skin absorption are available in the literature (Liu and Martin 2019; Champmartin et al. 2020). These studies have consistently shown that BPS permeated the skin more slowly than BPA and that less than 1% of applied dose got the receptor fluid. However, 20% to 47% of the applied BPS dose remained in

the skin depending on the vehicle (Champmartin et al. 2020), and was consequently potentially absorbable. In both studies BPS was mainly absorbed without biotransformation.

There are no *in vitro* studies on D-8 and PF201's skin absorption.

1.12   Aim of this study

Our aim was to study the skin absorption of BPA and its main alternatives in thermal paper, namely BPS, D-8 and Pergafast 201 *in vitro*. In order to achieve this goal, this project was divided into three parts. This dissertation has been organised following the research of these three parts. Each part has been published in peer-review journals and is presented as an annex to this dissertation.

The first part is the development and validation of an analytical method to quantify colour developers in *in vitro* skin absorption samples, and is described in Annex I "Simultaneous quantification of bisphenol A, its glucuronide metabolite and commercial alternatives by LC-MS/MS intended for *in vitro* skin absorption samples".

 The second part is the *in vitro* study on skin absorption of colour developers, and is described in Annex II "Skin absorption of Bisphenol A and its alternatives in thermal paper".

The third part is the study of how experimental parameters affect BPA skin absorption *in vitro*, and is described in Annex III "Influence of experimental parameters on in vitro human skin permeation of Bisphenol A".

The next two chapters give a summary of the main results of the three annexes (Chapter 2), and a discussion on the results (Chapter 3).

2. Main results

2.1 Analysis of colour developers

We developed and validated a sensitive LC-MS/MS method for the direct and simultaneous quantification of BPA, BPA-G, BPS, D-8, PF201 in *in vitro* skin absorption samples where receptor fluid was saline. The materials and methods are thoroughly described in Annex 1, chapter "Experimental procedures". Briefly, the analytes in calibration standard solutions, quality control (QC) solutions and samples were extracted and concentrated by solid phase extraction SPE (C18 cartridge), and analysed by LC-MS/MS. For LC-MS/MS we used a C18 column and an electrospray ionisation source (ESI) in negative ion mode. Our method was in line with guidelines of bioanalytical method validation (FDA 2018) but with higher acceptance thresholds for lower limits of quantification (LLOQ) and QC solutions' accuracy and precision. The lower limit of quantification (LLOQ) of this analytical method was 0.2 μg/L for all five analytes. The upper limit of quantification (ULOQ) was 200 μg/L for BPA, and 20 μg/L for BPA-G, BPS, D-8, and PF201. Linearity was good, with $R^2 \geq 0.998$ for all the analytes. Slope variability ($\%RSD_{slope}$) was equal to or under 8.4 for all analytes except for BPS, for which %RSDslope was 14.8. Accuracy values were within ±8% of nominal concentration for low and high QCs of all analytes. Intra-day precision and intermediate precision were both under 10% for all analytes, except BPA low QC, where they reached respectively 12.2% and 15.5%.

Matrix effect, extraction recovery, and process efficiency were evaluated using the method of Matuszewski, Constanzer, and Chavez-Eng (2003) (Table 3 of 1). The results showed that matrix effects were negligible for D-8 and PF201, and were strong for BPA at low concentrations, BPA-G and BPS even after correction using internal standards. Overall process efficiency (calculated as the product of matrix effect and extraction recovery) was good for BPA high QC solutions, BPA-G, D-8 and PF201 (100-113%). Process efficiency was low for BPS (71-80%) and BPA low QC solutions (134%). Matrix in skin absorption samples was saline that that been in contact with skin for up to 24 h ($saline_{skin}$). Calibration standards and QC solutions were prepared in saline. Therefore, we assessed the use of saline as a surrogate for $saline_{skin}$. The slopes of the calibration curves prepared in matrix ($saline_{skin}$) or in surrogate matrix (saline) differed by −5% for BPA, 4% for BPA-G, −16% for BPS, 8% for D-8, and 4% for PF201 (Table 4, Annex 1)). All analytes in aqueous solutions and in matrix were stable under typical benchtop, storage and long-term conditions. Stock solutions in methanol were stable up to 6 months, except for PF201 (peak area was reduced by 90% upon storage at −20 °C for 6 months).

2.2 Skin absorption of colour developers

We used the developed method to quantify BPA, BPA-G, BPS, D-8, and PF201 in *in vitro* skin absorption samples. For the *in vitro* experiments, we used flow-through diffusion cells with saline as receptor fluid. Then, we exposed *ex vivo* human skin to aqueous solutions of the test chemicals for 24 hours. A detailed description of the methods used is available in chapter "Materials and methods" of Annex II. A first series of experiments aimed at determining the skin permeation kinetics (steady state). We applied large volumes ($100 \, \mu l/cm^2$) of tested chemicals in aqueous solution on 200 µm-thick viable human skin to reach an infinite dose. The results are shown in Table 4. In these conditions, steady state was reached by BPS, but not by BPA and D-8. PF201 was <LLOQ in most receptor fluid samples. BPA-G in the receptor fluid was under the limit of quantification after 24 h of exposure. A second series of experiments aimed at quantifying the test chemicals in the different *in vitro* system compartments (mass balance). We applied $100 \, \mu l/cm^2$ of tested chemicals in aqueous solution on 800 µm-thick previously frozen ($-20°C$) human skin. The results of mass balance experiments are shown in Table 5.

2.3 Effect of experimental parameters on BPA *in vitro* skin absorption

Finally, we studied the effect that different experimental parameters have on BPA skin permeation kinetics *in vitro*. We used the same experimental set up as in Demierre et al. (2012)'s study for the sake of comparison (diffusion cells, flow, receptor fluid, sampling times), and we changed four parameters: either skin thickness (800, 400, 200 µm), BPA concentration (250, 164, 18 mg/l), skin state (fresh or frozen), or vehicle volume (1000, 100, $10 \, \mu l/cm^2$). We analysed the receptor fluid samples to obtain BPA absorption profiles for the different experimental conditions. We used HPLC-FL to analyse the samples because this method did not require any sample preparation. The analytical method is described in Annex III, section 2.3 "Sample assays").-We estimated J, K_p and t_{lag} values from BPA absorption profiles. We further analysed J, K_p and t_{lag} as a function of the four studied experimental parameters (skin thickness, skin state, vehicle volume, and BPA concentration) using a linear mixed-effect model. Skin donor was used as a random effect. Restricted Maximum Likelihood was used to fit this mixed model. Table 3 of Annex III shows the experimental conditions and all the results for the different assays. Briefly, steady state conditions were achieved when $1000 \, \mu l/cm^2$ of BPA 250 mg/l were applied on the skin. In these conditions K_p values ranged $1.6–5.2 \times 10^{-3}$ cm/h depending on skin thickness. J decreased 3-fold with increasing skin thickness from 200 to 400/800 µm (P < 0.05), 2-fold with decreasing vehicle volume from 1000 to $100 \, \mu l/cm^2$, 3-fold with fresh (viable) skin compared to previously frozen skin, and 11-fold with a 14-fold decrease in BPA concentration.

27

Table 4 - Summary of skin exposure conditions and results of permeation kinetic experiments, following an application of 100 µl/cm² aq solution on 200 µm-thick viable human skin.

[a] Number of skin samples tested from three skin donors.

Chemical	n[a]	Concentration [mg/	Mean (±SD) amount in receptor fluid after 24 h of exposure		Mean (±SD) kinetic parameters		
			µg/cm²	% of applied dose	t_{lag} [h]	J_{peak}[c] x 10⁻² [µg/cm²/h]	K_p x 10⁻⁴ [cm/h]
BPA	12	250	8.00 (±3.05)	32 (±12)	NA	67 (±30)	NA
BPS	12	250	0.05 (±0.03)	0.2 (±0.1)	7.6	0.6 (±0.9)[d]	0.24 (±0.35)
D-8	10	20	0.41 (±0.18)	20 (±9)	NA	4.1 (±2.0)	NA
PF201	11	3[b]	<LLOQ	<LLOQ	NA	NA	NA

[b] Water solubility has been reported to be 35 mg/l but we could only dissolve 3 mg/l.
[c] J calculated at the steepest linear portion of the absorption profile
[d] J_{ss}
NA, not applicable.

Table 5 - Summary of skin exposure conditions and results of mass balance experiments, following an application of 100 µl/cm² aq solution on 800 µm-thick previously frozen (-20°C) human skin.

Chemical	n[a]	Dose [µg/cm²]	Mean (± SD) amount in the different compartments after 24 h of exposure									
			µg/cm²					% of applied dose				
			Skin swabs	Donor chamber	Skin	Receptor fluid[b]	Recovery (total)	Skin swabs	Donor chamber	Skin	Receptor fluid[b]	Recovery (total)
BPA	8	25	14 (±1.0)	0.5 (±0.6)	3.7 (±3.4)	6.4 (±3.1)	25 (±3.1)	57 (±4.2)	1.0 (±1.8)	15 (±14)	25 (±13)	98 (±13)
BPS	7	25	18 (±3.7)	0.4 (±0.6)	2.5 (±1.6)	0.1 (±0.0)	21 (±3.5)	71 (±14)	2.1 (±2.4)	11 (±6.8)	0.4 (±0.2)	84 (±14)
D-8	7	2	1.1 (±0.7)	0.1 (±0.1)	0.4 (±0.1)	0.5 (±0.3)	1.7 (±0.6)	39 (±18)	3.9 (±5.0)	16 (±5.4)	17 (±12)	76 (±13)
PF201	8	0.3	0.09 (±0.07)	<LLOQ	0.01 (±0.00)	<LLOQ	0.09 (±0.07)	22 (±20)	<LLOQ	1.5 (±0.9)	<LLOQ	24 (±22)

[a] Number of skin samples tested from three skin donors.
[b] Sum of the amount quantified in the receptor fluid collected for 24 hours and in the receptor fluid remained in the receptor chamber.

3. Discussion and perspectives

In Chapter 1 we introduced the problematic of human exposure to thermal paper colour developers. We summarised toxicological data and exposure data on the most used colour developers. As colour developers can migrate on the skin and be absorbed, we introduced the concept of skin absorption and the different ways to assess it. We summarised also the methods to analyse colour developers, because quantification is a necessary step in skin absorption assays. The aim of this dissertation was to assess *in vitro* skin absorption of the four most used colour developers in Switzerland. Therefore, we developed a method to quantify these colour developers in *in vitro* skin absorption samples (Annex 1) and we used it to study their skin absorption *in vitro* (Annex II). Finally, we studied the effect that some experimental parameters have on *in vitro* skin absorption of BPA, to understand the variability of the literature data and to compare them with our results (Annex III). Chapter 2 presented a summary of the results of the researches described and discussed in detail in Annexes 1 to 3. Chapter 3 is a discussion of our results, as well as a presentation of the limitations of our study and of the future perspectives.

3.1 Analysis of colour developers

As pointed out in section 1.10.2 "Analytical methods for the quantification of BPA, BPS, D-8 and PF201", bisphenols are routinely analysed in different matrices. Nowadays the gold standard for bisphenol analysis is LC-MS/MS. Only one study had developed an LC-MS/MS method to quantify BPA, BPS, D-8 and PF201 in methanol used for the extraction of these colour developers from thermal papers (Goldinger et al. 2015). However, we needed an analytical method to analyse them in a more complex liquid matrix, such as our *in vitro* skin absorption samples. Therefore, we developed and validated a method for this purpose (Annex 1).

A problem in BPA analysis is the contamination from BPA contained in plastics used for laboratory analyses (Ye et al. 2013). Therefore, we tested pipette tips, PTFE filters, solvents, and several SPE cartridges, and BPA was detectable but under the LLOQ (1% - 16% of the LLOQ signal).

We tested also the analytes stability and did not observe any particular issues, except for PF201 stock solutions in methanol, which had a 90% peak area loss after being stored for 6 months at -20ºC. This confirms other studies reporting PF201 instability in protic organic solvents (Goldinger et al. 2015; Eckardt and Simat 2017) and in acidic aqueous solutions (Eckardt and Simat 2017).

The receptor fluid of our *in vitro* assays was relatively simple, i.e. saline. Nonetheless, sample pre-treatment was necessary. Without any pre-treatment, ion suppression of the analytes was observed over few analyses. The

addition of ammonia in the mobile phase improved the detector response because it enhanced the analyte ionisation [M-OH + OH⁻ → M-O⁻ + H₂O], but was not enough to avoid signal decrease during the analytical run. This effect was overcome by sample pre-treatment with solid phase extraction (SPE). After SPE cartridge selection and solvent optimization, the SPE recoveries ranged within ±10% of the nominal QC concentrations, except for BPS QC_{low} (114%) and BPA-G QCs (83-88%). Surrogate matrix assessment showed that the calibration curves prepared in matrix ($saline_{skin}$) and in surrogate matrix (saline) had slope differences, especially for BPS. However, we considered these differences low enough to justify the use of saline as a surrogate matrix, given the scarcity of human skin samples for skin absorption studies. For method validation, we followed the Food and Drug Administration (FDA) guidelines (FDA 2018). However, we set higher accuracy and precision acceptance criteria for LLOQ and quality control solutions (QC_{low} and QC_{high}) than the recommended by the FDA. This was due to the lower accuracy for BPA LLOQ and QC_{low} (as shown in Table 2 of Annex 1) compared to the other analytes, and to the matrix effects on BPA and BPS (as shown in Table 3 of Annex 1). The matrix effect on BPS (68-70%) could not be compensated by the internal standard (BPA-G-[$^{13}C_{12}$]), probably due to their difference in chemical structures and retention times. The higher variability and matrix effects for BPA QC_{low} compared to the other analytes could be due to BPA ubiquitous contamination from plastics and solvents: in blank solutions, BPA signal was 45% of LLOQ, while BPA-G, BPS, D-8 and PF201 signals were <7% of LLOQ. Even though this value could not justify the strong matrix effect on BPA QC_{low}, it indicated that BPA background contamination was still possible and could affect the results at low concentrations. Matrix effects on BPA QC_{low} could only partly be compensated (125%) even using BPA isotope-labelled analogue BPA-[D_6] as internal standard. Coupled with an extraction recovery of 107%, this matrix effect on BPA QC_{low} led to a process efficiency of 134%. For BPA QC_{high} the internal standard could compensate well for matrix effect (97%) and recovery (106%), leading to a high process efficiency (103%). Surprisingly, BPA-G-[$^{13}C_{12}$] could not correct for BPA-G matrix effects (123% for QC_{low} and 136% for QC_{high}). These were compensated by BPA-G extraction recoveries (83%-88%), leading to an overall process efficiency of 108% for BPA-G QC_{low} and 113% for BPA-G QC_{high}. For D-8 and PF201, we observed no or little matrix effects and a good overall process efficiency (≤110%). We deemed this method sensitive and robust for the analysis of *in vitro* skin absorption samples and we applied it to the skin absorption assays that are discussed in the next section.

3.2 Skin absorption of colour developers

As pointed out in the introduction (Chapter 1, section 1.9), *in vitro* skin absorption assays can be carried out either under finite or infinite dose conditions. The goal of using finite doses is to replicate exposure conditions, and to

know how much of the applied dose is unabsorbed, absorbed in the skin, and absorbed in the receptor fluid (mass balance). The goal of infinite dose conditions is to calculate the skin absorption kinetics of the permeants from their skin absorption profiles. Most skin absorption laboratories use radio-labelled permeants, as scintillation counting has high sensitivity, simplifies sample analysis, and does not depend on permeant degradation or metabolism. This is particularly useful for mass balance (Walters 2002).

In this research project, we tested unlabelled permeants because our laboratory is not equipped to work with radioactive compounds. We decided to use doses that were deemed to be infinite (100 μl/cm^2) to increase the probability of detecting the permeants with our analytical method. We determined both the skin absorption profiles (i.e. permeation curves of Figures 1 to 4, Annex II) and the mass balance using the infinite dose approach. In these conditions, our BPA applied dose (25 μg/cm^2) was approximately 20 times greater than reported finger exposure for dry skin, and in line with wet skin (Chapter 1.5, on "Migration from thermal paper to human skin"). D-8 dose (2 μg/cm^2) was in the range of dermal exposures for dry skin, and 5-12 times smaller for wet skin. PF201 dose (0.3 μg/cm^2) was in the range of dermal exposures for dry skin, and 15-60 times smaller for wet skin. BPS dose (25 μg/cm^2) was approximately 30 times greater than the reported range of dermal exposures for dry skin, and 5-15 times greater for wet skin.

Our results in Table 4 show that BPS had a peak permeation rate 2 orders of magnitude smaller than BPA. D-8 permeation rate was 16 times smaller than BPA. This was likely due to the 13 times smaller concentration of D-8 compared to BPA, suggesting that D-8 skin permeation may be comparable or somewhat smaller than BPA. PF201 was not detected in the receptor fluid, indicating that PF201 did not permeate the skin as the parent compound, but PF201 storage and/or metabolism in the skin could not be ruled out. These results are in line with the main physicochemical properties of our test substances (Table 6). As introduced in Chapter 1, section 1.8.1, logK$_{OW}$ and MW are two key parameters for the diffusion of chemicals through the stratum corneum (Guy and Potts 1993). Efficient permeants in general have a MW < 500 and are lipophilic. All four tested colour developers follow this general rule, but PF201 has the highest MW almost approaching the 500 limit, and a lower logK$_{OW}$ compared to BPA and D-8. BPS has a similar MW as BPA and D-8 (all three MWs are <300), and the lowest logK$_{OW}$.

Table 6 – Main physicochemical properties of BPA, BPS, D-8, and PF201 (US EPA 2015a).

	BPA	BPS	D-8	Pergafast 201
CAS number	80-05-7	80-09-1	95235-30-6	232938-43-1
Molecular formula	$C_{15}H_{16}O_2$	$O_2S(C_6H_4OH)_2$	$C_{15}H_{16}O_4S$	$C_{21}H_{20}N_2O_6S_2$
MW	228.29	250.27	292.35	460.52
Solubility in water (mg/l)	120 – 300	1.1×10^3 (20°C)	21, 19.7	35 at 20°C
Log K_{ow}	2.2 3.32	1.2	3.36	2.6

BPA and D-8 skin absorption profiles had a decrease after 10 hours, but not BPS (Figure 1 of Annex II). The applied dose was enough to achieve the steady state for BPS, but not enough for the two colour developers with higher skin permeability (BPA and D-8). Therefore, we were able to calculate K_p and t_{lag} values for BPS. The dose necessary the reach steady state depends on the permeants skin permeability: the higher the permeability, the higher the dose. Therefore, maintaining infinite dose conditions can be problematic for permeable substances, especially the lipophilic ones (Selzer et al. 2013). Finite and infinite doses were further studied and discussed in the third part of this dissertation (Annex III).

Our results on BPS are in line with reported data in that BPS absorption is consistently lower than BPA (Liu and Martin 2019; Champmartin et al. 2020). However, each study reported different K_p and t_{lag} values (Table 7). These differences could be due to different experimental parameters, as shown for BPA in results' section 2.3 and discussion section 3.3. For BPA, we determined that skin thickness (200 vs. 400 µm) had the most influence on J. Also, vehicle volume did not affect significantly BPA's J when vehicle volume varied between 100 and 1000 µl/cm². However, vehicle volume could potentially lead to significant changes in J for vehicle volumes variations between 10 and 100 µl/cm². Assuming that these experimental parameters affect similarly BPS and BPA at least qualitatively, the difference in skin thickness and in vehicle volume could explain the 9-fold difference in K_p between our study and Champmartin et al. (2020). The considerable lower BPS concentration used by Liu and Martin (2019) compared to our study (1 and 5 mg/l in vs. 250 mg/l, see Table 7) should theoretically lead to lower J values. However, the J value that Liu and Martin (2019) determined was similar to our study. This is likely due to the 3D skin model, which could be more permeable than ex-vivo human skin, leading to K_p values two orders of magnitude greater than ours. In conclusion, considerable differences in skin type and diffusion system did not allow result comparisons between our study and Liu and Martin (2019).

Table 7 – Experimental set up and results of published BPS skin absorption studies.

	Reale et al. (2020)	Liu and Martin (2019)	Champmartin et al. (2020)
Experimental parameters			
Skin type	Human	Human skin model	Human
Skin thickness [µm]	200	120	476
Skin condition	Viable	3D model	Viable
Total skin samples	12	3	8
Diffusion system	Flow-through	Static diffusion device in 6-well plates	Static
BPS concentration [mg/l]	250	1, 5	740
Vehicle	Water	Water	Water
Vehicle volume [µl/cm^2]	100	1494, 1540	50
BPS dose [µg/cm^2]	25	1.5, 7.7	20
Receptor fluid	Saline	Phosphate-buffered saline	RPMI-1640 medium supplemented with 0.2% gentamycin, 2.5% penicillin-streptomycin and 2% bovine serum albumin.
Exposure time [h]	24	25	40
Results			
J_{ss} x 10^{-2} [µg/cm^2/h]	0.6 ± 0.9	0.9 ± 1.4, 1.7 ± 1.2 [a]	0.10 ± 0.02
K_p x 10^{-4} [cm/h]	0.24 ± 0.35	90 ± 150, 30 ± 20 [a]	0.026
T_{lag} [h]	$7.6 \pm$	Not reported	0.6 ± 3.8
Mass balance [b]			
Unabsorbed dose [%]	73	74, 84 [a]	47
Skin dose [%	11	16, 17 [a]	47
Receptor fluid [%]	0.4	8, 6.4 [a]	<1

[a] Results reported for 1.5 and 7.7 µg/cm^2 doses, respectively

[b] Results expressed as percent of the applied dose.

Mass balance results allow a comparison between BPA and BPS, as the recovery was within the acceptable values as per the OECD (2004a) guidelines (Table 5). Dose absorbed in receptor fluid was greater for BPA than BPS. Unabsorbed dose (skin swabs + donor chamber rinsing) was greater for BPS than BPA. Amounts in skin were similar for BPA and BPS. BPA amounts in skin (15% of the dose) were in line with results reported in the literature, all in the 12 – 27 % range. BPA absorbed dose (25%) was in the middle of the reported range (1 – 46 %). Most of BPS dose was not absorbed (73%), part was retained in the skin (11%), and a very low amount was in the receptor fluid (0.4 %). These results are in line with published studies in that at least half of the BPS applied dose was not absorbed and low amounts were found in the receptor fluid (Table 7). Champmartin et al. (2020) also found low amounts of BPS in the receptor fluid (<1%), and higher amounts in the skin (47%).

Mass balance assays for D-8 and PF201 had low recoveries. D-8 mass balance results were close to the recommended range of 100 ± 20% for non-radiolabelled test substances (OECD, 2011), while PF201 had especially low recoveries. We hypothesize that degradation in contact with the skin may play a major role in PF201 skin absorption, because the skin has an acidic pH (5.5). For D-8 the reasons for these recoveries can be several: tape-stripping, which was carried out but not included in the mass balance because tape strips could not be analysed, low cotton swabs recoveries, metabolism, skin protein binding, and degradation. Mass balance results are further discussed in Annex II, chapter on Discussion.

As mentioned in the introduction (Section 1.6, Figure 4), quantifying metabolites of an absorbed chemical is important to calculate the biologically effective dose. Most toxicological studies use the oral route of exposure to determine dose-response curves. If there is a considerable difference in the oral and skin metabolism of a chemical, oral dose-response relationships are not applicable to the dermal route of exposure. This is particularly important for chemicals with a high first-pass metabolism in the liver, such as BPA. Figure 2 of Introduction (Section 1.3 on "Toxicokinetics") showed that after oral dosing in humans, 90% of BPA dose undergoes first-pass metabolism and 10% of the dose the systemic circulation (Gundert-Remy, Mielke, and Bernauer 2013). Here we show that BPA-glucuronide was negligible in the receptor fluid after 24 hours of exposure. Our results on BPA skin metabolism are similar to other studies using diffusion cells (Marquet et al. 2011; Champmartin et al. 2020). Studies using multi-well plates detected higher amounts of BPA conjugated metabolites, probably because of the different methods, which tend to overestimate metabolism (EFSA 2015). Overall, our results confirm that there are considerable differences in BPA metabolism between dermal and oral routes of exposures. These differences will likely result in higher bioavailability of BPA from dermal exposure despite the lower skin absorption compared to oral absorption.

3.3 Effect of experimental parameters on BPA *in vitro* skin absorption

Results of *in vitro* studies on BPA skin absorption are inconsistent, due to the use of different materials and experimental conditions. Here we assessed the influence that some experimental parameters have on BPA human skin absorption using flow-through diffusion cells. The variation of J due to changing BPA concentration, vehicle volume, skin thickness and status (viable or frozen) are summarized in Figure 7.
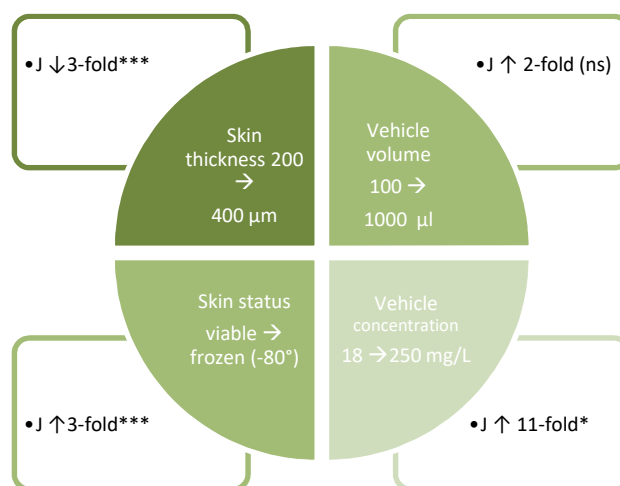
Figure 7 - Summary of the effects that different experimental parameters have on BPA skin permeation kinetics. ***, P ≤ 0.001; **, P ≤ 0.01; *, P ≤ 0.05; ns, not significant (P > 0.05). P values were calculated from Restricted Maximum Likelihood statistical analysis.

The qualitative influence of the studied experimental parameters on skin permeability is well known. Increasing a permeant's concentration leads to faster skin permeation, while increasing skin thickness leads to a slower skin permeation of chemicals (as shown in Introduction, equations 3 and 6). An increase in aqueous vehicle volume is associated to an increase in permeation rate due to an increased skin hydration (Introduction, section 1.8.1 on "Skin properties affecting absorption"). Also, the permeability of skin frozen at -20 ºC is considered to be similar to viable skin, and the OECD (2004a) accepts its use for *in vitro* skin absorption studies. Contradictory data exist on skin frozen at -80 ºC which can be more permeable (Barbero and Frasch 2016) or less permeable (Nielsen et al. 2011) than viable skin. Here, we quantified the effect that permeant concentration, vehicle volume, skin thickness, freezing skin at -80 ºC had on BPA permeation rate (figure 7). This quantification allowed the comparison of J values among ours and two other published studies (Toner et al. 2018; Demierre et al. 2012). We have concluded that J values agree among these studies when experimental differences are taken into account. No comparison of our J values was possible when too many parameters differed among studies.

Our results showed also that skin absorption of BPA in water reached the steady state only when 1000 μl/cm^2 of BPA solution 250 mg/l were applied (Table 3 in Annex III). This volume is 10 times greater than the minimal volume suggested by the OECD (2004a) for infinite dose experiments (100 μl/cm^2). This is the first time that steady-state has been reached for BPA. The derived steady state parameters can be used in *in silico* modelling of BPA skin permeation.

It is worth noting that we determined different K_p values depending on the skin thickness used in the *in vitro* experiments. K_p decreased significantly with skin thickness increasing from 200 to 400 μm. This is to be expected

because the permeant's permeability coefficient is inversely proportional to the pathlenght across the skin (eq.6 in section 1.10.1), and because the aqueous viable tissue provides a high resistance to the permeation of lipophilic chemicals (Wilkinson et al. 2006; van de Sandt et al. 2004), such as BPA. More specifically, the barrier resistance provided by the skin $(1/K_p)$ is defined by the resistances of both the stratum corneum (SC) and viable tissue (vt) (eq. 7) (Potts and Guy 1992; Cleek and Bunge 1993):

$$\frac{1}{K_p} = \frac{1}{K_{sc}} + \frac{1}{K_{vt}} \quad \text{(eq. 7)}$$

$$K_{sc} = K_{scv}\frac{D_{sc}}{L_{sc}} \text{ and } K_{vt} = K_{vtv}\frac{D_{vt}}{L_{vt}} \quad \text{(eq. 8)}$$

where K_{sc} and K_{vt} are the permeability coefficients, K_{scv} and K_{vtv} are the partition coefficients with the vehicle, D_{sc} and D_{vtv} are the diffusion coefficients, and L_{sc} and L_{vt} are the pathlengths in the SC and vt, respectively. As the diffusion through the viable tissue is in general much larger than through the stratum corneum, often the permeability across the skin is almost equal to the permeability of the stratum corneum alone $(1/K_p \approx 1/K_{SC})$ (Cleek and Bunge 1993). However, the contribution of the viable tissue to the overall resistance to permeation may not be negligible for lipophilic substances, such as BPA. This explains why increasing the viable tissue thickness led to an increased barrier resistance to BPA permeation, hence a lower K_p. Our results showed also that K_p decreased, but not significantly, with increasing skin thickness from 400 to 800 μm. This is not easily explained, and it seems to contradict the above discussion. The limited number of skin samples and skin donors for the 400 μm (n = 3, N = 1) versus the 800 μm skin thickness experiments (n = 10, N = 3) could be a source of error for the statistical analysis. However, similar results were obtained when comparing J through skin with different thicknesses from the same donor (data not shown). Also, we did not determine BPA retention in the skin, which could be influenced by the differences in skin thickness. Overall, these findings suggest that there is a complex relationship existing between lipophilicity, skin thickness, and skin permeation.

3.4 Limitations and futures perspectives

Several limitations are acknowledged in this study, and are thoroughly discussed in each annex. Here the main limitations and future perspectives are discussed. We developed an analytical method to quantify the skin metabolism of BPA, but not of BPS, D-8 and PF201, which still has yet to be developed. Consequently, we could not assess metabolism of BPS, D-8 and PF201 when viable skin was used. Data on D-8 and PF201 metabolism do not exist, while BPS metabolism in humans is mainly phase II conjugation. We deemed conjugation by the skin negligible as observed for BPA, which has recently been supported for BPS (Champmartin et al. 2020). Thus, we

did not add a deconjugation step. Our method could be further developed to include metabolites for all colour developers, once data on D-8 and PF201 metabolism become available. Also, our analytical method was developed for a matrix, i.e. saline that had been in contact with human dermis, but its applicability could potentially be widened to urine samples of human biomonitoring studies.

Mass balance assays included two tape strips, which were not analysed. Omitting permeants content in tape strips leads to underestimating the unabsorbed dose (also called dislodgeable dose in Annex II, as per OECD (2004a) definitions). Skin extraction recoveries were not assessed. However, the BPA amount extracted from skin was in line with data reported in the literature. This suggests that the method used for skin extraction was efficient. Saline was used as the receptor fluid in the experiments where skin metabolism was studied, instead of a cell culture medium. As explained in the introduction (1.9 In vitro skin absorption assays, paragraph on Receptor fluid), the OECD (2004a) recommends cell culture media to assess skin metabolism. In our study, we preferred using a simpler matrix (saline) because our test substances were not radiolabelled and were quantified by LC-MSMS. However, we used freshly excised human skin directly from the hospital surgery unit, and our experiments started no more than two hours from the plastic surgery.

Finally, colour developers are present as a powder in thermal paper, but we applied them on the skin as aqueous solutions. Water on skin causes vehicle-skin effects, such as an excessive skin hydration, which leads to greater skin permeation (Moss, Gullick, and Wilkinson 2015). Solids are often applied on skin in small amounts of acetone to overcome this issue, because acetone quickly evaporates leaving the powder more or less homogenously distributed across the skin surface. However, acetone increases skin permeability (Robert J. Scheuplein and Ross 1974). Therefore, we applied all four colour developers in aqueous solution, as other published studies. Consequently, we could compare our results with other existing studies on BPA skin absorption with aqueous donor solutions. The 100 and 1000 μl/cm² applied test solution experiments were likely to overestimate colour developers skin absorption for a dry (normal) skin scenario, but could simulate an exposure scenario of sweaty or moistened hands.

3.5 Conclusions

We showed that different experimental conditions led to significant variations of skin absorption results. This explained the inconsistencies in published BPA skin absorption results that has hampered their interpretation. We provide skin absorption kinetics for D-8, BPS, and PF201, and they were in decreasing order: BPA > D-8 >> BPS > PF201. Thus, BPS skin exposures would lead to lower internal doses compared to BPA and D-8. Dose

estimates are a necessary step in risk assessment, and help regulators evaluate public health risks associated with these colour developers. Future studies should (1) include the administration of colour developers in the solid state on the skin to better represent exposures from thermal papers, (2) determine possible skin metabolism of BPA alternatives, and (3) assess PF201 stability, as some of its degradation products could be available for skin absorption.

References

Ackermann, C., Flynn, G.L., Smith, W.M., 1987. Ether-water partitioning and permeability through nude mouse skin in vitro. II. Hydrocortisone 21-n-alkyl esters, alkanols and hydrophilic compounds. Int. J. Pharm. 36, 67–71. https://doi.org/10.1016/0378-5173(87)90238-9

Alabi, A., Caballero-Casero, N., Rubio, S., 2014. Quick and simple sample treatment for multiresidue analysis of bisphenols, bisphenol diglycidyl ethers and their derivatives in canned food prior to liquid chromatography and fluorescence detection. J. Chromatogr. A 1336, 23–33. https://doi.org/10.1016/j.chroma.2014.02.008

ANSES, 2013. Anses 2013 - Evaluation des risques du bisphenol A pour la sante humaine.

Ballesteros, O., Zafra, A., Navalón, A., Vílchez, J.L., 2006. Sensitive gas chromatographic–mass spectrometric method for the determination of phthalate esters, alkylphenols, bisphenol A and their chlorinated derivatives in wastewater samples. J. Chromatogr. A 1121, 154–162. https://doi.org/10.1016/j.chroma.2006.04.014

Barbero, A.M., Frasch, H.F., 2016. Effect of Frozen Human Epidermis Storage Duration and Cryoprotectant on Barrier Function Using Two Model Compounds. Skin Pharmacol. Physiol. 29, 31–40. https://doi.org/10.1159/000441038

Bernier, M.R., Vandenberg, L.N., 2017. Handling of thermal paper: Implications for dermal exposure to bisphenol A and its alternatives. PLOS ONE 12, e0178449. https://doi.org/10.1371/journal.pone.0178449

Biedermann, S., Tschudin, P., Grob, K., 2010. Transfer of bisphenol A from thermal printer paper to the skin. Anal. Bioanal. Chem. 398, 571–576. https://doi.org/10.1007/s00216-010-3936-9

Björnsdotter, M.K., Jonker, W., Legradi, J., Kool, J., Ballesteros-Gómez, A., 2017. Bisphenol A alternatives in thermal paper from the Netherlands, Spain, Sweden and Norway. Screening and potential toxicity. Sci. Total Environ. 601–602, 210–221. https://doi.org/10.1016/j.scitotenv.2017.05.171

Bos, J.D., Meinardi, M.M., 2000. The 500 Dalton rule for the skin penetration of chemical compounds and drugs. Exp. Dermatol. 9, 165–169. https://doi.org/10.1034/j.1600-0625.2000.009003165.x

Braun, J.M., Kalkbrenner, A.E., Calafat, A.M., Bernert, J.T., Ye, X., Silva, M.J., Barr, D.B., Sathyanarayana, S., Lanphear, B.P., 2011. Variability and predictors of urinary bisphenol A concentrations during pregnancy. Environ. Health Perspect. 119, 131–137. https://doi.org/10.1289/ehp.1002366

Brotons, J.A., Olea-Serrano, M.F., Villalobos, M., Pedraza, V., Olea, N., 1995. Xenoestrogens released from lacquer coatings in food cans. Environ. Health Perspect. 103, 608–612.

Caballero-Casero, N., Lunar, L., Rubio, S., 2016. Analytical methods for the determination of mixtures of bisphenols and derivatives in human and environmental exposure sources and biological fluids. A review. Anal. Chim. Acta 908, 22–53. https://doi.org/10.1016/j.aca.2015.12.034

Calafat, A.M., Kuklenyik, Z., Reidy, J.A., Caudill, S.P., Ekong, J., Needham, L.L., 2005. Urinary concentrations of bisphenol A and 4-nonylphenol in a human reference population. Environ. Health Perspect. 113, 391–395.

Champmartin, C., Marquet, F., Chedik, L., Décret, M.-J., Aubertin, M., Ferrari, E., Grandclaude, M.-C., Cosnier, F., 2020. Human in vitro percutaneous absorption of bisphenol S and bisphenol A: A comparative study. Chemosphere 252, 126525. https://doi.org/10.1016/j.chemosphere.2020.126525

Chang, C.-M., Chou, C.-C., Lee, M.-R., 2005. Determining leaching of bisphenol A from plastic containers by solid-phase microextraction and gas chromatography–mass spectrometry. Anal. Chim. Acta 539, 41–47. https://doi.org/10.1016/j.aca.2005.03.051

Cleek, R.L., Bunge, A.L., 1993. A New Method for Estimating Dermal Absorption from Chemical Exposure. 1. General Approach. Pharm. Res. 10, 497–506. https://doi.org/10.1023/A:1018981515480

Colorado-Yohar, S., Castillo-González, A., Sanchez-Meca, J., Aparicio, M., Sánchez-Rodríguez, D., Salamanca-Fernández, E., Ardanaz, E., Amiano, P., Fernández, M., Mendiola, J., Navarro-Mateu, F., López, M., 2021. Concentrations of bisphenol-A in adults from the general population: A systematic review and meta-analysis. Sci. Total Environ. 775, 145755. https://doi.org/10.1016/j.scitotenv.2021.145755

Cunha, S.C., Inácio, T., Almada, M., Ferreira, R., Fernandes, J.O., 2020. Gas chromatography–mass spectrometry analysis of nine bisphenols in canned meat products and human risk estimation. Food Res. Int. 135, 109293. https://doi.org/10.1016/j.foodres.2020.109293

Danish EPA, 2014. Alternative technologies and substances to bisphenol A (BPA) in thermal paper receipts, Environmental Project. The Danish Environmental Protection Agency.

Demierre, A.-L., Peter, R., Oberli, A., Bourqui-Pittet, M., 2012. Dermal penetration of bisphenol A in human skin contributes marginally to total exposure. Toxicol. Lett. 213, 305–308. https://doi.org/10.1016/j.toxlet.2012.07.001

ECHA, 2019. Use of bisphenol A and its alternatives in thermal paper in the EU: 2018 update. European Chemicals Agency.

Eckardt, M., Simat, T.J., 2017. Bisphenol A and alternatives in thermal paper receipts - a German market analysis from 2015 to 2017. Chemosphere 186, 1016–1025. https://doi.org/10.1016/j.chemosphere.2017.08.037

EFSA, 2015. Scientific Opinion on the risks to public health related to the presence of bisphenol A (BPA) in foodstuffs. EFSA J. 13, 3978. https://doi.org/10.2903/j.efsa.2015.3978

Ehrlich, S., Calafat, A.M., Humblet, O., Smith, T., Hauser, R., 2014. Handling of Thermal Receipts as a Source of Exposure to Bisphenol A. JAMA 311, 859. https://doi.org/10.1001/jama.2013.283735

FDA, U.S.F. & D.A., 2018. Bioanalytical Method Validation Guidance for Industry. Guidance document 44.

Flynn, G.L., 1990. Physicochemical determinants of skin absorption. in: Principles of Route to Route Extrapolation for Risk Assessment. Gerrity TR, Henry CJ, p. pp 93-127.

Flynn, G.L., 1985. Mechanism of percutaneous absorption from physicochemical evidence. in: Percutaneous Absorption. Mechanisms, Methodology, Drug Delivery. R.L. Bronaugh and H.I. Maibach, New York, pp. 17–42.

Franz, T.J., 1983. Kinetics of Cutaneous Drug Penetration. Int. J. Dermatol. 22, 499–505. https://doi.org/10.1111/j.1365-4362.1983.tb02187.x

Frederiksen, H., Nielsen, O., Koch, H.M., Skakkebaek, N.E., Juul, A., Jørgensen, N., Andersson, A.-M., 2020. Changes in urinary excretion of phthalates, phthalate substitutes, bisphenols and other polychlorinated and phenolic substances in young Danish men; 2009–2017. Int. J. Hyg. Environ. Health 223, 93–105. https://doi.org/10.1016/j.ijheh.2019.10.002

Gallart-Ayala, H., Moyano, E., Galceran, M.T., 2010. On-line solid phase extraction fast liquid chromatography–tandem mass spectrometry for the analysis of bisphenol A and its chlorinated derivatives in water samples. J. Chromatogr. A 1217, 3511–3518. https://doi.org/10.1016/j.chroma.2010.03.028

Gallo, P., Di Marco Pisciottano, I., Esposito, F., Fasano, E., Scognamiglio, G., Mita, G.D., Cirillo, T., 2017. Determination of BPA, BPB, BPF, BADGE and BFDGE in canned energy drinks by molecularly imprinted polymer cleaning up and UPLC with fluorescence detection. Food Chem. 220, 406–412. https://doi.org/10.1016/j.foodchem.2016.10.005

García-Prieto, A., Lunar, M.L., Rubio, S., Pérez-Bendito, D., 2008. Determination of urinary bisphenol A by coacervative microextraction and liquid chromatography–fluorescence detection. Anal. Chim. Acta 630, 19–27. https://doi.org/10.1016/j.aca.2008.09.060

Gayrard, V., Lacroix, M.Z., Grandin, F.C., Collet, S.H., Mila, H., Viguié, C., Gély, C.A., Rabozzi, B., Bouchard, M., Léandri, R., Toutain, P.-L., Picard-Hagen, N., 2019. Oral Systemic Bioavailability of Bisphenol A and Bisphenol S in Pigs. Environ. Health Perspect. 127, 77005. https://doi.org/10.1289/EHP4599

Geens, T., Aerts, D., Berthot, C., Bourguignon, J.-P., Goeyens, L., Lecomte, P., Maghuin-Rogister, G., Pironnet, A.-M., Pussemier, L., Scippo, M.-L., Van Loco, J., Covaci, A., 2012. A review of dietary and non-dietary exposure to bisphenol-A. Food Chem. Toxicol. Int. J. Publ. Br. Ind. Biol. Res. Assoc. 50, 3725–3740. https://doi.org/10.1016/j.fct.2012.07.059

Ghayda, R.A., Williams, P.L., Chavarro, J.E., Ford, J.B., Souter, I., Calafat, A.M., Hauser, R., Mínguez-Alarcón, L., 2019. Urinary bisphenol S concentrations: Potential predictors of and associations with semen quality parameters among men attending a fertility center. Environ. Int. 131, 105050. https://doi.org/10.1016/j.envint.2019.105050

Goldinger, D.M., Demierre, A.-L., Zoller, O., Rupp, H., Reinhard, H., Magnin, R., Becker, T.W., Bourqui-Pittet, M., 2015. Endocrine activity of alternatives to BPA found in thermal paper in Switzerland. Regul. Toxicol. Pharmacol. 71, 453–462. https://doi.org/10.1016/j.yrtph.2015.01.002

Gundert-Remy, U., Mielke, H., Bernauer, U., 2013. Commentary: Dermal penetration of bisphenol A—Consequences for risk assessment. Toxicol. Lett. 217, 159–161. https://doi.org/10.1016/j.toxlet.2012.12.009

Guy, R.H., Potts, R.O., 1993. Penetration of industrial chemicals across the skin: a predictive model. Am. J. Ind. Med. 23, 711–719. https://doi.org/10.1002/ajim.4700230505

Hazel, G.-C., 2016. Novel (Trans)dermal Drug Delivery Strategies: Micro- and Nano-scale Assessments. Springer.

Heinälä, M., Ylinen, K., Tuomi, T., Santonen, T., Porras, S.P., 2017. Assessment of Occupational Exposure to Bisphenol A in Five Different Production Companies in Finland. Ann. Work Expo. Health 61, 44–55. https://doi.org/10.1093/annweh/wxw006

Hines, C.J., Jackson, M.V., Deddens, J.A., Clark, J.C., Ye, X., Christianson, A.L., Meadows, J.W., Calafat, A.M., 2017. Urinary Bisphenol A (BPA) Concentrations among Workers in Industries that Manufacture and Use BPA in the USA. Ann. Work Expo. Health 61, 164–182. https://doi.org/10.1093/annweh/wxw021

Hopf, N.B., Champmartin, C., Schenk, L., Berthet, A., Chedik, L., Du Plessis, J.L., Franken, A., Frasch, F., Gaskin, S., Johanson, G., Julander, A., Kasting, G., Kilo, S., Larese Filon, F., Marquet, F., Midander, K., Reale, E., Bunge, A.L., 2020. Reflections on the OECD guidelines for in vitro skin absorption studies. Regul. Toxicol. Pharmacol. 117, 104752. https://doi.org/10.1016/j.yrtph.2020.104752

Hormann, A.M., Saal, F.S. vom, Nagel, S.C., Stahlhut, R.W., Moyer, C.L., Ellersieck, M.R., Welshons, W.V., Toutain, P.-L., Taylor, J.A., 2014. Holding Thermal Receipt Paper and Eating Food after Using Hand

Sanitizer Results in High Serum Bioactive and Urine Total Levels of Bisphenol A (BPA). PLOS ONE 9, e110509. https://doi.org/10.1371/journal.pone.0110509

Kaddar, N., Harthé, C., Déchaud, H., Mappus, E., Pugeat, M., 2008. Cutaneous Penetration of Bisphenol A in Pig Skin. J. Toxicol. Environ. Health A 71, 471–473. https://doi.org/10.1080/15287390801906824

Kazemi, S., Bahramifar, N., Moghadamnia, A.A., Jorsarae, S.G.A., 2016. Detection of Bisphenol A and Nonylphenol in Rat's Blood Serum, Tissue and Impact on Reproductive System. Electron. Physician 8, 2772–2780. https://doi.org/10.19082/2772

Khmiri, I., Côté, J., Mantha, M., Khemiri, R., Lacroix, M., Gely, C., Toutain, P.-L., Picard-Hagen, N., Gayrard, V., Bouchard, M., 2020. Toxicokinetics of bisphenol-S and its glucuronide in plasma and urine following oral and dermal exposure in volunteers for the interpretation of biomonitoring data. Environ. Int. 138, 105644. https://doi.org/10.1016/j.envint.2020.105644

Kubwabo, C., Kosarac, I., Stewart, B., Gauthier, B.R., Lalonde, K., Lalonde, P.J., 2009. Migration of bisphenol A from plastic baby bottles, baby bottle liners and reusable polycarbonate drinking bottles. Food Addit. Contam. Part Chem. Anal. Control Expo. Risk Assess. 26, 928–937. https://doi.org/10.1080/02652030802706725

Laganà, A., Bacaloni, A., De Leva, I., Faberi, A., Fago, G., Marino, A., 2004. Analytical methodologies for determining the occurrence of endocrine disrupting chemicals in sewage treatment plants and natural waters. Anal. Chim. Acta 501, 79–88. https://doi.org/10.1016/j.aca.2003.09.020

Lassen, C., Mikkelsen, S.H., Brandt, U.K., 2011. Migration of bisphenol A from cash register receipts and baby dummies (No. 110 2011), Survey of Chemical Substances in Consumer Products. Danish Environmental Protection Agency.

Lehmler, H.-J., Liu, B., Gadogbe, M., Bao, W., 2018. Exposure to Bisphenol A, Bisphenol F, and Bisphenol S in U.S. Adults and Children: The National Health and Nutrition Examination Survey 2013-2014. ACS Omega 3, 6523–6532. https://doi.org/10.1021/acsomega.8b00824

Li, Q., Wang, X., Yuan, D., 2009. Preparation of solid-phase microextraction fiber coated with single-walled carbon nanotubes by electrophoretic deposition and its application in extracting phenols from aqueous samples. J. Chromatogr. A 1216, 1305–1311. https://doi.org/10.1016/j.chroma.2008.12.082

Liu, J., Martin, J.W., 2019. Comparison of Bisphenol A and Bisphenol S Percutaneous Absorption and Biotransformation. Environ. Health Perspect. 127, 67008. https://doi.org/10.1289/EHP5044

Liu, J., Martin, J.W., 2017. Prolonged Exposure to Bisphenol A from Single Dermal Contact Events. Environ. Sci. Technol. 51, 9940–9949. https://doi.org/10.1021/acs.est.7b03093

Mao, L., Sun, C., Zhang, H., Li, Y., Wu, D., 2004. Determination of environmental estrogens in human urine by high performance liquid chromatography after fluorescent derivatization with p-nitrobenzoyl chloride. Anal. Chim. Acta 522, 241–246. https://doi.org/10.1016/j.aca.2004.04.071

Marquet, F., Payan, J.-P., Beydon, D., Wathier, L., Grandclaude, M.-C., Ferrari, E., 2011. In vivo and ex vivo percutaneous absorption of [14C]-bisphenol A in rats: a possible extrapolation to human absorption? Arch. Toxicol. 85, 1035–1043. https://doi.org/10.1007/s00204-011-0651-z

Matthews, J.B., Twomey, K., Zacharewski, T.R., 2001. In vitro and in vivo interactions of bisphenol A and its metabolite, bisphenol A glucuronide, with estrogen receptors alpha and beta. Chem. Res. Toxicol. 14, 149–157. https://doi.org/10.1021/tx0001833

Matuszewski, B.K., Constanzer, M.L., Chavez-Eng, C.M., 2003. Strategies for the assessment of matrix effect in quantitative bioanalytical methods based on HPLC-MS/MS. Anal. Chem. 75, 3019–3030.

Merchant and Research Consulting, 2013. World BPA Production Grew by Over 372,000 Tonnes in 2012 | Merchant Research & Consulting, Ltd. [WWW Document]. URL https://mcgroup.co.uk/news/20131108/bpa-production-grew-372000-tonnes.html (accessed 12.9.20).

Mitani, K., Narimatsu, S., Izushi, F., Kataoka, H., 2003. Simple and rapid analysis of endocrine disruptors in liquid medicines and intravenous injection solutions by automated in-tube solid-phase microextraction/high performance liquid chromatography. J. Pharm. Biomed. Anal. 32, 469–478. https://doi.org/10.1016/S0731-7085(03)00221-8

Mol, H.G., Sunarto, S., Steijger, O.M., 2000. Determination of endocrine disruptors in water after derivatization with N-methyl-N-(tert.-butyldimethyltrifluoroacetamide) using gas chromatography with mass spectrometric detection. J. Chromatogr. A 879, 97–112.

Mørck, T.J., Sorda, G., Bechi, N., Rasmussen, B.S., Nielsen, J.B., Ietta, F., Rytting, E., Mathiesen, L., Paulesu, L., Knudsen, L.E., 2010. Placental transport and in vitro effects of Bisphenol A. Reprod. Toxicol. 30, 131–137. https://doi.org/10.1016/j.reprotox.2010.02.007

Moss, G., Gullick, D., Wilkinson, S., 2015. Predictive Methods in Percutaneous Absorption. Springer-Verlag, Berlin Heidelberg. https://doi.org/10.1007/978-3-662-47371-9

Ndaw, S., Remy, A., Denis, F., Marsan, P., Jargot, D., Robert, A., 2018. Occupational exposure of cashiers to bisphenol S via thermal paper. Toxicol. Lett. 298, 106–111. https://doi.org/10.1016/j.toxlet.2018.05.026

Ndaw, S., Remy, A., Jargot, D., Robert, A., 2016. Occupational exposure of cashiers to Bisphenol A via thermal paper: urinary biomonitoring study. Int. Arch. Occup. Environ. Health 89, 935–946. https://doi.org/10.1007/s00420-016-1132-8

Nielsen, J.B., Plasencia, I., Sørensen, J.A., Bagatolli, L.A., 2011. Storage conditions of skin affect tissue structure and subsequent in vitro percutaneous penetration. Skin Pharmacol. Physiol. 24, 93–102. https://doi.org/10.1159/000322304

OECD, 2011. Organisation for Economic Co-operation and Development, Series on Testing and Assessment Nº. 156, Guidance Notes on Dermal Absorption.

OECD, 2004a. Organisation for Economic Co-operation and Development, Guidelines for the testing of chemicals, Section 4, Test Nº 428: Skin absorption: In Vitro Method.

OECD, 2004b. Organisation for Economic Co-operation and Development, Series on Testing and Assessment Nº 28, Guidance Document for the Conduct of Skin Absorption Studies. OECD. https://doi.org/10.1787/9789264078796-en

OECD, 2004c. Organisation for Economic Co-operation and Development, Guidelines for the testing of chemicals, Section 4, Test No. 427: Skin Absorption: In Vivo Method. OECD Publishing.

Oh, J., Choi, J.W., Ahn, Y.-A., Kim, S., 2018. Pharmacokinetics of bisphenol S in humans after single oral administration. Environ. Int. 112, 127–133. https://doi.org/10.1016/j.envint.2017.11.020

Penalver, A., Pocurull, E., Borrull, F., Marcé, R.M., 2002. Method based on solid-phase microextraction–high-performance liquid chromatography with UV and electrochemical detection to determine estrogenic compounds in water samples. J. Chromatogr. A 964, 153–160.

Pottenger, L.H., Domoradzki, J.Y., Markham, D.A., Hansen, S.C., Cagen, S.Z., Waechter, J.M., 2000. The Relative Bioavailability and Metabolism of Bisphenol A in Rats Is Dependent upon the Route of Administration. Toxicol. Sci. 54, 3–18. https://doi.org/10.1093/toxsci/54.1.3

Potts, R.O., Guy, R.H., 1992. Predicting Skin Permeability. Pharm. Res. 9, 663–669. https://doi.org/10.1023/A:1015810312465

Reale, E., Vernez, D., Hopf, N.B., 2020. Skin Absorption of Bisphenol A and Its Alternatives in Thermal Paper. Ann. Work Expo. Health. https://doi.org/10.1093/annweh/wxaa095

Roberts, M.S., Anderson, R.A., Swarbrick, J., 1977. Permeability of human epidermis to phenolic compounds. J. Pharm. Pharmacol. 29, 677–683. https://doi.org/10.1111/j.2042-7158.1977.tb11434.x

Rocha, B.A., Azevedo, L.F., Gallimberti, M., Campiglia, A.D., Jr, F.B., 2015. High Levels of Bisphenol A and Bisphenol S in Brazilian Thermal Paper Receipts and Estimation of Daily Exposure. J. Toxicol. Environ. Health A 0, 1–8. https://doi.org/10.1080/15287394.2015.1083519

Rodriguez-Mozaz, S., López de Alda, M.J., Barceló, D., 2004. Monitoring of estrogens, pesticides and bisphenol A in natural waters and drinking water treatment plants by solid-phase extraction–liquid chromatography–mass spectrometry. J. Chromatogr. A 1045, 85–92. https://doi.org/10.1016/j.chroma.2004.06.040

Rubin, B.S., 2011. Bisphenol A: an endocrine disruptor with widespread exposure and multiple effects. J. Steroid Biochem. Mol. Biol. 127, 27–34. https://doi.org/10.1016/j.jsbmb.2011.05.002

Russo, G., Barbato, F., Cardone, E., Fattore, M., Albrizio, S., Grumetto, L., 2018. Bisphenol A and Bisphenol S release in milk under household conditions from baby bottles marketed in Italy. J. Environ. Sci. Health B 53, 116–120. https://doi.org/10.1080/03601234.2017.1388662

Sahle, F.F., Gebre-Mariam, T., Dobner, B., Wohlrab, J., Neubert, R.H.H., 2015. Skin Diseases Associated with the Depletion of Stratum Corneum Lipids and Stratum Corneum Lipid Substitution Therapy. Skin Pharmacol. Physiol. 28, 42–55. https://doi.org/10.1159/000360009

Sánchez-Avila, J., Bonet, J., Velasco, G., Lacorte, S., 2009. Determination and occurrence of phthalates, alkylphenols, bisphenol A, PBDEs, PCBs and PAHs in an industrial sewage grid discharging to a Municipal Wastewater Treatment Plant. Sci. Total Environ. 407, 4157–4167. https://doi.org/10.1016/j.scitotenv.2009.03.016

Scheuplein, R.J., Blank, I.H., 1971. Permeability of the skin. Physiol. Rev. 51, 702–747. https://doi.org/10.1152/physrev.1971.51.4.702

Scheuplein, R.J., Ross, L.W., 1974. Mechanism of Percutaneous Absorption. V. Percutaneous Absorption of Solvent Deposited Solids. J. Invest. Dermatol. 62, 353–360. https://doi.org/10.1111/1523-1747.ep12701619

Selzer, D., Abdel-Mottaleb, M.M.A., Hahn, T., Schaefer, U.F., Neumann, D., 2013. Finite and infinite dosing: Difficulties in measurements, evaluations and predictions. Adv. Drug Deliv. Rev., Modeling the human skin barrier - Towards a better understanding of dermal absorption 65, 278–294. https://doi.org/10.1016/j.addr.2012.06.010

Skledar, D.G., Schmidt, J., Fic, A., Klopčič, I., Trontelj, J., Dolenc, M.S., Finel, M., Mašič, L.P., 2016. Influence of metabolism on endocrine activities of bisphenol S. Chemosphere 157, 152–159. https://doi.org/10.1016/j.chemosphere.2016.05.027

Sun, C., Leong, L.P., Barlow, P.J., Chan, S.H., Bloodworth, B.C., 2006. Single laboratory validation of a method for the determination of Bisphenol A, Bisphenol A diglycidyl ether and its derivatives in canned foods by reversed-phase liquid chromatography. J. Chromatogr. A 1129, 145–148. https://doi.org/10.1016/j.chroma.2006.08.018

Teeguarden, J.G., Twaddle, N.C., Churchwell, M.I., Yang, X., Fisher, J.W., Seryak, L.M., Doerge, D.R., 2015. 24-hour human urine and serum profiles of bisphenol A: Evidence against sublingual absorption following ingestion in soup. Toxicol. Appl. Pharmacol. 288, 131–142. https://doi.org/10.1016/j.taap.2015.01.009

Thayer, K.A., Doerge, D.R., Hunt, D., Schurman, S.H., Twaddle, N.C., Churchwell, M.I., Garantziotis, S., Kissling, G.E., Easterling, M.R., Bucher, J.R., Birnbaum, L.S., 2015. Pharmacokinetics of bisphenol A in humans following a single oral administration. Environ. Int. 83, 107–115. https://doi.org/10.1016/j.envint.2015.06.008

Thayer, K.A., Taylor, K.W., Garantziotis, S., Schurman, S.H., Kissling, G.E., Hunt, D., Herbert, B., Church, R., Jankowich, R., Churchwell, M.I., Scheri, R.C., Birnbaum, L.S., Bucher, J.R., 2016. Bisphenol A, Bisphenol S, and 4-Hydroxyphenyl 4-Isoprooxyphenylsulfone (BPSIP) in Urine and Blood of Cashiers. Environ. Health Perspect. 124, 437–444. https://doi.org/10.1289/ehp.1409427

Tominaga, T., Negishi, T., Hirooka, H., Miyachi, A., Inoue, A., Hayasaka, I., Yoshikawa, Y., 2006. Toxicokinetics of bisphenol A in rats, monkeys and chimpanzees by the LC–MS/MS method. Toxicology 226, 208–217. https://doi.org/10.1016/j.tox.2006.07.004

Toner, F., Allan, G., Dimond, S.S., Waechter, J.M., Beyer, D., 2018. In vitro percutaneous absorption and metabolism of Bisphenol A (BPA) through fresh human skin. Toxicol. Vitro Int. J. Publ. Assoc. BIBRA 47, 147–155. https://doi.org/10.1016/j.tiv.2017.11.002

Tuzimski, T., Szubartowski, S., Gadzała-Kopciuch, R., Miturski, A., Wójtowicz-Marzec, M., Kwaśniewski, W., Buszewski, B., 2020. Comparison of DAD and FLD Detection for Identification of Selected Bisphenols in Human Breast Milk Samples and Their Quantitative Analysis by LC-MS/MS. J. AOAC Int. 103, 1029–1042. https://doi.org/10.1093/jaoacint/qsaa027

US EPA, 2015a. Bisphenol A Alternatives in Thermal Paper (No. [Supercedes version dated January 2014]). United States Environmental Protection Agency.

US EPA, 2015b. Exposure Assessment Tools by Routes - Dermal [WWW Document]. US EPA. URL https://www.epa.gov/expobox/exposure-assessment-tools-routes-dermal (accessed 11.10.20).

van de Sandt, J.J.M., van Burgsteden, J.A., Cage, S., Carmichael, P.L., Dick, I., Kenyon, S., Korinth, G., Larese, F., Limasset, J.C., Maas, W.J.M., Montomoli, L., Nielsen, J.B., Payan, J.-P., Robinson, E., Sartorelli, P., Schaller, K.H., Wilkinson, S.C., Williams, F.M., 2004. In vitro predictions of skin absorption of caffeine, testosterone, and benzoic acid: a multi-centre comparison study. Regul. Toxicol. Pharmacol. 39, 271–281. https://doi.org/10.1016/j.yrtph.2004.02.004

van Es, D.S., 2014. Analysis of alternatives for BPA in thermal paper.pdf (No. Report 1515). Wageningen UR Food & Biobased Research, Wageningen.

Vandenberg, L.N., Chahoud, I., Heindel, J.J., Padmanabhan, V., Paumgartten, F.J.R., Schoenfelder, G., 2010. Urinary, Circulating, and Tissue Biomonitoring Studies Indicate Widespread Exposure to Bisphenol A. Environ. Health Perspect. 118, 1055–1070. https://doi.org/10.1289/ehp.0901716

Vandenberg, L.N., Gerona, R.R., Kannan, K., Taylor, J.A., van Breemen, R.B., Dickenson, C.A., Liao, C., Yuan, Y., Newbold, R.R., Padmanabhan, V., vom Saal, F.S., Woodruff, T.J., 2014. A round robin approach to the analysis of bisphenol a (BPA) in human blood samples. Environ. Health 13, 25. https://doi.org/10.1186/1476-069X-13-25

Vandenberg, L.N., Welshons, W.V., vom Saal, F.S., Toutain, P.-L., Myers, J.P., 2014. Should oral gavage be abandoned in toxicity testing of endocrine disruptors? Environ. Health 13, 46. https://doi.org/10.1186/1476-069X-13-46

Vervliet, P., Gys, C., Caballero-Casero, N., Covaci, A., 2019. Current-use of developers in thermal paper from 14 countries using liquid chromatography coupled to quadrupole time-of-flight mass spectrometry. Toxicology 416, 54–61. https://doi.org/10.1016/j.tox.2019.02.003

Völkel, W., Colnot, T., Csanády, G.A., Filser, J.G., Dekant, W., 2002. Metabolism and kinetics of bisphenol a in humans at low doses following oral administration. Chem. Res. Toxicol. 15, 1281–1287.

Waldman, J.M., Gavin, Q., Anderson, M., Hoover, S., Alvaran, J., Ip, H.S.S., Fenster, L., Wu, N.T., Krowech, G., Plummer, L., Israel, L., Das, R., She, J., 2016. Exposures to environmental phenols in Southern California firefighters and findings of elevated urinary benzophenone-3 levels. Environ. Int. 88, 281–287. https://doi.org/10.1016/j.envint.2015.11.014

Walters, K.A., 2002. Dermatological and Transdermal Formulations. CRC Press.

Wang, Q., Zhu, L., Chen, M., Ma, X., Wang, X., Xia, J., 2017. Simultaneously determination of bisphenol A and its alternatives in sediment by ultrasound-assisted and solid phase extractions followed by derivatization using GC-MS. Chemosphere 169, 709–715. https://doi.org/10.1016/j.chemosphere.2016.11.095

Wetherill, Y.B., Akingbemi, B.T., Kanno, J., McLachlan, J.A., Nadal, A., Sonnenschein, C., Watson, C.S., Zoeller, R.T., Belcher, S.M., 2007. In vitro molecular mechanisms of bisphenol A action. Reprod. Toxicol. Elmsford N 24, 178–198. https://doi.org/10.1016/j.reprotox.2007.05.010

WHO (Ed.), 2006. Dermal absorption, Environmental Health Criteria. World Health Organization, Geneva.

Wilhelm, K.-P., Zhai, H., Maibach, H.I., 2012. Dermatotoxicology, 8th ed. Informa Healthcare.

Wilkinson, S.C., Maas, W.J.M., Nielsen, J.B., Greaves, L.C., van de Sandt, J.J.M., Williams, F.M., 2006. Interactions of skin thickness and physicochemical properties of test compounds in percutaneous penetration studies. Int. Arch. Occup. Environ. Health 79, 405–413. https://doi.org/10.1007/s00420-005-0056-5

Xiao, Q., Li, Y., Ouyang, H., Xu, P., Wu, D., 2006. High-performance liquid chromatographic analysis of bisphenol A and 4-nonylphenol in serum, liver and testis tissues after oral administration to rats and its application to toxicokinetic study. J. Chromatogr. B 830, 322–329. https://doi.org/10.1016/j.jchromb.2005.11.024

Yamasaki, K., Noda, S., Imatanaka, N., Yakabe, Y., 2004. Comparative study of the uterotrophic potency of 14 chemicals in a uterotrophic assay and their receptor-binding affinity. Toxicol. Lett. 146, 111–120. https://doi.org/10.1016/j.toxlet.2003.07.003

Yang, Yunjia, Lu, L., Zhang, J., Yang, Yi, Wu, Y., Shao, B., 2014. Simultaneous determination of seven bisphenols in environmental water and solid samples by liquid chromatography–electrospray tandem mass spectrometry. J. Chromatogr. A 1328, 26–34. https://doi.org/10.1016/j.chroma.2013.12.074

Yang, Yunjia, Yang, Yi, Zhang, J., Shao, B., Yin, J., 2019. Assessment of bisphenol A alternatives in paper products from the Chinese market and their dermal exposure in the general population. Environ. Pollut. Barking Essex 1987 244, 238–246. https://doi.org/10.1016/j.envpol.2018.10.049

Ye, X., Kuklenyik, Z., Needham, L.L., Calafat, A.M., 2006. Measuring environmental phenols and chlorinated organic chemicals in breast milk using automated on-line column-switching–high performance liquid chromatography–isotope dilution tandem mass spectrometry. J. Chromatogr. B 831, 110–115. https://doi.org/10.1016/j.jchromb.2005.11.050

Ye, X., Kuklenyik, Z., Needham, L.L., Calafat, A.M., 2005. Quantification of urinary conjugates of bisphenol A, 2,5-dichlorophenol, and 2-hydroxy-4-methoxybenzophenone in humans by online solid phase extraction-high performance liquid chromatography-tandem mass spectrometry. Anal. Bioanal. Chem. 383, 638–644. https://doi.org/10.1007/s00216-005-0019-4

Ye, X., Zhou, X., Hennings, R., Kramer, J., Calafat, A.M., 2013. Potential external contamination with bisphenol A and other ubiquitous organic environmental chemicals during biomonitoring analysis: an elusive laboratory challenge. Environ. Health Perspect. 121, 283–286. https://doi.org/10.1289/ehp.1206093

Zalko, D., Jacques, C., Duplan, H., Bruel, S., Perdu, E., 2011. Viable skin efficiently absorbs and metabolizes bisphenol A. Chemosphere 82, 424–430. https://doi.org/10.1016/j.chemosphere.2010.09.058

Zarzycki, P.K., Włodarczyk, E., Baran, M.J., 2009. Determination of endocrine disrupting compounds using temperature-dependent inclusion chromatography. J. Chromatogr. A 1216, 7602–7611. https://doi.org/10.1016/j.chroma.2009.03.067

Zhang, Q., Grice, J.E., Wang, G., Roberts, M.S., 2009. Cutaneous metabolism in transdermal drug delivery. Curr. Drug Metab. 10, 227–235. https://doi.org/10.2174/138920009787846350

Zhao, J.-L., Ying, G.-G., Wang, L., Yang, J.-F., Yang, X.-B., Yang, L.-H., Li, X., 2009. Determination of phenolic endocrine disrupting chemicals and acidic pharmaceuticals in surface water of the Pearl Rivers in South China by gas chromatography–negative chemical ionization–mass spectrometry. Sci. Total Environ. 407, 962–974. https://doi.org/10.1016/j.scitotenv.2008.09.048

Zhou, X., Kramer, J.P., Calafat, A.M., Ye, X., 2014. Automated on-line column-switching high performance liquid chromatography isotope dilution tandem mass spectrometry method for the quantification of bisphenol A, bisphenol F, bisphenol S, and 11 other phenols in urine. J. Chromatogr. B 944, 152–156. https://doi.org/10.1016/j.jchromb.2013.11.009

Annex I

Simultaneous Quantification of Bisphenol A, Its Glucuronide Metabolite and Commercial Alternatives by LC-MS/MS for *In Vitro* Skin Absorption Evaluation

Elena Reale[a], Silvia Fustinoni[b,c], Rosa Mercadante[c], Elisa Polledri[c], Nancy B. Hopf[a,d]*

[a] Center for Primary Care and Public Health (Unisanté), University of Lausanne, Route de la Corniche 2, 1066 Epalinges, Switzerland. Elena.Reale@unisante.ch, Nancy.Hopf@unisante.ch

[b] Environmental and Industrial Toxicology Unit, Fondazione IRCCS Ca' Granda Ospedale Maggiore Policlinico, Via S. Barnaba 8, 20122 Milan, Italy. silvia.fustinoni@unimi.it

[c] EPIGET - Epidemiology, Epigenetics, and Toxicology Lab, Department of Clinical Sciences and Community Health, Università degli Studi di Milano, Via S. Barnaba 8, 20122 Milano, Italy. silvia.fustinoni@unimi.it, rosa.mercadante@unimi.it, elisa.polledri@unimi.it

[d] Swiss Centre for Applied Human Toxicology (SCAHT), Missionsstrasse 64, 4055 Basel, Switzerland

Abstract

Bisphenol A (BPA) is the most used color developer in thermal paper products such as cashiers' receipts, followed by Bisphenol S (BPS), Wincon 8 (D-8), and Pergafast 201 (PF201). These chemicals can migrate from the paper onto the skin and possibly be absorbed and metabolized. Until now, D-8 and PF201 have not been analyzed in biological matrices, nor has a method been developed to simultaneously quantify them even though they are often found as mixtures. Our aim was to develop and validate a method to quantify BPA, its glucuronide metabolite (BPA-G), BPS, D-8 and PF201 in *in vitro* skin absorption samples. After solid-phase extraction and reversed-phase chromatography, we quantified the substances in saline that had been in contact with human dermis for 24 h using a triple quadrupole mass detector equipped with an electrospray ionization source. We assessed the method in three *in vitro* skin absorption assays using *ex-vivo* human skin from one skin donor per test substance. The quantification ranges of our method were 0.2 - 200 µg/L for BPA and 0.2 - 20 µg/L for BPA-G, BPS, D-8, and PF201. Accuracies were within ±8% of nominal concentrations. Intra-day and total precisions (%RSD) were <10% for all analytes, except for BPA in low-concentration quality control solutions (low QCs) (12.2% and 15.5%, respectively). Overall, the process efficiency was 100-113% for all analytes, except BPS low and high QCs (80% and 71%, respectively) and BPA low QCs (134%). The absorbed dose ranged from 0.02% to 49% depending on the test substance, and was not determinable for PF201. This is the first analytical method to quantify simultaneously BPA, BPA-G, and BPA alternatives in saline from *in vitro* skin absorption samples.

1. Introduction

Bisphenol A (BPA) is a high production volume chemical and an endocrine disruptor[1–4]. It is mainly used in polycarbonate plastics and epoxy resins. Typical products are food containers, inside liners in canned food and cash register receipts. BPA is the color developer of the thermal papers[5–9] used for cash register receipts and can migrate from the paper onto the skin when handled[10]. Ndaw and co-workers[11,12] reported a significant increase in urinary total (free + conjugated) BPA and Bisphenol S (BPS) concentrations among cashiers handling thermal paper receipts.

Due to its endocrine-disruptive effects and possible skin exposures, BPA has been gradually replaced in thermal papers by alternative substances such as BPS, Wincon 8 (D-8), and Pergafast 201 (PF201).[8,13–16] BPS is a bisphenol, D-8 is a phenol, and PF201 is phenol-free (Table 1). Based on limited *in vitro* assays, BPS acts as a weak estrogen and its endocrine activity is less than that of BPA[15], D-8 acts as an estrogen antagonist[17], and PF201

does not have any estrogenic activity[18]. The U.S. EPA[18] assessed the human health hazards associated with BPA alternatives in thermal paper, and designated these as high concerns for repeated dose toxicity (BPS) and developmental toxicity (PF201).

Several studies have focused on assessing *in vitro* BPA skin absorption and metabolism.[19–23] BPA is metabolized to its glucuronide conjugate (BPA-G) in the skin.[23] BPA metabolism is important because BPA's conjugated metabolites lack estrogenic activity.[24] Comparably to BPA, BPS undergoes phase II metabolism[25,26] and the BPS-glucuronide does not activate hormone receptors.[26] To our knowledge, there are no studies on D-8 and PF201 metabolism. BPA can penetrate the skin and reach the systemic circulation. Only one study exists on BPS *in vitro* skin absorption,[27] and none for D-8 or PF201. Skin absorption data are necessary to assess cashiers' exposures to these substances from handling thermal papers. This will ultimately help in developing risk assessments and assessing health risks in populations with exposures to BPA, BPS, D-8, and PF201.

Skin absorption studies are generally performed either on animals or *in vitro*. A chemical's ability to permeate skin is measured in *in vitro* skin experiments, which consist of a donor and receptor chamber separated by the skin membrane. The chemical of interest is applied onto the skin in the donor chamber, and the chemical and/or its metabolites are quantified in the receptor fluid. A frequently used receptor fluid is saline (0.9% w/v NaCl). Extensive literature exists on the quantification of BPA and BPS in matrices such as urine, blood, tissues, maternal milk, food, drinks, and surface water.[12,25,28–32] BPA-G and other BPA conjugated metabolites are usually measured indirectly after enzymatic hydrolysis in urine by measuring the unconjugated BPA and expressed as total BPA (total - unconjugated = conjugated). Commercial BPA-G as well as labeled standards have become available. These have made it possible to directly quantify BPA-G in biological matrices.[33]

Solid-phase extraction (SPE) coupled with liquid chromatography-tandem mass spectrometry (LC-MS/MS) achieves the best sensitivity for quantification of BPA and its conjugated metabolites in biological matrices.[29–31,33–35] This is also true for BPS, D-8, and PF201 extracted in methanol from thermal paper.[13,15,36] Other analytical instruments have been used for bisphenols, such as high-performance liquid chromatography (HPLC) with fluorescence [20,37] or diode-array detection (DAD).[14,38,39] A few previously published articles described D-8 and PF201 analyses in methanol. The focus of these studies was to determine D-8 and PF201 concentration by direct extraction from thermal papers.[8,13–15,36] To our knowledge, no study has quantified BPA alternatives in liquid matrices similar to biological fluids. Furthermore, these color developer substances are often found as mixtures and analytical methods that could quantify them simultaneously would therefore be advantageous.

Our aims were first to develop a sensitive analytical chemical method to quantify simultaneously BPA, BPA-G, BPS, D-8, and PF201 in saline using LC-MS/MS, and then to validate this novel method with samples obtained from *in vitro* skin absorption experiments.
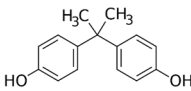
2. Experimental Procedures

2.1 Materials and Chemicals
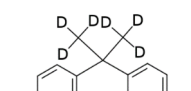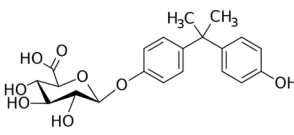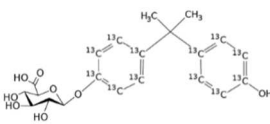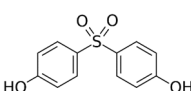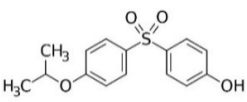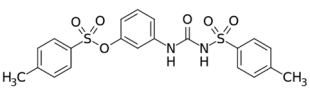
BPA, BPA-G, and BPS were purchased from Sigma-Aldrich Chemie GmbH, Buchs, Switzerland. D-8 and PF201 were bought from Santa Cruz Biotechnology, Heidelberg, Germany. Bisphenol A-D6 (BPA-[D_6]) and bisphenol A-$^{13}C_{12}$ β-D-glucuronide (BPA-G-[$^{13}C_{12}$]) were obtained from Toronto Research Chemicals, Toronto, ON, Canada. The CAS Registry Numbers, chemical structures, and molecular weights of the analytes and the internal standards used for quantification are shown in Table 1.

LC/MS-grade acetonitrile, methanol (MeOH), and water were obtained by Carlo Erba Reagents, Milan, Italy. Saline was prepared by dissolving 0.9% (w/v) sodium chloride (purissim. p.a. ≥ 99.5%, supplied by Sigma-Aldrich Chemie GmbH, Buchs, Switzerland) in Milli-Q water (Millipore, Milford, MA, USA). Ammonium hydroxide solution (NH4OH ≥ 25% in water, eluent additive for LC-MS) was supplied by Sigma-Aldrich Chemie GmbH, Buchs, Switzerland.

2.2 Standard Solutions

A stock solution (1 mg/mL) was prepared in LC-MS-grade MeOH for BPA, BPA-G, BPS, D-8, and PF201, as well as for the internal standards BPA-[D6] and BPA-G-[$^{13}C_{12}$]. Two intermediate solutions containing all five analytes at 200 µg/L and 2 µg/L were prepared by dilution of the stock solutions in saline. Six calibration standard solutions ranging from 0.02 to 200 µg/L were obtained by diluting intermediate solutions in saline. Quality control solutions (QCs) were prepared at 0.4 µg/L (low QC) and 10 µg/L (high QC) in saline. A mixed internal standard solution (ISS) containing BPA-[D_6] and BPA-G-[$^{13}C_{12}$] was prepared in saline (10 mg/L). Stock solutions of BPA, BPA-G, BPS and D-8 and intermediate solutions were stored at -20°C for up to 6 months. As PF201 was stable in water and unstable in MeOH, PF201 stock solution had to be freshly prepared when new intermediate solution was needed. Calibration standard solutions were freshly prepared from intermediate solutions on every analysis day.

Table 1. Chemical structures, molecular weights (MW), retention times, retention time variability (%RSD), collision energies, and multiple reaction monitoring (MRM) transitions for the detection and quantification of the different analytes.

Compound	Acronym	CAS nº	MW	Structure	Retention time (min)	%RSD retention time	MRM transitions[a]		Collision energy (eV)[a]
							Precursor ion	Product ion	
Bisphenol A	BPA	80-05-7	228.29		5.0	0.2	**227.1**	**212.4**	**16**
							227.1	133.1	23
Bisphenol A-d₆	BPA-d₆	86588-58-1	234.32		5.0	0.2	**233.1**	**138.1**	**27**
							233.1	93.1	31
Bisphenol A mono-β-D-glucuronide	BPA-G	267244-08-6	404.41		3.5	0.3	**403.7**	**228.1**	**26**
							403.7	113.1	15
Bisphenol A-¹³C₁₂ β-D-Glucuronide	BPA-G-¹³C₁₂	1313730-08-3	416.32		3.5	0.2	**415.2**	**239.1**	**26**
							415.2	113.1	15
Bisphenol S	BPS	80-09-1	250.27		0.5	1.7	**249.0**	**108.0**	**27**
							249.0	156.0	21
Wincon 8	D-8	95235-30-6	292.35		3.8	0.1	**291.0**	**248.0**	**21**
							291.0	184.0	29
Pergafast 201	PF201	232938-43-1	460.52		3.8	0.1	**459.2**	**170.0**	**19**
							459.2	106.0	41

[a] Data in bold are for quantifiers, other data are for qualifiers.

2.3 Solid-phase Extraction (SPE)

Calibration standard solutions, QC solutions, and samples (3 mL) were spiked with 15 µL of the ISS and then directly loaded onto SPE cartridges (Isolute C18 200 mg/6 mL; Biotage AB, Uppsala, Sweden). SPE cartridges were previously conditioned with 2 mL of MeOH , and equilibrated with 2mL of water. After washing (2 x 2 mL

water), the analytes were eluted (2 x 2 mL MeOH) through a polytetrafluoroethylene filter (PTFE, 0.45 μm, 4 mm diameter; BGB Analytik, Switzerland). Conditioning, equilibration, washing, and elution were carried out using a manifold system (Pressure+, Biotage AB, Uppsala, Sweden). The eluate was evaporated to dryness under a nitrogen stream, and the residue was dissolved in 300 μl of water.

2.4 LC-MS/MS

Calibration standard solutions, QC solutions or samples were injected (10 μl) in the LC system (UltiMate 3000 HPLC system, Thermo Fisher, Fisher Scientific, Reinach, Switzerland) equipped with a packed column (C18 column, 100 x 2.1 mm, 1.8 μm, Eclipse Plus, Zorbax, Agilent Technology, Basel, Switzerland) kept at 40°C. The mobile phase was a mixture of water and acetonitrile, each containing 5 mM of ammonium hydroxide, operating at a flow rate of 0.4 mL/min with the following gradient: 98% water (0.5 min); decreased to 50% water (1 min); 50% water (2 min); increased to 98% water (1 min), and 98% water (3 min).

A triple-quadrupole mass spectrometer (MS/MS) equipped with a heated electrospray ionization (H-ESI) source (TSQ Quantiva, Thermo Fisher, Fisher Scientific, Reinach, Switzerland) was used for detection. The MS conditions were optimized as follows: spray voltage, -3300 V; sheath gas, auxiliary gas, and sweep gas pressures of 25, 13, and 0 respectively (arbitrary units); ion transfer tube temperature, 298°C; and vaporizer temperature, 270°C. The MS/MS system was set on multiple reaction monitoring (MRM), with the H-ESI source in negative ion mode. Peak integration, MS quantitation, and data processing were carried out with Thermo Scientific Chromeleon 7.2 Chromatography Data System (CDS) software.

2.5 Sample quantification

Internal calibration with isotope-labelled internal standards was used for quantification. BPA-[D_6] was used as internal standard for BPA, while BPA-G-[$^{13}C_{12}$] was used as internal standard for BPA-G, BPS, D-8, and PF201. Calibration curves were obtained by analysing the calibration standard solutions in saline containing ISS. The calibration plot of standard/internal standard peak areas ratios (y) versus calibration standard nominal concentrations (x) was fitted by least-squares linear regression with a weighting factor of 1/x.

2.6 Method development

The following parameters were studied to SPE conditions: SPE cartridge types and sizes for maximum retention and minimum BPA contamination from cartridge plastics; BPA presence in the solvents used for analyses; wash and elution solvent volumes; and number of wash and elution steps to yield the maximum recovery. MS conditions,

MRM transitions, and collision energies were optimized combining autotuning and manual tuning of a 5 mg/L aqueous standard solution directly infused in the MS system without passing through the LC. LC conditions were optimized by testing several different columns as well as different mobile-phase solvents and gradients. The following LC columns were tested for method development were the Hypersil Gold PFP (50 x 2.1 mm, 3 µm, Thermo), Acquity UPLC HSS T3 (75 x 2.1 mm, 1.8 µm, Waters), Zorbax Eclipse Plus C18 (100 x 2.1 mm, 1.8 µm, Agilent), Zorbax Eclipse XDB-C8 (150 x 2.1 mm, 3 µm, Agilent), Hypersil Gold Phenyl (50 x 2.1 mm, 1.9 µm, Thermo), XBridge - RP18 (50 x 4.6 mm, 3.5 µm, Waters), Acquity BEH C18 (50 x 2.1 mm, 1.7 µm, Waters), Synergi Hydro RP (75 x 3 mm, 4 µm, Phenomenex), Synergi MAX – RP (75 x 3 mm, 4 µm, Phenomenex), Gemini-NX C18 (30 x 4.6 mm, 3 µm, Phenomenex), ODP2 HP-2D (150 x 2.0 mm, 5 µm, Shodex).

2.7 Method validation

Validation of the optimized method included five runs carried out on 5 days over a 2-week period. Four concentrations were prepared and quantified in triplicate in each run: the two lowest calibration standards (0.02 and 0.2 µg/L), and the low and high QC solutions. Calibration curves were generated and linearity assessed by means of their coefficient of determination (R^2). Slope variability was calculated as the standard deviation of five slopes expressed in % of the mean (coefficient of variation or relative standard deviation, %RSD). The lower limit of quantification (LLOQ) was defined as the lowest concentration on the calibration curve that could be quantified within 30 % of relative bias (% of nominal concentration) and precision (%RSD) during validation. Precision and accuracy were calculated for the low and high QC solutions. Acceptance threshold for accuracy and precision was 20%. Accuracy or relative bias was calculated as the percent ratio of the mean concentration to the nominal concentration. Precision was calculated as intra-day precision (repeatability) and intermediate precision. These were determined with an ANOVA-based variance decomposition, and they were expressed as %RSD. For intra-day precision, %RSD was calculated as the square root of the intra-day variance, divided by the mean of all results. [40] The intra-day variance (s_r^2) was calculated as the mean of the daily variances (eq. 1):

$$s_r^2 = \frac{\sum_{d=1}^{D}\sum_{r=1}^{n}(x_{dr} - \bar{x}_d)^2}{D\,(n-1)} \qquad (1)$$

where D is the total number of days, n is the number of replicates per day, x_{dr} is the result for replicate r on day d, an $\bar{x}_d$ is the average of all replicates on day d.

For intermediate precision, %RSD was calculated as the square root of the total variance s_R^2 divided by the mean of all results. The total variance s_R^2 was calculated as the sum of the intra-day variance s_r^2 and the between-day variance s_g^2 (eq. 2) [40]:

$$s_R^2 = s_r^2 + s_g^2 \ \ (\text{if } s_g^2 \geq 0) \qquad (2)$$

$$s_R^2 = s_r^2 \ \ (\text{if } s_g^2 < 0)$$

$$s_g^2 = \frac{\sum_{d=1}^{D}(\bar{x}_d - \bar{\bar{x}})^2}{D - 1} - \frac{s_r^2}{n}$$

where $\bar{\bar{x}}$ indicates the average of all results.

Matrix effect, extraction recovery, and process efficiency were evaluated using the method of Matuszewski and co-workers [41] for five replicates of low and high QC solutions. Matrix effect (ME%) was calculated as the percent peak area ratio of QC solutions where the analytes were spiked after the SPE and QC solutions prepared in neat reconstitution solvent (water). Extraction recovery (RE%) was calculated as the percent peak area ratio of QC solutions spiked before and after the SPE. Process efficiency (PE%) was calculated as the product of matrix effect and extraction recovery.

The use of pure saline as a surrogate matrix for the preparation of calibration standards and QCs was evaluated. Three different matrices, consisting of saline that had been in contact with three different dermis specimens for 24 h, were used to prepare three calibration curves. The mean slope of these calibration curves was compared with the mean slope of calibration curves (n=3) prepared in pure saline.

Specificity was assessed by verifying the absence of interfering peaks in five different blank samples. Blank samples were composed of saline that had been in contact with human dermis from five different skin donors for 24 h during skin absorption experiments (see 'Skin absorption experiments').

Carry-over is a systematic error that is derived from the analytes' signals from a preceding sample introduced into the next sample, and was assessed by injecting four blanks immediately following the 200 µg/L calibration standard. Carry-over was calculated as the mean percent ratio of the analytes' peak areas in each blank over the LLOQ peak area (n = 8).

The stability of analytes in aqueous solutions and in matrix was studied. All spiked aqueous and matrix solutions for stability testing were prepared in duplicates. For aqueous solutions, stability was assessed by comparing the area under the peak of a freshly prepared aqueous solution containing all analytes (5 mg/L) with that of stored solutions at varying temperatures and times. These solutions were diluted 100 times before they were injected in the LC system. For analytes in matrix, stability was assessed by comparing the concentration of a freshly prepared matrix solution containing all analytes (10 µg/L) with that of stored matrix solutions at varying temperatures and times.

2.8 Skin absorption experiments

Samples from skin absorption experiments were analyzed to test the efficiency of the developed LC-MS/MS method. Skin absorption and metabolism were measured *in vitro* using diffusion cells.[42] In each cell a human skin flap separates a donor chamber, where the tested chemical is applied, and a receptor fluid, into which the tested chemical migrates after diffusing through the skin. In our experiments we used flow-through diffusion cells (11.28 mm internal diameter, 1 cm^2 area, PermeGear, obtained from SES Analytical System, Bechenheim, Germany), and saline as receptor fluid. Saline was continuously stirred and pumped (50 µL/min; peristaltic pump from Ismatec IPC-N, IDEX Health and Science GmbH, Wertheim-Mondfeld, Germany) through the receptor chamber. Cells were kept at 32°C by a heated water-bath circulator (Haake SC 100 Digital Immersion Circulator, 100°C w/cla, Thermo Scientific, Newington, NH, USA). *Ex-vivo* full thickness human abdominal skin was obtained immediately following surgery from the Plastic and Reconstructive Surgery Department (DAL) at the Centre Hospitalier Universitaire Vaudois (CHUV, Lausanne, Switzerland) (ethical protocol 264/12). Skin was rinsed with saline and dermatomed (AcculanII, B. Braun/Aesculap, Sempach, Switzerland) to 800 µm thickness. The skin was then cut into circular sections and mounted onto the flow-through diffusion cells with the stratum corneum side facing up. After a 30-min stabilization period, the skin flaps were exposed to 100 µL of test solutions for 24 h. Test solutions of BPA, BPS, D-8 and PF201 were prepared in water (250 mg/L, 250 mg/L, 20 mg/L and 3 mg/L, respectively). Their concentrations were verified using the analytical method described here for saline except for three steps: the test solutions were not extracted (SPE), calibration standards were prepared in water, and external calibration was used for quantification. Each substance was tested in three *ex-vivo* human skin flaps (n=3) from one skin donor (N=1). Trans-epidermal water loss (TEWL) (VapoMeter wireless, Delfin Technologies Ltd., Kuopio, Finland) was tested after the 30-min stabilization period as well as at the end of each experiment to confirm skin integrity throughout the whole experiment. Skin flaps with a TEWL greater than 11 g/m^2/h were excluded.[43] Receptor fluid was sampled by a fraction collector (FC 204, Gilson Inc., Middleton, WI, USA) at several time intervals over 24 h. Receptor fluid samples were quantified using the developed analytical method. The analyte concentration was set at LLOQ/2 whenever the analysis resulted in a value below the lower limit of quantification (<LLOQ). If two out of the three skin flaps tested per substance at any time point give < LLOQ results, then the mean analyte concentration was set as < LLOQ at that time point.

3. Results

3.1 Analytical method development and validation

Analytical column, SPE, and solvents. The first HPLC columns tested for method development were the Thermo Hypersil Gold PFP, Waters Acquity UPLC HSS T3, and Agilent Zorbax Eclipse Plus C18. The best analyte separation, peak shapes, and peak intensities were observed with the Zorbax Eclipse Plus C18 column, but BPS was not retained (retention time (RT) = 0.6 min). Therefore, several other chromatographic columns were tested (see 'Method development'). BPS's RT was the longest using Agilent Zorbax Eclipse XDB-C8 (1.25 min) and Shodex ODP2 HP-2D (1.5 min) columns. However, the Zorbax Eclipse XDB-C8 column had lower peak intensities compared to other columns, and the Shodex ODP2 HP-2D led to considerably worse calibration linearity. Overall, the best performance was observed using the Zorbax Eclipse Plus C18 and the Acquity BEH C18, for which BPS's RT was 0.6 and 0.3 min, respectively. Therefore, the column selected for further method development and validation was the Zorbax Eclipse Plus C18.

Several adjustments were made to the solvents used as mobile phase and in their gradient. In the literature, BPA analysis in biological matrices by LC-MS/MS often used C18 columns and water:MeOH [25,44] or water:acetonitrile mobile phases.[12,29] Therefore, both options were studied. The presence of NaCl (0.9% w/v) produced a strong ion suppression for BPA and BPA-D_6 regardless of using water:MeOH or water:acetonitrile. Working in negative ion mode and adding ammonia in the mobile phases increased the sensitivity, as it enhanced the formation of the parent ion [M-H]⁻. However, sample preparation by SPE was still necessary to increase the sensitivity. For the Agilent Zorbax Eclipse Plus C18 water:acetonitrile with 5 mM ammonium hydroxide was the selected mobile phase that gave well-resolved and symmetrical peaks with stable retention times. Different gradients were tested, starting from 2% to 100% organic phase and gradually reducing the organic phase span and gradient times. The final gradient gave the best compromise between resolution and run time.

Solvents and other materials used for routine analysis, such as plastic pipet tips, SPE cartridges, and PTFE filters were tested for BPA contamination. All these materials showed BPA signals ranging from 1% to 16% of the LLOQ signal. Overall, BPA signal in blank solutions was 45% of LLOQ signal. For BPA-G, BPS, D-8 and PF201, the blank solutions' signals ranged between 4% and 7%.

MS quantifiers. Table 1 shows the multiple reaction monitoring (MRM) transitions used to quantify and confirm the analytes and internal standards, the collision energies needed to produce the desired product ions, and the retention times of their chromatographic peaks. The most abundant product ion was used as the quantifier (marked

in bold in the table), and the second most abundant product ion was used as the qualifier. The extracted ion chromatograms (XICs) of all five analytes are shown in Figure 1. Each chromatogram was obtained by registering the MRM transition of the molecular ion [M-H]$^-$ to produce the quantifier in blank solutions and in calibration standard solutions at the LLOQ (Figure 1).

Calibration curve and limits of quantification. Table 2 shows the calibration curve, accuracy, and precision. The lower limit of quantification (LLOQ) was 0.2 µg/L for all five analytes. The upper limit of quantification was 200 µg/L for BPA, and 20 µg/L for BPA-G, BPS, D-8, and PF201. Linearity was good with R2 ≥ 0.998 for all the analytes. Slope variability (%RSD$_{slope}$) was equal to or under 8.4 for all analytes except BPS, for which %RSD$_{slope}$ was 14.8.

Accuracy and Precision. Accuracy values were within ±8% of nominal concentration for low and high QCs of all analytes. Intra-day precision and intermediate precision were both under 10% for all analytes, except BPA low QC, where they reached respectively 12.2 % and 15.5 %.

Matrix Effect, Extraction Recovery and Process Efficiency. All results of the extraction recovery, matrix effect and overall process efficiency are listed in Table 3.

Justification of Surrogate Matrix. The slopes of the calibration curves prepared in matrix or in surrogate matrix differed by -5% for BPA, 4% for BPA-G, -16% for BPS, 8% for D-8, and 4% for PF201 (Table 4). The slope variability (%RSD$_{slope}$) of the calibration curves in matrix was 20%, 32%, 7%, 4% and 5% for BPA, BPA-G, BPS, D-8, and PF201, respectively.
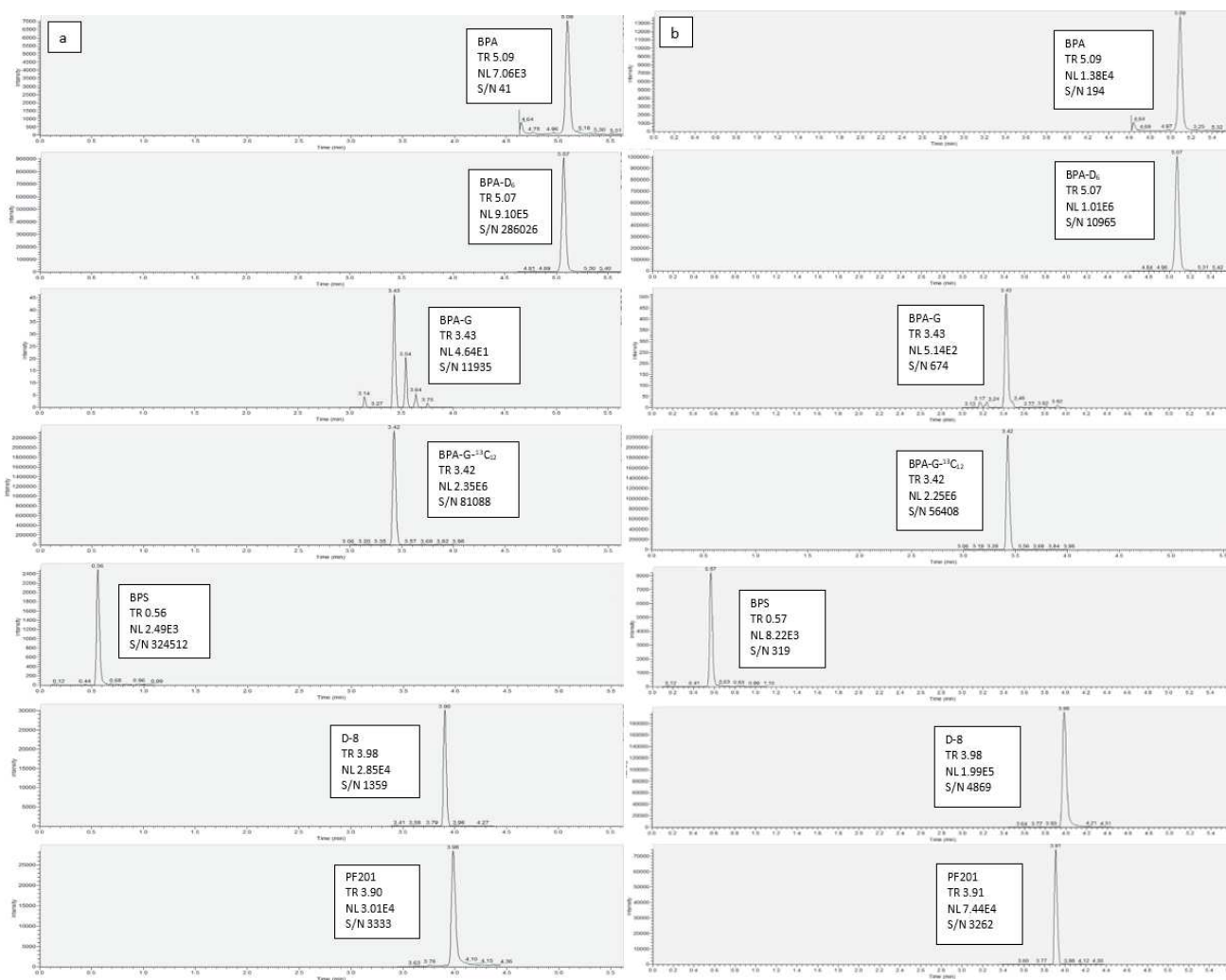
Figure 1. Extracted ion chromatograms (XICs) of BPA, BPA-D$_6$, BPA-G, BPA-G-^{13}C$_{12}$, BPS, D-8, and PF201 in blank solutions (a) and in calibration standard solutions at the LLOQ = 0.2 μg/L (b). TR = retention time, NL = normalization level, S/N = signal-to-noise ratio.

Table 2. Calibration curve data, including lower limit of quantification (LLOQ) and upper limit of quantification (ULOQ), and precision and accuracy of the analytical method for each investigated substance.

| | Calibration curve | | | | | | Accuracy (n = 15) | | | Precision (n = 3, 5 days)[c] | | | | | |
| | | | | | | | % of nominal concentration | | | Intra-day (%RSD) | | | Intermediate (%RSD) | | |
Analyte	Investigated range (µg/L)	LLOQ – ULOQ (µg/L)	Slope	Intercept	R²	%RSD slope	LLOQ (min – max)	QC low[a] (min – max)	QC high[b] (min – max)	LLOQ	QC low[a]	QC high[b]	LLOQ	QC low[a]	QC high[b]
BPA	0.02-200	0.2-200	2.011	0.3380	0.999	4.1	118 (96 –129)	108 (91 – 122)	100 (93 – 107)	16.3	12.2	2.9	17.5	15.5	6.4
BPA-G	0.02-200	0.2-20	0.158	0.0011	0.999	8.4	102 (89 – 120)	101 (90 – 104)	93 (89 – 98)	5.3	5.1	2.8	11.9	8.5	4.5
BPS	0.02-200	0.2-20	3.144	0.0668	0.999	14.8	100 (78 – 109)	101 (94 – 105)	106 (100 – 115)	8.2	8.8	9.4	14.3	8.8	9.9
D-8	0.02-200	0.2-20	25.137	0.2656	0.999	6.8	101 (98 – 102)	104 (103 – 105)	100 (97 – 103)	3.4	3.4	3.5	3.7	3.4	3.7
PF201	0.02-200	0.2-20	11.127	0.6087	0.998	5.5	94 (81 – 101)	102 (98 – 111)	104 (101 – 107)	6.2	7.5	7.2	10.1	7.9	7.2

[a] 0.4 µg/L
[b] 10 µg/L
[c] Precision is presented as intra-day and intermediate (intra + inter-day) percent relative standard deviation (%RSD).

Table 3. Matrix effect, extraction recovery, and overall process efficiency as defined by Matuszewski et al. [41]

Analyte	Nominal concentration (µg/L)	% Extraction recovery		% Matrix effect		% Process efficiency	
		without IS	with IS	without IS	with IS	without IS	with IS
BPA	0.4	84	107	180	125	151	134
	10	82	106	107	97	87	103
BPA-G	0.4	78	88	123	123	95	108
	10	71	83	137	136	98	113
BPS	0.4	100	114	70	70	70	80
	10	90	105	69	68	62	71
D-8	0.4	97	110	100	100	97	110
	10	91	107	98	97	90	103
PF201	0.4	89	101	101	101	90	102
	10	84	98	103	101	86	100

Table 4. Justification of the use of saline as surrogate matrix for the saline that has been in contact with human dermis up to 24h.

	Slope (± SD)		% Δ[a]
Analyte	Calibration in surrogate matrix	Calibration in matrix	% relative difference of the calibration curve slopes obtained in surrogate matrix and in the real matrix
BPA	4.427 (± 0.52)	4.646 (± 0.92)	-5
BPA-G	0.094 (± 0.03)	0.090 (± 0.03)	4
BPS	2.352 (± 0.65)	2.815 (± 0.20)	-16
D-8	48.48 (± 8.49)	44.97 (± 1.60)	8
PF201	24.27 (± 5.24)	23.37 (± 1.25)	4

[a] The difference (% Δ) in mean slope of calibration curves prepared in surrogate matrix vs. matrix is shown (n = 3).

Specificity. Monitoring two transitions per analyte by the MS/MS system provided high specificity. However, as shown in Figure 1, no interferences were detected in our experimental conditions.

Carry-over. The mean (n=8) carry-over for BPA was the ratio of the BPA peak area in the blank divided by the peak area of the LLOQ. The blank was the first injected blank, after the ULOQ. Mean carry-over for BPA was 42% of the LLOQ (0.083 µg/L). The second blank was 22% (0.044 µg/L), the third was 18% (0.037 µg/L), and the fourth was 17% (0.034 µg/L). Carry-over values in the first, second, third, and fourth blanks were respectively 4%, 3%, 3%, and 4% of the LLOQ (0.007-0.008 µg/L) for BPA-G; 1%, 1%, 1%, and 1% of the LLOQ (0.001 µg/L) for BPS; 132%, 20%, 14%, and 13% of the LLOQ (0.26, 0.041, 0.029, and 0.026 µg/L) for D-8; and 14%, 12%, 11%, and 11% of the LLOQ (0.023-0.027 µg/L) for PF201.

Stability. Stability tests showed that in aqueous solution all analytes were stable for at least 7 days at room temperature. All analytes except BPA-G were stable for at least 80 days at +4 °C (Table 5). In matrix, all analytes were stable for at least 1 day at room temperature, and at least 80 days at -20 °C. Stock solutions of BPA, BPA-G, BPS, and D-8 in MeOH were stable for up to 6 months (peak area variation ± 20%). PF201 stock solution's peak area was reduced by 90% upon storage at -20°C for 6 months.

Table 5. Stability of the analytes in different matrices.

Compound	Storage conditions								
	In H$_2$O					In matrix			
	T$_{room}$		+4°C			T$_{room}$	-20°C		
	24h	7 days	24h	7 days	80 days	24h	3 freeze/thaw cycles (24h)	7 days	80 days
BPA	103	107	113	99	100	93	115	75	98
BPA-G	102	108	111	115	81	82	90	88	110
BPS	109	105	104	110	100	109	117	88	93
D-8	100	111	113	116	101	113	111	98	101
PF201	93	116	103	127	102	95	97	97	90

3.2 Application of the developed method to skin absorption samples

Samples from preliminary skin absorption testing were analyzed to evaluate the analytical method's feasibility. The extracted ion chromatograms (XICs) of the analytes in our skin absorption samples are shown in Figure 2. Amounts of BPA, BPA-G, BPS, and D-8 over the LLOQ were quantified within the validated ranges (Table 6).

Figure 2. Extracted ion chromatograms (XICs) of BPA, BPA-G, BPS, D-8, and PF201 in a sample obtained from skin absorption experiments. TR = retention time, NL = normalization level, C = concentration.

Even though PF201 was quantified in a few samples, the overall value was < LLOQ, as two out of three repeats were <LLOQ. After 24 h of skin exposure to the test solutions, the total dose recovered in the receptor fluid was

48.6%, 0.02%, 0.08%, and 27.4% of the applied dose for BPA, BPA-G, BPS, and D-8, respectively, and was not determinable for PF201. Intra-skin absorption variability (%RSD) at the different time points ranged from 17% to 110% for BPA, 43% to 63% for BPA-G, 74% to 104% for BPS, and 9% to 66% for D-8.

Table 6. Dose recovered (% of applied dose) in receptor fluid of *in vitro* skin absorption assays sampled at different times points after the beginning of skin exposure.

Time (h)	% of applied dose (± SD)[a]									
	BPA		**BPA-G**		**BPS**		**D-8**		**PF201**	
0	0.005	± 0.001	n.d.		n.d.		n.d.		n.d.	
1	0.019	± 0.020	n.d.		n.d.		n.d.		n.d.	
2	0.427	± 0.383	n.d.		n.d.		n.d.		n.d.	
3	1.355	± 0.891	0.003	± 0.002	n.d.		0.331	± 0.220	n.d.	
4	2.427	± 1.306	0.004	± 0.002	n.d.		0.881	± 0.411	n.d.	
5	3.328	± 1.555	0.004	± 0.002	n.d.		1.789	± 1.141	n.d.	
6	3.946	± 1.712	0.003	± 0.002	n.d.		1.872	± 0.592	n.d.	
8	9.588	± 3.710	0.005	± 0.002	n.d.		5.131	± 1.820	n.d.	
10	9.406	± 2.999	n.d.		0.008	± 0.007	5.730	± 1.365	n.d.	
12	6.460	± 1.486	n.d.		0.010	± 0.010	4.179	± 0.776	n.d.	
14	4.236	± 0.923	n.d.		0.010	± 0.008	2.688	± 0.358	n.d.	
16	2.700	± 0.501	n.d.		0.011	± 0.009	1.650	± 0.155	n.d.	
18	1.805	± 0.350	n.d.		0.011	± 0.008	1.102	± 0.149	n.d.	
20	1.254	± 0.216	n.d.		0.010	± 0.008	0.821	± 0.117	n.d.	
22	0.923	± 0.166	n.d.		0.010	± 0.007	0.639	± 0.072	n.d.	
24	0.699	± 0.131	n.d.		0.009	± 0.006	0.523	± 0.075	n.d.	
Total	48.578	± 14.435	0.019	± 0.010	0.080	± 0.078	27.335	± 7.020	n.d.	

[a] Values are expressed as mean results ± SD (n=3). For BPA-G the dose recovered is expressed as % of BPA applied dose.
n.d. = not determinable because two or three out of three skin samples gave results of analyte concentration <LLOQ (LLOQ = 0.2 µg/L).

4. Discussion

We developed and validated a method for the simultaneous quantification of BPA, BPA-G, BPS, D-8, and PF201 in saline from *in vitro* skin absorption assays. Our results show that this method is selective, accurate and precise over wide concentration ranges, as well as applicable to samples from *in vitro* human skin absorption experiments.

Sample analysis without any pre-treatment was assessed. The presence of 0.9% NaCl in saline led to ion suppression and loss in sensitivity for all analytes over few analyses within the same run (data not shown). The

addition of a base, such as ammonia, in the mobile phase improved the analytes' ionization and increased H-ESI response. This effect has also been reported by Furey and co-workers[45] and Tan and coworkers.[46] However, a decrease of the peak areas was observed during the analytical run. This effect was overcome by sample pre-treatment with Solid-phase extraction (SPE).

Several SPE cartridges were tested for maximum analyte retention. As BPA is used in polycarbonate plastics, SPE cartridges were also tested for possible BPA presence and leakage from the plastic. Assay contamination by ubiquitous BPA has been reported to be an issue in some cases,[34,47,48] while well controlled in others.[49,50] In our studies, all cartridges had BPA concentrations below the LLOQ but still detectable. The smallest BPA peaks were detected using 6 mL cartridges. A possible explanation is that the higher capacity of 6 mL vs. 3 mL cartridges limited the contact area between the sample and the cartridge's plastic walls. Similar results were obtained using Water Oasis HLB 1 mL cartridge. The lowest BPA signals were detected using J.T. Baker Bakerbond SPE™ C18 and Biotage Isolute C18 cartridges. Isolute C18 cartridges were chosen for method development and routine analysis because they were optimal for our sample volume and were less expensive.

In method validation, the higher variability for BPA's low QC was likely due to the ubiquitous contamination of BPA. For all analytes, most of the variability derived from repeatability s^2_r, and not from the inter-day variance s^2_g. The differences in the slope of the calibration curves prepared in matrix or in surrogate matrix were not negligible, especially for BPS. They were deemed sufficiently low, however, to justify the use of saline as a surrogate matrix given the scarcity of human skin samples for skin absorption studies. The higher slope variability of BPS's calibration curves in surrogate matrix compared to the other analytes was likely due to the lack of BPS retention on the chromatographic column. Calibration slope variability higher than 5% indicates the presence of relative matrix effects [51]. The calibration slope variability in matrix was >5% for BPA, BPA-G, and BPS, while ≤5% for D-8 and PF201. This was in accordance with our matrix effect study results where no or little matrix effects were observed for D-8 and PF201. Extraction recoveries ranged between 98% and 101% for PF201 and between 107% and 110% for D-8. This resulted in a good overall process efficiency of 110 % and 103% for D-8 low and high QCs, and 102% and 100% for PF201. Less efficient was the analytical process for BPS (PE% = 80% and 71% for the low and high QCs, respectively). This was mostly due to the matrix effects, which were 70% for the low QC and 68% for the high QCs. The use of BPA-G-[$^{13}C_{12}$] as an internal standard for BPS was not able to correct for matrix effects. This was probably because of the difference in chemical structure and their retention times. Surprisingly, BPA-G-[$^{13}C_{12}$] was not able to correct for matrix effects for BPA-G either. This led to an ion enhancement of 123% and 136% for BPA-G low and high QCs respectively. BPA-G matrix effects were compensated by extraction recoveries ranging from 83% to 88%, which resulted in overall process efficiency of

108% for BPA-G low QC and 113% for BPA-G high QC. Recoveries using Biotage Isolute C18 cartridges ranged within ±10% of the nominal QC concentrations, except for BPS low QC (114%) and BPA-G high QC (83%), after optimizing the wash/eluent solvents and volume and correcting with the internal standard for all analytes. BPA isotope-labeled analogue BPA-[D$_6$] was able to compensate for BPA high-QCs' matrix effect (97%) and recovery (106%), leading to a high process efficiency (103%). BPA low-QCs were affected by a stronger matrix effect that the internal standard could partly correct (125%). Coupled with an extraction recovery of 107%, this led to a process efficiency of 134%. We hypothesize that the presence of ubiquitous BPA (in plastics and solvents) could be a cause of the high value observed in the matrix effect study, given the high BPA signal in blank solutions (45% of LLOQ signal for BPA, <7% of LLOQ signal for BPA-G, BPS, D-8, and PF201). This value could not justify the high matrix effect on the BPA low QCs, but indicated that BPA background contamination was still possible and could affect the results at low concentrations.

Commonly, guidelines on bioanalytical method validation[52,53] require that the analyte response in a carry-over blank is less than 20% of the LLOQ response. Therefore, three blanks should be injected for samples with BPA concentration >200 µg/L, while for D-8 at this concentration one blank is necessary. This concentration is 10 times higher than D-8's ULOQ. No carry-over blank injections are necessary for BPA-G, BPS, and PF201.

Our stability test results in aqueous solution and in matrix were similar to results obtained by Ye and co-workers.[54] They reported BPA-conjugated species in urine to be stable for at least 7 days at +4 °C, and for at least 180 days at -70°C. Our stability test results in MeOH confirm the high instability of PF201 in protic and slightly acidic solutions reported by Eckardt and Simat.[14]

Our method was applicable to *in vitro* skin absorption assays. The high intra-skin absorption variability was most likely due to the skin samples, i.e., due to possible slightly different skin thicknesses, skin elasticity, number of stretchmarks, and amount of hair. These skin permeation results are only preliminary, as they were obtained using skin samples from only one donor per test substance. Including additional skin donors is necessary to use these results for risk assessment. Even if only preliminary, our results suggest that BPA and D-8 had the highest skin absorption. This is in line with the octanol/water partition coefficient (log K$_{ow}$) of the test substances, which is a key parameter for the diffusion of chemicals through the stratum corneum [55]. BPA and D-8 are more lipophilic (log K$_{ow}$ = 3.3 and 3.4, respectively) than PF201 and BPS (log K$_{ow}$ = 1.2 and 2.6, respectively). Lipophilic substances with molecular weight < 500 Da can permeate the skin via the stratum corneum intercellular lipid lamellae. This is the most efficient diffusion route. PF201 has the highest molecular weight among the four test substances and the lowest log K ow. This could explain PF201's concentrations <LLOQ in most of our samples.

Skin metabolism is particularly important for chemicals with a high first-pass metabolism in the liver, e.g. BPA. After oral dosing in humans, 90% of the BPA dose undergoes first-pass metabolism and 10% of the dose enters the systemic circulation.[56] Our results show that BPA metabolism to BPA-G was negligible in *ex-vivo* human skin. These differences in metabolism between dermal and oral routes of exposures will likely result in higher bioavailability of BPA from dermal exposure despite the lower skin absorption compared to oral absorption.

A limitation of our study was that the analytical method was not developed to quantify the skin metabolism of BPS, D-8 and PF201. BPS metabolism in humans is known and is mainly phase II conjugation, as observed for BPA metabolism. We deemed conjugation by the skin negligible, which has recently been supported for BPS.[57] Thus, we did not add a deconjugation step. Our method could be further developed to include metabolites for all color developers, once data on D-8 and PF201 metabolism become available. Another limitation of our study was the higher acceptance criteria for LLOQ and QC solutions' accuracy and precision, compared to values recommended by guidelines on bioanalytical method validation. This was due to some critical points, namely the lower accuracy of BPA at low-QCs compared to BPA-G, BPS, D-8, and PF201, and the matrix effects on BPA and BPS. However, *in vitro* skin absorption experiments are characterized by a high variability due to inter-individual and intra-individual differences in the skin samples, which make our method fit for its intended purpose. Finally, this analytical method was developed for a matrix, i.e., saline that had been in contact with human dermis, but its applicability could potentially be widened to urine samples of human biomonitoring studies.

In summary, a sensitive LC-MS/MS method was developed and validated for the quantification of BPA, BPA-G and BPA alternatives used as color developers in thermal paper receipts. Our method was in line with guidelines of bioanalytical method validation [53] but with higher acceptance thresholds for LLOQ and QC accuracy and precision. Our method was robust for the analysis of samples from *in vitro* human skin absorption experiments, where the matrix was saline that had been in contact with human dermis for up to 24 h. In our preliminary *in vitro* assays, BPA and D-8 had the highest potential for human skin absorption, and BPA skin metabolism to BPA-G was negligible.

References

(1)   Chen, M.-Y.; Ike, M.; Fujita, M. Acute Toxicity, Mutagenicity, and Estrogenicity of Bisphenol-A and Other Bisphenols. *Environ. Toxicol.* **2002**, *17* (1), 80–86.

(2)   Fic, A.; Žegura, B.; Gramec, D.; Mašič, L. P. Estrogenic and Androgenic Activities of TBBA and TBMEPH, Metabolites of Novel Brominated Flame Retardants, and Selected Bisphenols, Using the XenoScreen XL YES/YAS Assay. *Chemosphere* **2014**, *112*, 362–369. https://doi.org/10.1016/j.chemosphere.2014.04.080.

(3)   Richter, C. A.; Birnbaum, L. S.; Farabollini, F.; Newbold, R. R.; Rubin, B. S.; Talsness, C. E.; Vandenbergh, J. G.; Walser-Kuntz, D. R.; vom Saal, F. S. In Vivo Effects of Bisphenol A in Laboratory Rodent Studies. *Reprod. Toxicol.* **2007**, *24* (2), 199–224. https://doi.org/10.1016/j.reprotox.2007.06.004.

(4)   Wetherill, Y. B.; Akingbemi, B. T.; Kanno, J.; McLachlan, J. A.; Nadal, A.; Sonnenschein, C.; Watson, C. S.; Zoeller, R. T.; Belcher, S. M. In Vitro Molecular Mechanisms of Bisphenol A Action. *Reprod. Toxicol.* **2007**, *24* (2), 178–198. https://doi.org/10.1016/j.reprotox.2007.05.010.

(5)   Liu, J.; Martin, J. W. Prolonged Exposure to Bisphenol A from Single Dermal Contact Events. *Environmental Science & Technology* **2017**, *51* (17), 9940–9949. https://doi.org/10.1021/acs.est.7b03093.

(6)   Mendum, T.; Stoler, E.; VanBenschoten, H.; Warner, J. C. Concentration of Bisphenol A in Thermal Paper. *Green Chemistry Letters and Reviews* **2011**, *4* (1), 81–86. https://doi.org/10.1080/17518253.2010.502908.

(7)   Porras, S. P.; Heinälä, M.; Santonen, T. Bisphenol A Exposure via Thermal Paper Receipts. *Toxicology Letters* **2014**, *230* (3), 413–420. https://doi.org/10.1016/j.toxlet.2014.08.020.

(8)   Vervliet, P.; Gys, C.; Caballero-Casero, N.; Covaci, A. Current-Use of Developers in Thermal Paper from 14 Countries Using Liquid Chromatography Coupled to Quadrupole Time-of-Flight Mass Spectrometry. *Toxicology* **2019**, *416*, 54–61. https://doi.org/10.1016/j.tox.2019.02.003.

(9)   von Goetz, N.; Pirow, R.; Hart, A.; Bradley, E.; Poças, F.; Arcella, D.; Lillegard, I. T. L.; Simoneau, C.; van Engelen, J.; Husoy, T.; Theobald, A.; Leclercq, C. Including Non-Dietary Sources into an Exposure Assessment of the European Food Safety Authority: The Challenge of Multi-Sector Chemicals Such as Bisphenol A. *Regulatory Toxicology and Pharmacology* **2017**, *85*, 70–78. https://doi.org/10.1016/j.yrtph.2017.02.004.

(10)   Biedermann, S.; Tschudin, P.; Grob, K. Transfer of Bisphenol A from Thermal Printer Paper to the Skin. *Analytical and Bioanalytical Chemistry* **2010**, *398* (1), 571–576. https://doi.org/10.1007/s00216-010-3936-9.

(11)   Ndaw, S.; Remy, A.; Denis, F.; Marsan, P.; Jargot, D.; Robert, A. Occupational Exposure of Cashiers to Bisphenol S via Thermal Paper. *Toxicol. Lett.* **2018**, *298*, 106–111. https://doi.org/10.1016/j.toxlet.2018.05.026.

(12)   Ndaw, S.; Remy, A.; Jargot, D.; Robert, A. Occupational Exposure of Cashiers to Bisphenol A via Thermal Paper: Urinary Biomonitoring Study. *International Archives of Occupational and Environmental Health* **2016**, *89* (6), 935–946. https://doi.org/10.1007/s00420-016-1132-8.

(13)   Björnsdotter, M. K.; Jonker, W.; Legradi, J.; Kool, J.; Ballesteros-Gómez, A. Bisphenol A Alternatives in Thermal Paper from the Netherlands, Spain, Sweden and Norway. Screening and Potential Toxicity. *Science of The Total Environment* **2017**, *601–602*, 210–221. https://doi.org/10.1016/j.scitotenv.2017.05.171.

(14)   Eckardt, M.; Simat, T. J. Bisphenol A and Alternatives in Thermal Paper Receipts - a German Market Analysis from 2015 to 2017. *Chemosphere* **2017**, *186*, 1016–1025. https://doi.org/10.1016/j.chemosphere.2017.08.037.

(15)   Goldinger, D. M.; Demierre, A.-L.; Zoller, O.; Rupp, H.; Reinhard, H.; Magnin, R.; Becker, T. W.; Bourqui-Pittet, M. Endocrine Activity of Alternatives to BPA Found in Thermal Paper in Switzerland. *Regulatory Toxicology and Pharmacology* **2015**, *71* (3), 453–462. https://doi.org/10.1016/j.yrtph.2015.01.002.

(16)   Russo, G.; Barbato, F.; Grumetto, L. Monitoring of Bisphenol A and Bisphenol S in Thermal Paper Receipts from the Italian Market and Estimated Transdermal Human Intake: A Pilot Study. *Sci. Total Environ.* **2017**, *599–600*, 68–75. https://doi.org/10.1016/j.scitotenv.2017.04.192.

(17)   Kuruto-Niwa, R.; Nozawa, R.; Miyakoshi, T.; Shiozawa, T.; Terao, Y. Estrogenic Activity of Alkylphenols, Bisphenol S, and Their Chlorinated Derivatives Using a GFP Expression System. *Environ. Toxicol. Pharmacol.* **2005**, *19* (1), 121–130. https://doi.org/10.1016/j.etap.2004.05.009.

(18)   US EPA. *Bisphenol A Alternatives in Thermal Paper, Final Report.*; United States Environmental Protection Agency, 2014.

(19)   Demierre, A.-L.; Peter, R.; Oberli, A.; Bourqui-Pittet, M. Dermal Penetration of Bisphenol A in Human Skin Contributes Marginally to Total Exposure. *Toxicology Letters* **2012**, *213* (3), 305–308. https://doi.org/10.1016/j.toxlet.2012.07.001.

(20) Marquet, F.; Payan, J.-P.; Beydon, D.; Wathier, L.; Grandclaude, M.-C.; Ferrari, E. In Vivo and Ex Vivo Percutaneous Absorption of [14C]-Bisphenol A in Rats: A Possible Extrapolation to Human Absorption? *Archives of Toxicology* **2011**, *85* (9), 1035–1043. https://doi.org/10.1007/s00204-011-0651-z.

(21) Mørck, T. J.; Sorda, G.; Bechi, N.; Rasmussen, B. S.; Nielsen, J. B.; Ietta, F.; Rytting, E.; Mathiesen, L.; Paulesu, L.; Knudsen, L. E. Placental Transport and in Vitro Effects of Bisphenol A. *Reproductive Toxicology* **2010**, *30* (1), 131–137. https://doi.org/10.1016/j.reprotox.2010.02.007.

(22) Toner, F.; Allan, G.; Dimond, S. S.; Waechter, J. M.; Beyer, D. In Vitro Percutaneous Absorption and Metabolism of Bisphenol A (BPA) through Fresh Human Skin. *Toxicol In Vitro* **2018**, *47*, 147–155. https://doi.org/10.1016/j.tiv.2017.11.002.

(23) Zalko, D.; Jacques, C.; Duplan, H.; Bruel, S.; Perdu, E. Viable Skin Efficiently Absorbs and Metabolizes Bisphenol A. *Chemosphere* **2011**, *82* (3), 424–430. https://doi.org/10.1016/j.chemosphere.2010.09.058.

(24) Snyder, R. W.; Maness, S. C.; Gaido, K. W.; Welsch, F.; Sumner, S. C.; Fennell, T. R. Metabolism and Disposition of Bisphenol A in Female Rats. *Toxicol. Appl. Pharmacol.* **2000**, *168* (3), 225–234. https://doi.org/10.1006/taap.2000.9051.

(25) Zhou, X.; Kramer, J. P.; Calafat, A. M.; Ye, X. Automated On-Line Column-Switching High Performance Liquid Chromatography Isotope Dilution Tandem Mass Spectrometry Method for the Quantification of Bisphenol A, Bisphenol F, Bisphenol S, and 11 Other Phenols in Urine. *Journal of Chromatography B* **2014**, *944*, 152–156. https://doi.org/10.1016/j.jchromb.2013.11.009.

(26) Skledar, D. G.; Schmidt, J.; Fic, A.; Klopčič, I.; Trontelj, J.; Dolenc, M. S.; Finel, M.; Mašič, L. P. Influence of Metabolism on Endocrine Activities of Bisphenol S. *Chemosphere* **2016**, *157*, 152–159. https://doi.org/10.1016/j.chemosphere.2016.05.027.

(27) Liu, J.; Martin, J. W. Comparison of Bisphenol A and Bisphenol S Percutaneous Absorption and Biotransformation. *Environ. Health Perspect.* **2019**, *127* (6), 67008. https://doi.org/10.1289/EHP5044.

(28) Huysman, S.; Van Meulebroek, L.; Janssens, O.; Vanryckeghem, F.; Van Langenhove, H.; Demeestere, K.; Vanhaecke, L. Targeted Quantification and Untargeted Screening of Alkylphenols, Bisphenol A and Phthalates in Aquatic Matrices Using Ultra-High-Performance Liquid Chromatography Coupled to Hybrid Q-Orbitrap Mass Spectrometry. *Anal. Chim. Acta* **2019**, *1049*, 141–151. https://doi.org/10.1016/j.aca.2018.10.045.

(29) Lee, S.; Kim, C.; Youn, H.; Choi, K. Thyroid Hormone Disrupting Potentials of Bisphenol A and Its Analogues - in Vitro Comparison Study Employing Rat Pituitary (GH3) and Thyroid Follicular (FRTL-5) Cells. *Toxicology in Vitro* **2017**, *40*, 297–304. https://doi.org/10.1016/j.tiv.2017.02.004.

(30) Thayer, K. A.; Taylor, K. W.; Garantziotis, S.; Schurman, S.; Kissling, G. E.; Hunt, D.; Herbert, B.; Church, R.; Jankowich, R.; Churchwell, M. I.; Scheri, R. C.; Birnbaum, L. S.; Bucher, J. R. Bisphenol A, Bisphenol S, and 4-Hydroxyphenyl 4-Isoprooxyphenylsulfone (BPSIP) in Urine and Blood of Cashiers. *Environmental Health Perspectives* **2015**. https://doi.org/10.1289/ehp.1409427.

(31) Van Overmeire, I.; Vrijens, K.; Nawrot, T.; Van Nieuwenhuyse, A.; Van Loco, J.; Reyns, T. Simultaneous Determination of Parabens, Bisphenols and Alkylphenols in Human Placenta by Ultra-High Performance Liquid Chromatography-Tandem Mass Spectrometry. *J. Chromatogr. B Analyt. Technol. Biomed. Life Sci.* **2019**, *1121*, 96–102. https://doi.org/10.1016/j.jchromb.2019.05.012.

(32) Ye, X.; Kuklenyik, Z.; Needham, L. L.; Calafat, A. M. Measuring Environmental Phenols and Chlorinated Organic Chemicals in Breast Milk Using Automated On-Line Column-Switching–High Performance Liquid Chromatography–Isotope Dilution Tandem Mass Spectrometry. *Journal of Chromatography B* **2006**, *831* (1–2), 110–115. https://doi.org/10.1016/j.jchromb.2005.11.050.

(33) Andra, S. S.; Austin, C.; Yang, J.; Patel, D.; Arora, M. Recent Advances in Simultaneous Analysis of Bisphenol A and Its Conjugates in Human Matrices: Exposure Biomarker Perspectives. *Sci. Total Environ.* **2016**, *572*, 770–781. https://doi.org/10.1016/j.scitotenv.2016.07.062.

(34) Teeguarden, J. G.; Calafat, A. M.; Ye, X.; Doerge, D. R.; Churchwell, M. I.; Gunawan, R.; Graham, M. K. Twenty-Four Hour Human Urine and Serum Profiles of Bisphenol A during High-Dietary Exposure. *Toxicol Sci* **2011**, *123* (1), 48–57. https://doi.org/10.1093/toxsci/kfr160.

(35) Yao, Y.; Shao, Y.; Zhan, M.; Zou, X.; Qu, W.; Zhou, Y. Rapid and Sensitive Determination of Nine Bisphenol Analogues, Three Amphenicol Antibiotics, and Six Phthalate Metabolites in Human Urine Samples Using UHPLC-MS/MS. *Anal Bioanal Chem* **2018**, *410* (16), 3871–3883. https://doi.org/10.1007/s00216-018-1062-2.

(36) Yang, Y.; Yang, Y.; Zhang, J.; Shao, B.; Yin, J. Assessment of Bisphenol A Alternatives in Paper Products from the Chinese Market and Their Dermal Exposure in the General Population. *Environ. Pollut.* **2019**, *244*, 238–246. https://doi.org/10.1016/j.envpol.2018.10.049.

(37) García-Prieto, A.; Lunar, M. L.; Rubio, S.; Pérez-Bendito, D. Determination of Urinary Bisphenol A by Coacervative Microextraction and Liquid Chromatography–Fluorescence Detection. *Analytica Chimica Acta* **2008**, *630* (1), 19–27. https://doi.org/10.1016/j.aca.2008.09.060.

(38) Li, Q.; Wang, X.; Yuan, D. Preparation of Solid-Phase Microextraction Fiber Coated with Single-Walled Carbon Nanotubes by Electrophoretic Deposition and Its Application in Extracting Phenols from

Aqueous Samples. *Journal of Chromatography A* **2009**, *1216* (9), 1305–1311. https://doi.org/10.1016/j.chroma.2008.12.082.

(39)   Zarzycki, P. K.; Włodarczyk, E.; Baran, M. J. Determination of Endocrine Disrupting Compounds Using Temperature-Dependent Inclusion Chromatography. *Journal of Chromatography A* **2009**, *1216* (44), 7602–7611. https://doi.org/10.1016/j.chroma.2009.03.067.

(40)   Chesher, D. Evaluating Assay Precision. *Clin Biochem Rev* **2008**, *29* (Suppl 1), S23–S26.

(41)   Matuszewski, B. K.; Constanzer, M. L.; Chavez-Eng, C. M. Strategies for the Assessment of Matrix Effect in Quantitative Bioanalytical Methods Based on HPLC-MS/MS. *Anal. Chem.* **2003**, *75* (13), 3019–3030.

(42)   OECD. Organisation for Economic Co-Operation and Development, Guidelines for the Testing of Chemicals, Section 4, Test Nº 428: Skin Absorption: In Vitro Method; 2004.

(43)   Pinnagoda, J.; Tupker, R. A.; Agner, T.; Serup, J. Guidelines for Transepidermal Water Loss (TEWL) Measurement. A Report from the Standardization Group of the European Society of Contact Dermatitis. *Contact Derm.* **1990**, *22* (3), 164–178. https://doi.org/10.1111/j.1600-0536.1990.tb01553.x.

(44)   Yang, Y.; Guan, J.; Yin, J.; Shao, B.; Li, H. Urinary Levels of Bisphenol Analogues in Residents Living near a Manufacturing Plant in South China. *Chemosphere* **2014**, *112*, 481–486. https://doi.org/10.1016/j.chemosphere.2014.05.004.

(45)   Furey, A.; Moriarty, M.; Bane, V.; Kinsella, B.; Lehane, M. Ion Suppression; a Critical Review on Causes, Evaluation, Prevention and Applications. *Talanta* **2013**, *115*, 104–122. https://doi.org/10.1016/j.talanta.2013.03.048.

(46)   Tan, D.; Jin, J.; Wang, L.; Zhao, X.; Guo, C.; Sun, X.; Dhanjai, null; Lu, X.; Chen, J. Ammonium Hydroxide Enhancing Electrospray Response and Boosting Sensitivity of Bisphenol A and Its Analogs. *Talanta* **2018**, *182*, 590–594. https://doi.org/10.1016/j.talanta.2018.02.033.

(47)   Twaddle, N. C.; Churchwell, M. I.; Vanlandingham, M.; Doerge, D. R. Quantification of Deuterated Bisphenol A in Serum, Tissues, and Excreta from Adult Sprague-Dawley Rats Using Liquid Chromatography with Tandem Mass Spectrometry. *Rapid Commun. Mass Spectrom.* **2010**, *24* (20), 3011–3020. https://doi.org/10.1002/rcm.4733.

(48)   Ye, X.; Zhou, X.; Hennings, R.; Kramer, J.; Calafat, A. M. Potential External Contamination with Bisphenol A and Other Ubiquitous Organic Environmental Chemicals during Biomonitoring Analysis: An Elusive Laboratory Challenge. *Environ. Health Perspect.* **2013**, *121* (3), 283–286. https://doi.org/10.1289/ehp.1206093.

(49) Vandenberg, L. N.; Gerona, R. R.; Kannan, K.; Taylor, J. A.; van Breemen, R. B.; Dickenson, C. A.; Liao, C.; Yuan, Y.; Newbold, R. R.; Padmanabhan, V.; vom Saal, F. S.; Woodruff, T. J. A Round Robin Approach to the Analysis of Bisphenol a (BPA) in Human Blood Samples. *Environ Health* **2014**, *13*, 25. https://doi.org/10.1186/1476-069X-13-25.

(50) vom Saal, F. S.; Welshons, W. V. Evidence That Bisphenol A (BPA) Can Be Accurately Measured without Contamination in Human Serum and Urine, and That BPA Causes Numerous Hazards from Multiple Routes of Exposure. *Molecular and Cellular Endocrinology* **2014**, *398* (1–2), 101–113. https://doi.org/10.1016/j.mce.2014.09.028.

(51) Matuszewski, B. K. Standard Line Slopes as a Measure of a Relative Matrix Effect in Quantitative HPLC-MS Bioanalysis. *J. Chromatogr. B Analyt. Technol. Biomed. Life Sci.* **2006**, *830* (2), 293–300. https://doi.org/10.1016/j.jchromb.2005.11.009.

(52) ICH. International Council for Harmonisation (ICH), Bioanalytical Method Validation M10; ICH Harmonised Guideline; 2018; p 63.

(53) FDA, U. S. F. & D. A. Bioanalytical Method Validation Guidance for Industry. **2018**, 44.

(54) Ye, X.; Bishop, A. M.; Reidy, J. A.; Needham, L. L.; Calafat, A. M. Temporal Stability of the Conjugated Species of Bisphenol A, Parabens, and Other Environmental Phenols in Human Urine. *J Expos Sci Environ Epidemiol* **2007**, *17* (6), 567–572. https://doi.org/10.1038/sj.jes.7500566.

(55) Guy, R. H.; Potts, R. O. Penetration of Industrial Chemicals across the Skin: A Predictive Model. *Am. J. Ind. Med.* **1993**, *23* (5), 711–719. https://doi.org/10.1002/ajim.4700230505.

(56) Gundert-Remy, U.; Mielke, H.; Bernauer, U. Commentary: Dermal Penetration of Bisphenol A—Consequences for Risk Assessment. *Toxicology Letters* **2013**, *217* (2), 159–161. https://doi.org/10.1016/j.toxlet.2012.12.009.

(57) Champmartin, C.; Marquet, F.; Chedik, L.; Décret, M.-J.; Aubertin, M.; Ferrari, E.; Grandclaude, M.-C.; Cosnier, F. Human in Vitro Percutaneous Absorption of Bisphenol S and Bisphenol A: A Comparative Study. *Chemosphere* **2020**, *252*, 126525. https://doi.org/10.1016/j.chemosphere.2020.126525.

Annex II

Skin absorption of Bisphenol A and its alternatives in thermal paper

E. Reale[a], D. Vernez[a,b], N. B. Hopf[a,b]

[a] Center for Primary Care and Public Health (Unisanté), University of Lausanne, Switzerland - Department of Occupational and Environmental Health (DSTE), Route de la Corniche 2, 1066 Epalinges, Switzerland

[b] Swiss Centre for Applied Human Toxicology (SCAHT), Missionsstrasse 64, 4055 Basel, Switzerland

Corresponding author: Nancy B Hopf PhD, Center for Primary Care and Public Health (Unisanté), Route de la Corniche 2, 1066 Epalinges-Lausanne, Switzerland, Nancy.Hopf@unisante.ch

Abstract

Introduction: Bisphenol A (BPA) is the most used colour developer in thermal paper for cashiers receipts, labels and tickets. BPA can migrate onto the skin and be absorbed when handling these papers. BPA is a known endocrine disruptor and is therefore being replaced in thermal paper by some alternatives such as Bisphenol S (BPS), D-8 and Pergafast201® (PF201). To our knowledge, no studies have characterised skin permeation of these BPA alternatives.

Methods: We measured/characterised skin absorption for BPA, BPS, D-8, and PF201 through ex-vivo human skin using flow-through diffusion cells according to OECD guideline 428. Skin samples were 7-12 per test substance from three different skin donors. Skin metabolism was studied for BPA. Dermal absorption was expressed as the amount of the BPA alternatives in the receptor fluid over applied dose in percent (%).

Results: The absorbed dose after 24 hours of exposure was 25% for BPA, 17% for D-8, 0.4% for BPS and <LLOQ for PF201. The amount of BPA-glucuronide in the receptor fluid after 24 hours was under the limit of quantification (LLOQ = 0.2 µg/l). Despite the 10-fold lower concentration of the aq solution applied on the skin, D-8's permeation rate J_{MAX} was 5-fold higher than the one for BPS (0.032 vs. 0.006 µg/cm^2/h). Neither D-8 nor BPS permeated readily through the skin (t_{lag} = 3.9 h for D-8, 6.4 h for BPS). None of PF201's skin permeation kinetic parameters could be determined because this BPA analogue was not quantifiable in the receptor fluid in our test conditions.

Conclusions: Skin absorption was in decreasing order: BPA > D-8 >> BPS > PF201. These results are in agreement with their $logK_{ow}$ and molecular weights. We provided here the necessary data to estimate the extent of skin absorption of BPA analogues, which is a necessary step in risk assessment, and ultimately evaluate public health risks posed by D-8, PBS, and PF201.

1. Introduction

Bisphenol A (BPA) is one of the largest high production volume chemicals (OECD). The second largest source of human BPA exposure after food and beverage packaging is thermal paper (cash receipts, parking, airline and cinema tickets, luggage tags, bus and train tickets, grocery weight tickets) (EFSA, 2015). BPA is in the powdery coating on one side of the thermal paper. It has been found in 100/124, 78/100, and 195/308 thermal paper products by Goldinger et al. (2015), Björnsdotter et al. (2017), Vervliet et al. (2019), respectively. Skin contact with BPA in thermal paper contributed to the overall body burden among occupationally exposed populations, such as cashiers (Braun et al., 2003; Ndaw et al., 2016; Thayer et al., 2016) and workers in industries manufacturing and using BPA (Heinälä et al., 2017; Hines et al., 2017). These studies show that BPA migrates from the thermal paper onto the skin (Biedermann et al., 2010; Hormann et al., 2014) and is absorbed (Marquet et al., 2011; Demierre et al., 2012; Toner et al., 2018; Liu and Martin, 2019). Most of the absorbed BPA is not or is only slightly metabolised by the skin (Marquet et al., 2011; Zalko et al., 2011; Toner et al., 2018; Liu and Martin, 2019), and goes directly into the systemic circulation. BPA metabolites such as glucuronide and sulphate conjugates are not toxic and consequently, metabolism is of importance in assessing BPA toxicity. In 2016, BPA was classified as a presumed human reproductive toxicant (category 1B), and the European Union decided to restrict BPA in thermal paper to no more than 0.02% (w/w) by 2020 (EU 2016/2235). Several chemicals have been or are in the process of replacing BPA in thermal papers. These alternative developers could potentially migrate from thermal paper and be absorbed by the skin as shown for BPA. Moreover, thermal paper products usually contain one major developer with other developers often used as secondary developers or present in trace levels (Björnsdotter et al. 2017; Vervliet et al. 2019).

The most used BPA alternatives in cash receipts are Bisphenol S (BPS), Pergafast 201® (PF201), and Wincon 8 (D-8) (Table 1). The US EPA has classified BPS and PF201 as high-hazard colour developers for repeated dose toxicity and developmental toxicity, respectively (US EPA 2014). D-8 was considered of moderate hazard for these endpoints and with limited evidence of endocrine activity (US EPA 2014; Goldinger et al. 2015). Other less used developers are: D-90, 4-(4-hydroxy-3-prop-2-enylphenyl)sulfonyl-2-prop-2-enylphenol (TGSA), and 4-(4-phenylmethoxyphenyl)sulfonylphenol (BPS-MAE). Rare developers are urea urethane (UU) and 1,7-bis(4-hydroxyphenylthio)-3,5-dioxaheptane (DD-70). A structural analogue of BPS, 2,4-BPS, was detected in 20.8% of the samples, and it is likely to be an impurity of BPS (Vervliet et al., 2019; Yang et al., 2019). BPA has the highest concentration in thermal paper (medians 15.0 – 15.9 mg/g (Eckardt and Simat 2017), mean

Table 1 – Detection frequency of colour developers in thermal paper products.

	Björnsdotter et al. (2017)	Eckardt and Simat (2017)*	Goldinger et al. (2015)	Vervliet et al. (2019)	Yang et al. (2019)
n	100	114/98/99	124	308	120
Countries	Norway, Netherlands, Spain and Sweden	Germany	Switzerland	14 countries in Europe, Asia, North America and Oceania	China
	% of n	% of n	% of n	% of n	% of n
BPA	78	48/47/53	81	63	77
BPS	49	11/9/6	3	22	72
Pergafast 201	49	34/34/40	9	12	NA
D-8	24	6/7/1	7	8	33
D-90	7	NA	NA	4	19
TGSA	7	NA	NA	4	25
BPS-MAE	2	NA	NA	2	52
UU	NA	0/0/3	NA	0.6	NA
DD-70	NA	NA	NA	0.3	NA

(*) Numbers listed by collection years 2015/2016/2017

13.5 mg/g (Goldinger et al., 2015), mean 3.61 mg/g (Yang et al., 2019)), followed by BPS, Pergafast 201® and D-8 . In the study of Eckardt and Simat (2017), BPS, Pergafast 201® and D-8 concentrations ranged from 1.4 to 19.2 mg/g paper (median values between 2.5 and 14.7 mg/g). Similar values were reported by Goldinger et al. (2015) (concentration range 3.3 – 13.2 mg/g, median values between 4.6 – 12.0), while lower values were consistently measured in Chinese samples (mean values range 0.209 – 1.15, Yang et al. (2019)). The Danish Environmental Protection Agency (EPA) found similar concentrations for BPA, BPS and Pergafast 201® in thermal paper where the developers' content had been confirmed by the manufacturer (10.8, 11.6, 10.4 mg/g respectively) (Danish EPA, 2014).

Reported mean values of amount of BPA transferred from thermal paper to dry (i.e. normal condition) fingers was 1.1 µg/finger (Biedermann et al., 2010), 1.4 µg/finger (Lassen et al., 2011), and 1.1 µg/finger (Danish EPA, 2014). Eckardt and Simat (2017) observed no significant difference in the amount transferred when comparing samples with different colour developers (BPA, BPS, Pergafast 201®, and D-8), and ranged from 0.05 to 6.0 µg/finger (mean 0.8 µg/finger, median 0.3 µg/finger). By contrast, the Danish EPA reported mean values lower than BPA

for both BPS (0.8 µg/finger) and Pergafast 201® (0.4 µg/finger). Liu and Martin (2019) reported higher values for BPS (3.9 µg/hand wipe, range 0.71 – 10 µg/hand wipe) than BPA (0.77 µg/hand wipe, range 0.07 – 3.0 µg). Transfer of BPA from thermal paper is greater on humid, sweaty, oily or hand-lotion skin compared to dry skin (Biedermann et al., 2010; Lassen et al., 2011; Danish EPA, 2014). When skin was moistened by water or artificial sweat, Eckardt and Simat (2017) found that the amount of BPA transferred (mean 35 µg/finger, range 21 – 42 µg/finger) was higher than BPS, D-8 and Pergafast 201® (mean range 9 - 14 µg/finger, values range 2.3 – 24.6 µg/finger). Again, the Danish EPA (2014) observed greater amounts of BPA (17.7 µg/finger) and Pergafast 201® (17.1 µg/finger) compared to BPS (3.1 µg/finger).
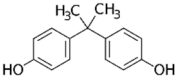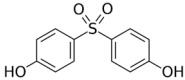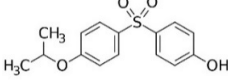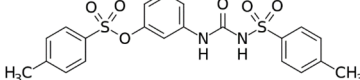
Colour developers could possibly be absorbed through the skin after migrating from thermal paper. BPA skin absorption has been extensively studied *in vitro* and is shown to be absorbed by the skin (Marquet et al., 2011; Demierre et al., 2012; Toner et al., 2018). Skin absorption of the alternative developers is poorly understood. Only two *in vitro* and *in vivo* study on BPS (Liu and Martin 2019; Champmartin et al. 2020) exist in the literature. To our knowledge, no other alternative developers have been assessed for potential skin absorption. The aim of this study was to characterise skin absorption of the BPA alternatives most frequently used in thermal papers, namely BPS, D-8, and Pergafast 201®, and to compare these to BPA. An *in vitro* study was carried out using human skin and flow-through diffusion cells (Franz cells), and following the "OECD Guideline 428 for Skin absorption". We determined both permeability kinetics and mass balance. The results provide insights on skin absorption rates and absorbed doses of colour developers replacing BPA that can be used in exposure assessments.

2. Materials and Methods

2.1 Chemicals

BPA, BPA-glucuronide and BPS were purchased from Sigma-Aldrich Chemie GmbH, Buchs, Switzerland. D-8 and PF201 were bought from Santa Cruz Biotechnology, Heidelberg, Germany. The CAS numbers and some chemical and physical properties of the three test substances are shown in Table 2. Bisphenol A-d6 (BPA-[D$_6$]) and bisphenol A-^{13}C$_{12}$ β-D-glucuronide (BPA-G-[^{13}C$_{12}$]) were obtained from Toronto Research Chemicals, Toronto, ON, Canada. Carlo Erba LC/MS-grade acetonitrile, methanol (MeOH), and water were obtained by Thommen-Furler AG, Büren, Switzerland. Saline was prepared by dissolving 0.9% (w/v) sodium chloride (purissim. p.a. ≥ 99.5%, supplied by Sigma-Aldrich Chemie GmbH, Buchs, Switzerland) in Milli-Q® water (Milli-Q® Advantage ultra-pure water system, Millipore, Milford, MA, USA).

Table 2 - Some physicochemical properties of BPA and its alternatives used in thermal paper: BPS, D-8, and Pergafast 201® (Source: EPA, 2014).

	Bisphenol A	Bisphenol S	D-8	Pergafast 201®
Structure				
Acronym	BPA	BPS	D-8	PF201
CAS number	80-05-7	80-09-1	95235-30-6	232938-43-1
Molar mass (g/mol)	228.29	250.27	292.35	460.52
Physical description	Dry powder	Dry powder	Dry powder	Dry powder
Solubility in water (mg/l)	120 – 301 (measured)	500-1100 (20°C)	19.7 (measured) at pH 6.85 21 (measured)	35 (measured) 35 at 20°C (measured)
Log k_{ow}	3.3 (measured)	1.2 (measured)	3.36 (measured)	2.6 (measured)

2.2 Test preparations

Water was chosen as a donor vehicle to mimic a solid colour developer deposited on skin. The colour developer will partition into sweat, a necessary step for skin absorption. Aqueous working solutions were prepared separately for BPA, BPS, D-8 and PF201 (250 mg/l, 250 mg/l, 20 mg/l and 3 mg/l, respectively). These concentrations were confirmed by analysis according to the method described in Chapter 2.4 except for calibration solutions that were in water instead of saline, which required no sample preparation. We applied 100 µl/cm^2 of the test preparations on the skin to achieve an infinite dose. This gave the following skin exposures: 25 µg/cm^2 for BPA, 25 µg/cm^2 for BPS, 2 µg/cm^2 for D-8, and 0.3 µg/cm^2 for PF201. All four substances were soluble in donor and receptor fluids at the tested concentrations as required by the OECD guidelines (OECD 2004b, 2004a).

2.3 Skin absorption assays

We did two types of skin absorption assays: skin permeation kinetics assays, where we studied the absorption over time, and mass balance assays, where we studied the absorption in the different system compartments (i.e. skin, skin wash, donor compartment, receptor fluid).

2.3.1 *In vitro skin absorption system*

We conducted skin absorption assays following OECD Guideline 428 (OECD 2004a) and OECD Guidance notes 28 (OECD 2004b), using jacketed flow-through diffusion cells (11.28 mm internal diameter, PermeGear®

obtained from SES Analytical System, Bechenheim, Germany). A heated water-bath circulator (Haake SC 100 Digital Immersion Circulator, 100 °C w/cla, Thermo Scientific, Newington, NH, USA) kept the skin flaps mounted on diffusion cells at 32°C. Receptor fluid was saline continuously stirred (multi-cell V9-CB stirrer, PermeGear® obtained from SES Analytical System, Bechenheim, Germany) and pumped through the receptor chamber (50 µl/min; peristaltic pump from Ismatec IPC-N, IDEX Health and Science GmbH, Wertheim-Mondfeld, Germany). The receptor fluid was collected automatically with a fraction collector (FC 204, Gilson Inc., Middleton, WI, USA) for skin permeation kinetics assays.

2.3.2 Human skin preparation

We obtained human abdominal skin from the Plastic and Reconstructive Surgery Department at the Vaud University Hospital Centre (CHUV, Lausanne, Switzerland) immediately after surgery (ethical protocol 264/12). Patient data were kept anonymous, and the only known data were the patients' gender and age. The skin samples were excised from three different skin donors (N = 3) for each tested chemical. Occasionally samples from a same skin donor were used for two test substances. A total of eight different skin donors were used for the four test substances. The total number of skin samples per test chemical was n = 12 for BPA, n = 12 for BPS, n = 10 for D-8, and n = 11 for PG201. Skin was rinsed with saline, dried with paper tissues and dermatomed at 200 µm thickness (Acculan®II, B. Braun/Aesculap, Sempach, Switzerland). The use of 200 µm-thick skin allowed the determination of the permeation rate without the depot effect that exist for thicker skin (500 - 1000 µm) (OECD 2011). We cut the skin into circular flaps, mounted them on the diffusion cells, and let them equilibrate for 30 minutes. We followed the same protocol for the mass balance experiments, except that skin had been frozen (-20°C) and dermatomed at 800 µm. Skin was used frozen due to easier availability of skin samples. Frozen skin was easier to dermatome to 800 µm thickness compared to 200 µm. Moreover, the 800 µm-thick skin in mass balance assays allowed the determination of the amount retained in the skin. Skin was thawed at room temperature before cutting and mounting the skin flaps onto the diffusion cells.

2.3.3 Skin integrity

We assessed skin integrity using a trans-epidermal water loss (TEWL) meter (VapoMeter wireless, Delfin Technologies Ltd., Kuopio, Finland) at the beginning and the end of each experiment. Skin flaps with a TEWL above 11 g/m²/h were discarded (Pinnagoda et al., 1990).

2.3.4 Skin absorption assays

We started the experiment once the skin samples had achieved a steady TEWL reading and skin were exposed (unoccluded) to the test preparations for 24 hours. The experiments started within two hours from retrieving the skin from the surgery unit. The receptor fluid was automatically sampled every hour from 0 to 6 hours, and every two hours from 6 to 24 hours in the permeation kinetics assays. In the mass balance assays, we collected the receptor fluid in glass vial during the 24-hour experiment. We washed the skin by adding water (200 µl) and rubbing gently with a cotton swab that we put into a glass vial. We repeated this washing procedure three times. We added water/acetonitrile 80:20 mixture (3 ml for BPA, 4 ml for BPS, D-8, and PF201) to the vial with the three cotton swabs. We extracted the substances from the cotton swab to the solution by sonicating the vial for ten minutes. We washed the donor chamber with by adding water/acetonitrile solution (0.5 ml), swirling the liquid inside the chamber, and then removing it to a glass vial. We repeated the donor chamber washing three times for each. We cut each skin flap to remove the non-exposed part. We tape stripped the exposed skin five times. We then dropped the skin flap into a glass vial with methanol (1 ml) and sonicated the vials for five minutes. We repeated this extraction process three times, and then pooled the 1 ml x 3 methanol aliquots in one vial.

2.4 Sample analysis

We quantified BPA, BPA-G, BPS, D-8 and PF201 in the receptor fluid and in water/acetonitrile samples by liquid chromatography tandem mass spectrometry (LC-MS/MS). The analytical method for the quantification in the receptor fluid was described in (Reale et al. 2020). Briefly, we prepared receptor fluid samples by solid phase extraction (SPE) (Isolute® C18 6 ml SPE cartridges; Biotage AB, Uppsala, Sweden). A C18 column (100 x 2.1 mm, 1.8 µm, Eclipse Plus, Zorbax, Agilent Technology, Basel, Switzerland) was used to separate the analytes with a HPLC (UltiMate 3000 HPLC system, Thermo Fisher, Fisher Scientific, Reinach, Switzerland) eluting with LC-grade water and acetonitrile containing ammonium hydroxide (5 mM). Triple quadrupole mass spectrometer (MS/MS) (TSQ Quantiva, Thermo Fisher, Fisher Scientific, Reinach, Switzerland) with an electrospray ionization (ESI) source in negative ion mode was used for detection. Internal calibration was done by adding BPA-[D_6] and BPA-[$^{13}C_{12}$] internal standards to samples and calibration standards. The lower limit of quantification (LLOQ) for all analytes was 0.2 µg/l. Method precision (%CV) and accuracy (% of nominal concentration) were tested over five different days. Precision of the quality control solutions at two different concentrations were in the range 93% - 108% and accuracy 3.7% - 15.5%. Extraction recovery corrected by internal standards was calculated as per Matuszewski et al. 2003 and ranged 83% - 110%. All analytes were stable in receptor fluid matrices as well as in water stored at -20°C at least for 80 days.

Conjugated metabolites of BPS, D-8 and PF201 were not quantified due to the lack of available analytical

method. Methanol used in skin extraction was evaporated to dryness under nitrogen stream. The residues were dissolved in water:acetonitrile 80:20 mixture (1 ml). Water/acetonitrile samples were diluted 10 times before injection in the LC system. Skin extraction recoveries were not determined. Cotton swabs extraction recoveries were 102% for BPA, 40% for BPS and D-8, and 49% for PF201. Tape strips were not analysed due to the lack of an analytical method for this matrix

2.5 Data analysis

For permeation kinetics assays, we plotted the permeation curves as cumulative amount of BPA in the receptor fluid per unit skin area over time for each skin sample. For each plot, we determined the maximum permeation rate (J_{MAX}, µg/cm^2/h) as the slope of the steepest linear portion. If the permeation rate achieved a constant value (steady-state) we calculated also the permeability coefficient (K_p, cm/h), and lag time (t_{lag}, h) as follows:

- K_p from Fick's first law for an infinite dose of a chemical applied on the skin $J = K_p \times C$, where C is the concentration (mg/l) of the test preparations ; and

- t_{lag} as the time to reach the steady-state, which is the time (x-axis) intercept of the steepest linear portion of the permeation curve.

Finally, we calculated the mean values of J_{MAX}, K_p and t_{lag} over all skin samples. For mass balance assays, we expressed the absorption as percent of the applied dose as well as µg/cm^2 in the different compartments i.e. skin, skin rinsing, donor chamber rinsing, and receptor fluid.

3. Results

3.1 Permeation kinetics assays

Results of the skin permeation kinetics assays are presented in Figure 1, and in Table 3. BPS reached steady-state after 7 hours. The permeation curves of BPA and D-8 started plateauing approximately after 12 hours. These plateaus suggest that steady-state conditions were not achieved. BPA had the greatest permeation rate J_{MAX} (0.67 µg/cm^2/h). BPS's J_{MAX} was approximately 110-fold lower than BPA's. D-8's skin absorption was slightly lower than BPA's: D-8's J_{MAX} was 16-fold lower than BPA due to the 12-fold difference in the concentration of the test preparation. D-8's J_{MAX} was 7-fold higher than BPS', despite the 10-fold lower applied concentration. After 24 hours of exposure, 32% (8.0 µg/cm^2) of BPA's applied dose had been absorbed in the receptor fluid versus 20% (0.4 µg/cm^2) of D-8 and only 0.2% (0.05 µg/cm^2) of BPS. BPA-glucuronide in the receptor fluid, after 24 hours of skin exposure to BPA, was detectable, but under the LLOQ of our analytical method in almost all the tested

samples. PF201's skin permeation kinetic parameters could not be determined because it was not quantifiable in the receptor fluid in our test conditions.

Table 3 - Summary of skin exposure conditions and results of skin permeation kinetics assays for the tested chemicals.

Chemical	n[a]	Concentration (aq) [mg/l]	Volume [µl/cm²]	Mean amount in receptor fluid after 24 h of exposure		t_{lag} [h]	J x 10⁻² [µg/cm²/h]	K_p x 10⁻⁴ [cm/h]
				µg/cm² (±SD)	% of applied dose (±SD)			
BPA (aq)	12	250	100	8.00 (±3.05)	32 (±12)	ND	67 (±30)	ND
BPS (aq)	12	250	100	0.05 (±0.03)	0.2 (±0.1)	7.6	0.6 (±0.9)	0.24 (±0.35)
D-8 (aq)	10	20	100	0.41 (±0.18)	20 (±9)	ND	4.1 (±2.0)	ND
Pergafast 201® (aq)	11	3[b]	100	<LLOQ	<LLOQ	ND	ND	ND

[a] Number of skin samples tested from three skin donors.
[b] Water solubility has been reported to be 35 mg/l but we could only dissolve 3 mg/l.
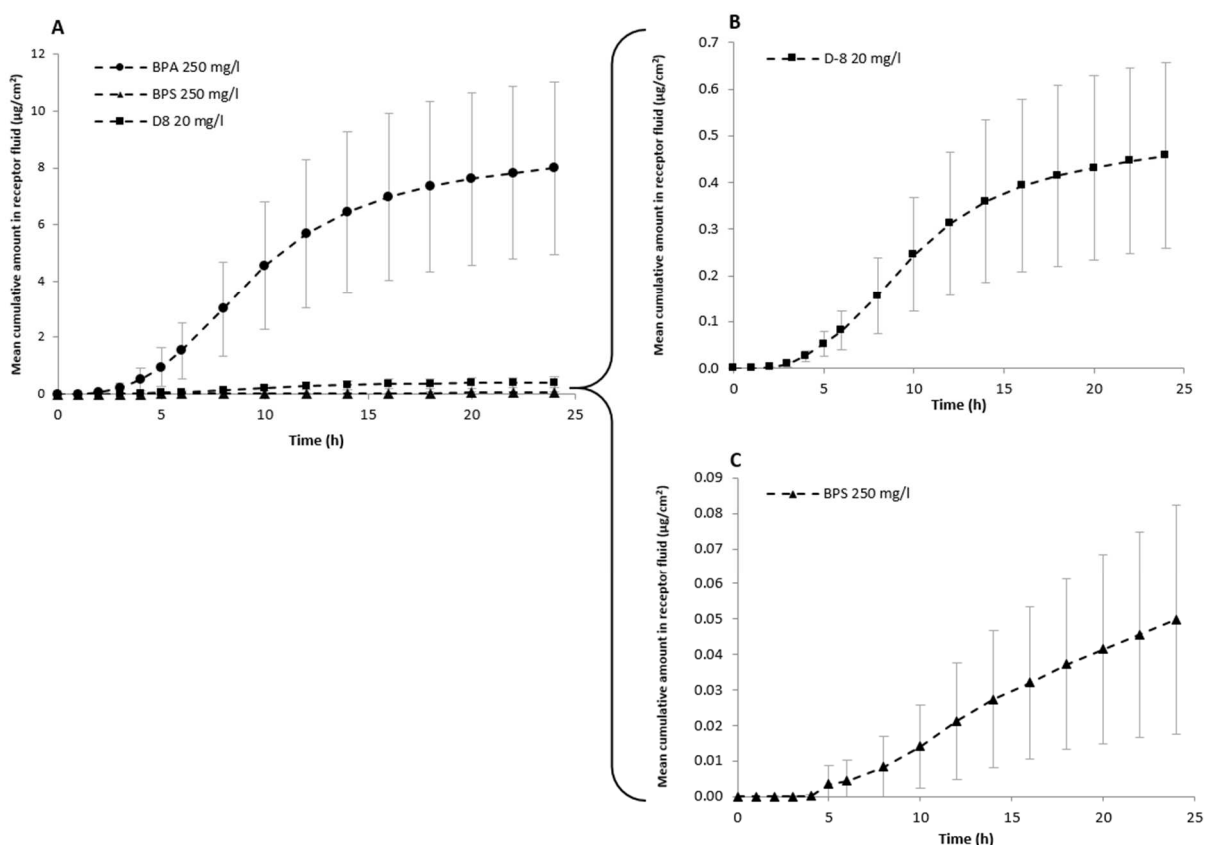ND, not determined.

Figure 1 - Mean permeation curve of BPA, BPS and D-8 (A), and expanded view of D-8 (B) and BPS (C). n = 12 for BPA, 12 for BPS, and 10 for D-8. Error bars represent the SD.

3.2 Mass balance assays

Mass balance assays results are presented in Table 4. The amount of applied dose quantified in the receptor fluid after 24-hour exposure (i.e. absorbed dose) was 0.4% (0.1 µg/cm^2) for BPS and 17% (0.5 µg/cm^2) for D-8 compared to 25% (6.4 µg/cm^2) for BPA. These values were similar to the absorbed dose observed in the skin

Table 4 - Mean and standard deviation (SD) of the amount of test chemicals quantified in the different compartments at the end of the experiments (24 h) following an application of 100 µl/cm^2 aq solution on 800 µm-thick frozen human skin. Results are expressed as percent of applied dose and as µg/cm^2

Chemical	BPA (n = 8)		BPS (n = 7)		D-8 (n = 7)		Pergafast 201® (n = 8)	
	Mean [%]	SD	Mean [%]	SD	Mean [%]	SD	Mean [%]	SD
Skin swabs	57	4.2	71	14	39	18	22	20
BPA in donor chamber	1.0	1.8	2.1	2.4	3.9	5.0	< LLOQ	
Skin	15	14	11	6.8	16	5.4	1.5	0.9
Receptor fluid [a]	25	13	0.4	0.2	17	12	< LLOQ	
Recovery (total)	98	13	84	14	76	13	24	22
	Mean [µg/cm^2]	SD	Mean [µg/cm^2]	SD	Mean [µg/cm^2]	SD	Mean [µg/cm^2]	SD
Skin swabs	14.22	1.0	17.7	3.7	1.1	0.7	0.09	0.07
BPA in donor chamber	0.5	0.6	0.4	0.6	0.09	0.10	<LLOQ	
Skin	3.7	3.4	2.5	1.6	0.4	0.1	0.01	0.00
Receptor fluid [a]	6.4	3.1	0.1	0.0	0.5	0.3	<LLOQ	
Recovery (total)	24.8	3.1	20.7	3.5	1.7	0.6	0.09	0.07

[a] Sum of the amount quantified in the receptor fluid collected for 24 hours and in the receptor fluid remained in the receptor chamber.

permeation kinetics assays (0.2% BPS, 20% D-8, 32% BPA). The dislodgeable dose (amount removed from skin by cotton swabs and donor chamber rinsing) was greater for BPS (73% of applied dose, 18 µg/cm^2) compared to BPA (58%, 15 µg/cm^2) and D-8 (43%, 1.2 µg/cm^2). The percent of applied dose quantified in the skin was similar for all three substances (11 – 16%, 0.4-3.7 µg/cm^2, Table 4). These do not include the tape strips samples, as we did not analyse these. Mass balance was 84% for BPS and 76% for D-8, which was lower compared to BPA (98%). For PF201 mass balance was 24%, which corresponded to the dislodgeable dose (22% of the applied dose in the skin swabs (0.1 µg/cm^2), and 1.5% in the skin (0.01 µg/cm^2)). PF201 was under the LLOQ in the donor chamber rinsing and in the receptor fluid.

4. Discussion

We studied the skin absorption of BPA and its main alternatives used in thermal paper. Our results show that the absorbed dose in the receptor fluid through frozen 800 µm skin after 24 hours of exposure was 25% ± 13% (6 µg/cm^2) for BPA, 17% ± 12% (0.5 µg/cm^2) for D-8, 0.4% ± 0.2% (0.1 µg/cm^2) for BPS and <LLOQ for PF201. Similar values were determined for viable 200 µm-thick skin. BPA skin absorption kinetics were similar to D-8, and 100 times greater than BPS. PF201 kinetics across the skin could not be determined because it was not quantifiable in the receptor fluid.

The reported mean transfer of BPA from thermal paper on hands is 1.4 µg/finger for dry skin (range 0.58 – 3.8 µg/finger), and 12.8 µg/finger for humid skin (range 2.63 – 30 µg/finger) (Lassen et al., 2011)). Here, we adopted the infinite dose strategy to be able to study the kinetics of the test substances through the skin, and to increase the probability of detecting these substances with our analytical method. Using the infinite dose approach, our BPA applied dose was 18 times greater than the reported finger exposure for dry skin, and in line with wet skin.

No data exist in the literature on D-8 migration from thermal paper to the skin. The Danish Environmental Protection Agency (Danish EPA, 2014) estimated D-8's potential skin migration based on its available physico-chemical properties. According to the Danish EPA, D-8 is expected to have a migration potential similar to that of BPA as it has chemical structure, molecular mass, and octanol-water partition coefficient (logK$_{ow}$) similar to BPA. In our study, D-8 dose was 2 µg/cm^2, which was in the range of dermal exposures reported for BPA (Lassen et al., 2011). PF201 dose (0.3 µg/cm^2) was in the reported range of dermal exposures to PF201 (0.28 – 0.50 µg/fingertip (Danish EPA, 2014)). For BPS, the reported range of migration on the skin is 0.73 – 0.85 µg/dry finger, and 1.6 – 4.8 µg/sweaty finger (Danish EPA, 2014)). BPS has a high water solubility (1,100 mg/l (US EPA, 2014)). Applying 100 µl of BPS in saturated solution would result in a dose 22 times greater than BPA, 140 times greater than reported finger exposure of dry skin to BPS, and 30-70 times greater than reported fingertip exposure of dry skin to BPS (0.73 – 0.85 µg/dry fingertip and 1.6 – 4.8 µg/sweaty fingertip (Danish EPA, 2014)). Therefore, we chose to use a BPS solution not at saturation but at the same concentration and dose used for BPA (250 mg/l, 25 µg/cm^2) to directly compare the permeation rate, which is dependent on the concentration. The applied BPS dose was 5 to 34 times higher than the reported range of BPS migration on the skin.

Table 5 - Experimental set up and results of BPA skin absorption studies in the literature.

Authors	Marquet et al. (2011)	Zalko et al. (2011)	Kaddar et al. (2008)	Mørck et al. (2010)	Demierre et al. (2012)	Toner et al. (2018)	Liu and Martin (2019)	Champmartin et al. (2020)	Our study
Skin parameters									
Skin type	Human	Human	Pig	Human	Human	Human	Human skin model	Human	Human
Skin thickness (µm)	400	500	Full thickness	800-1000	200	350-400	120	476	200, 800[a]
Skin condition	Frozen and viable	Viable	Frozen	Frozen	Frozen cadaver	Viable	3D model with metabolic activity	Viable	Viable, frozen[a]
Skin temperature (°C)	32	37	32	32	32	32	NA	32	32
total skin samples (n)	15	3	6	11	7	12	3	10	12
Skin donors (N)	6	Not reported	Not reported	Not reported	2	4	NA	Not reported	3
Methods									
System	Static diffusion cells	6-well plates for *ex vivo* organ cultures.	Static diffusion cells	Static diffusion cells	Flow through-diffusion cells	Flow through-diffusion cells, 12-well plate for metabolism	Static diffusion device in 6-well plates	Static diffusion cells	Flow through-diffusion cells
BPA concentration [mg/l]	4000	284[b]	10	3995[b]	194	300 (60, 12, 2.4)	1, 5	400	250
Vehicle	Acetone	DMEM[c]	Saline	Saline with 2% ethanol	Water	Phosphate buffered saline (PBS)	Water	Water	Water
Vehicle volume (µl/cm^2)	50	9.7	Not reported	Not reported	9.4	10	1538	50	100
BPA dose (µg/cm^2)	200	2.75	Not reported	Not reported	1.82	3 (0.6, 0.12, 0.04)	1.5, 7.7	20	25
Receptor fluid	RPMI, 2% BSA, 1% penicillin/streptomycin[d]	DMEM[d]	Saline	Saline with 5% BSA[d]	Saline	DMEM[d] + 1% ethanol + UDPGA[d] 2mM + PAPS[d] 40 µM	Phosphate-buffered saline	RPMI 1640 solution + 0.2% gentamycin + 2.5% penicillin-streptomycin + 2% BSA[d]	Saline
Exposure time (h)	24	72	10	48	24	24	25	40*	24
Results									
Metabolism (%)	< 2.5 (viable skin)[e]	27[f]	NA	NA	NA	8[g]	Not significant	88 was not metabolised	Not significant
Unabsorbed dose (%)	NA	3	65	45	57	72[h]	38[i]	Not reported	60
Skin (%)	NA	42	14	25	0.6 (epidermis + dermis), 24 (tape strips 1-2), 11 (tape strips 3-20)	13 (epidermis + dermis), 7.5 (tape strips 1-2), 2.5 (tape strips 3-20)	13	27	12 (epidermis + dermis)
Receptor fluid (%)	NA	46	1	13	8.6	3	46	41	29
Recovery (%)	NA	92	84	82	100	99	97	98	102

[a] Viable 200 µm-thick skin was used in the metabolism assay, frozen 800 µm-think skin in the mass balance assay.
[b] Calculated from the reported value 17.5 mM BPA.
[c] Calculated from the reported value 50 nmol BPA.
[d] Acronyms: RPMI Rosewell Park Memorial Institute medium, BSA bovine serum albumin, DMEM Dulbecco's Modified Eagle Medium, UDPGA Uridine 5'-diphosphoglucuronic acid, PAPS 3'-phosphoadenosine-5'-phosphosulfate
[e] BPA accounted for more than 97.5% of the radioactivity detected in the receptor fluid.
[f] Sum of BPA-glucuronide and BPA-sulphate
[g] Sum of BPA-glucuronide, BPA-sulphate and more polar compounds
[h] Results are reported only for the 3 µg/cm^2 dose
[i] Results are reported only for the 7.7 µg/cm^2 dose
NA not available

[*Modified from value written in Reale et al., Ann Work Expo Health. 2021 Mar 3;65(2):206-218]

Even under dose conditions ten times higher than the ones indicated in the OECD TG428 (100 µL/cm^2 of a saturated solution), steady-state was not reached for BPA and D-8. This has also been shown for other lipophilic permeants (Selzer et al. 2013) and was explained by donor depletion (high dermal delivery resulting in a reduction of the amount in the donor chamber). Actually, the amount of test substance to reach steady-state conditions depends on its permeability: the lower the permeability, the lower the dose necessary to reach steady-state. BPS was less permeable than BPA and D-8 and applying 100 µl/cm^2 of a BPS solution not at saturation led to steady-state.

Our results are in agreement with skin absorption estimates based on the test substances' molecular weight (MW) and logK$_{ow}$. These physico-chemical properties play an important role in passive diffusion of chemicals through the stratum corneum. The stratum corneum is the lipidic layer of the skin and is composed of corneocytes and inter-cellular lipid lamellae. The most efficient route of diffusion through the stratum corneum is the intercellular route among the lipid lamellae. Chemicals that follow this route have a MW lower than 500 Da and are lipophilic. BPS, D-8 and BPA have similar MWs in the range of 250-300 Da. BPA and D-8 have in addition similar logK$_{ow}$, while BPS has a lower logK$_{ow}$. Although BPA had an approximately 1.5-fold higher permeation rate and absorbed dose than D-8, this can be explained by the higher BPA concentration and dose applied onto the skin. Thus, we conclude that D-8's absorption was similar to BPA. As expected, BPS's skin absorption was consistently lower than BPA and D-8 (Figure 1 and Table 3). Percent dose of BPS in the skin and receptor fluid (11%) was a third compared to D-8 (33%).

BPA

Mass balance assays achieved an excellent recovery of BPA (98% ±13%). A comparison of our BPA mass balance results with literature data (Table 5) shows that all studies agree on the absorption in the skin (dermis + epidermis + stratum corneum excluding the first two tape strips) in the 12 % - 27% range. The largest difference among these studies is in the absorbed dose. The greatest absorbed dose (46%, 3.5 µg/cm^2) is reported by (Liu and Martin 2019), probably because of the use of a thinner (120 µm) 3D model skin and a high vehicle volume (1538 µl/cm^2). Also (Zalko et al. 2011) reported an absorbed dose of 46% (1.3 µg/cm^2), using 500 µm-thick skin and a low vehicle volume (10 µl/cm^2). The second greatest absorbed dose is reported by (Champmartin et al. 2020) (41%, 8.2 µg/cm^2) with a 476 µm-think skin and a 50 µl/cm^2 volume, followed by this study (25%, 6.4 µg/cm^2), using a thicker skin (800 µm) and a 100 µl/cm^2 volume. The lowest absorbed doses have been reported by (Kaddar et al., 2008; Demierre et al., 2012; Toner et al., 2018) (2%, 0.03-0.06 µg/cm^2) and (Mørck et al., 2010) (13%), and were probably due to the smaller vehicle volume used.

Our results show that BPA metabolism by skin into its glucuronide conjugate was negligible. A limitation of our study is the use of saline as the receptor fluid in the experiments where skin metabolism was studied. For skin metabolism studies cell culture media are the recommended receptor fluids (OECD, 2004b). Cell culture media support longer skin viability and it does not hinder the quantification of radiolabelled analytes, which are often used in this type of studies. In our study, we preferred the use of a simpler matrix (saline) because our test substances were not radio-labelled and were quantified by LC-MSMS. However, our experiments started no more than two hours from retrieving the skin. Such a short delay led to results in agreement with Marquet et al. (2011), who used cell culture media receptor fluid and reported that BPA was not at all or only very slightly metabolised by viable human skin (< 2.5% of the dose). Other two studies show higher values of BPA-conjugated metabolites and more polar compounds: 27% (Zalko et al., 2011) and 8% (Toner et al., 2018). The main difference is that these two studies did not use diffusion cells but a multi-well system. In this system, the skin sample soaks in receptor fluid containing the chemical of interest. This allows the study of the overall skin metabolic capacity neglecting chemical's skin permeation kinetics. The CEF-EFSA Panel considered this method an overestimation of *in vivo* skin metabolism (EFSA, 2015).

BPA alternatives

The low D-8 and BPS recoveries in mass balance assays could be due to various factors: tape-stripping samples not being included in the mass balance, low cotton swabs recoveries, metabolism, skin protein binding, or photo-degradation. Studies on BPS have reported metabolism into its glururonide and hydroxylated forms (Skledar et al., 2016), and photodegradation (Kovačič et al., 2019). For D-8, no data are available on its metabolism or stability. Considering that Liu and Martin (2019) and Champmartin et al. (2020) found no or limited BPS conjugated metabolites in their assays, and that we took special care to avoid photo-degradation (laboratory lights turned off during skin exposure to BPS, use of amber glass vials), plausible causes of low BPS mass balance are the exclusion of tape stripping samples, and the extraction efficiency of the skin and cotton swabs. D-8 and BPS mass balance results were close to the recommended range of 100 ± 20% for non-radiolabelled test substances (OECD, 2011). Our results for BPS mass balance showed that most BPS was in the dislodgeable dose (73%) and less in the skin (11%). This is in contrast with Champmartin et al. (2020) who found a large amount of BPS to remain in the skin (47%). The low recovery of PF201 in the mass balance assays could be due to metabolism, binding with skin proteins, and/or to its instability at skin pH (5.5 in humans). While there are no data on PF201 metabolism in the literature, it is known that PF201 is unstable in protic solvents at pH < 7 (Eckardt and Simat, 2017). Although we did not conduct stability tests, we observed that PF201 was stable in the aqueous test

preparation and in the receptor fluid. Therefore, a hypothesis is that PF201 hydrolysed in direct contact with the skin (pH = 5.5). If dermal absorption of PF201 is expected to be very limited or negligible, as already mentioned, the dislodgeable dose should be close to the applied dose, which is not the case. Therefore, even if PF201's metabolism by the skin and protein binding cannot be excluded, the low PF201 amount quantified in the skin rinsing (22% of applied dose) supports the hypothesis of PF201's hydrolysis in contact with skin. Overall, PF201 skin permeability is likely to be very low. Future studies are needed to better understand the possible PF 201 hydrolysis, metabolism and binding in the skin.

Our results for BPS are in line with Liu and Martin (2019) and Champmartin et al. (2020) in that BPS dermal absorption is consistently lower than BPA. However, in our study, BPS' K_p was two orders of magnitude lower than that of Liu and Martin (2019) (0.24×10^{-4} cm/h vs. 30×10^{-4} cm/h). This could be due to several differences in the experimental setup, as discussed for BPA. First, different skins and diffusion systems: our study used ex-vivo human skin and flow-through diffusion cells, while Liu and Martin (2019) used a 3D skin model consisting of organized human keratinocytes on tissue culture inserts and static diffusion cells designed specifically for the 3D skin model. Second, different skin thicknesses (200 μm in our study vs. 120 μm in Liu and Martin (2019)) and different vehicle volumes applied on the skin (100 μl/cm² in our study vs. 1538 μl/cm² in Liu and Martin (2019)). The effect of skin thickness on K_p is well-known as K_p is by definition inversely proportional to the skin thickness. The effect of hydration is known to increase skin permeability (Bunge et al., 2012; Frasch et al., 2014; Zhu et al., 2016). A higher skin thickness and a lower skin hydration (hence the lower volume of aqueous solution applied on the skin) could explain the lower BPS skin absorption in our study. Accordingly, Champmartin et al. (2020) used thicker skin (476 μm thickness) than both Liu and Martin and our studies as well as a vehicle volume (50 μl/cm²) that was half compared to our experiments and 30 times lower than Liu and Martin (2019). Champmartin et al obtained a K_p value only one order of magnitude lower than in our study (0.026×10^{-4} cm/h).

Limitations

Some limitations of this study have already been acknowledged, such as not assessing metabolism when viable skin was used, and not validating the skin extraction recovery. However, the BPA amount extracted from skin was in line with data reported in the literature. This suggests that the method used for skin extraction was efficient. Another limitation was not quantifying the amount of chemicals in the tape-strip samples, thus omitting this value in the recovery calculation. Colour developers are present as neat powder in thermal paper. We did not assess skin permeation of the neat powder or as in receipts per se. Applying colour developers as a powder on the skin might be closer to a scenario of a person touching thermal paper, although, this experimental set-up would not take into

account the pressure applied and rubbing of the receipts when they are handled. Applying an infinite dose in aqueous solution of the colour developers, as we did in our study, would simulate an exposure scenario of a solid on sweaty or moistened hands.

5. Conclusion

Overall, we can conclude qualitatively that skin absorption was in increasing order: PF201 < BPS << D-8 < BPA. These results are in agreement with these chemicals' log K_{ow} and MW. BPA metabolism by the skin was negligible in our test conditions. The absorbed dose in the receptor fluid was 25%, 17%, 0.4% and <LOQ for BPA, D-8, BPS and PF201, respectively. Low mass balance results for Pergafast 201® suggest that this molecule could undergo hydrolysis and/or binding when in contact with the stratum corneum.

Conflict of interest

The authors declare no competing interests.

References

Biedermann S, Tschudin P, Grob K. Transfer of bisphenol A from thermal printer paper to the skin. Analytical and Bioanalytical Chemistry. 2010 Sep;398(1):571–6.

Björnsdotter MK, Jonker W, Legradi J, Kool J, Ballesteros-Gómez A. Bisphenol A alternatives in thermal paper from the Netherlands, Spain, Sweden and Norway. Screening and potential toxicity. Science of The Total Environment. 2017 Dec 1;601–602:210–21.

Braun P, Moeder M, Popp P, Kuschk P, Engewald W, others. Trace analysis of technical nonylphenol, bisphenol A and 17α-ethinylestradiol in wastewater using solid-phase microextraction and gas chromatography–mass spectrometry. Journal of Chromatography A. 2003;988(1):41–51.

Bunge AL, Persichetti JM, Payan JP. Explaining skin permeation of 2-butoxyethanol from neat and aqueous solutions. Int J Pharm. 2012 Oct 1;435(1):50–62.

Champmartin C, Marquet F, Chedik L, Décret M-J, Aubertin M, Ferrari E, et al. Human in vitro percutaneous absorption of bisphenol S and bisphenol A: A comparative study. Chemosphere. 2020 Aug 1;252:126525.

Danish EPA. Alternative technologies and substances to bisphenol A (BPA) in thermal paper receipts. The Danish Environmental Protection Agency; 2014. (Environmental Project).

Demierre A-L, Peter R, Oberli A, Bourqui-Pittet M. Dermal penetration of bisphenol A in human skin contributes marginally to total exposure. Toxicology Letters. 2012 Sep;213(3):305–8.

Eckardt M, Simat TJ. Bisphenol A and alternatives in thermal paper receipts - a German market analysis from 2015 to 2017. Chemosphere. 2017 Nov;186:1016–25.

EFSA. Scientific Opinion on the risks to public health related to the presence of bisphenol A (BPA) in foodstuffs. EFSA Journal. 2015;13(1):3978.

EPA. Bisphenol A alternatives in thermal paper. United States Environmental Protection Agency; 2014.

Frasch HF, Barbero AM, Dotson GS, Bunge AL. Dermal permeation of 2-hydroxypropyl acrylate, a model water-miscible compound: Effects of concentration, thermodynamic activity and skin hydration. International Journal of Pharmaceutics. 2014 Jan;460(1–2):240–7.

Goldinger DM, Demierre A-L, Zoller O, Rupp H, Reinhard H, Magnin R, et al. Endocrine activity of alternatives to BPA found in thermal paper in Switzerland. Regulatory Toxicology and Pharmacology. 2015 Apr;71(3):453–62.

Heinälä M, Ylinen K, Tuomi T, Santonen T, Porras SP. Assessment of Occupational Exposure to Bisphenol A in Five Different Production Companies in Finland. Ann Work Expo Health. 2017 01;61(1):44–55.

Hines CJ, Jackson MV, Deddens JA, Clark JC, Ye X, Christianson AL, et al. Urinary Bisphenol A (BPA) Concentrations among Workers in Industries that Manufacture and Use BPA in the USA. Ann Work Expo Health. 2017 01;61(2):164–82.

Hormann AM, vom Saal FS, Nagel SC, Stahlhut RW, Moyer CL, Ellersieck MR, et al. Holding Thermal Receipt Paper and Eating Food after Using Hand Sanitizer Results in High Serum Bioactive and Urine Total Levels of Bisphenol A (BPA). PLoS One [Internet]. 2014 Oct 22 [cited 2015 Aug 24];9(10). Available from: http://www.ncbi.nlm.nih.gov/pmc/articles/PMC4206219/

Kaddar N, Harthé C, Déchaud H, Mappus E, Pugeat M. Cutaneous Penetration of Bisphenol A in Pig Skin. Journal of Toxicology and Environmental Health, Part A. 2008 Mar 12;71(8):471–3.

Kovačič A, Gys C, Kosjek T, Covaci A, Heath E. Photochemical degradation of BPF, BPS and BPZ in aqueous solution: Identification of transformation products and degradation kinetics. Science of The Total Environment. 2019 May;664:595–604.

Lassen C, Mikkelsen SH, Brandt UK. Migration of bisphenol A from cash register receipts and baby dummies. Danish Environmental Protection Agency; 2011 p. 67. (Survey of Chemical Substances in Consumer Products). Report No.: 110 2011.

Liu J, Martin JW. Comparison of Bisphenol A and Bisphenol S Percutaneous Absorption and Biotransformation. Environ Health Perspect. 2019 Jun;127(6):67008.

Marquet F, Payan J-P, Beydon D, Wathier L, Grandclaude M-C, Ferrari E. In vivo and ex vivo percutaneous absorption of [14C]-bisphenol A in rats: a possible extrapolation to human absorption? Archives of Toxicology. 2011 Sep;85(9):1035–43.

Matuszewski BK, Constanzer ML, Chavez-Eng CM. Strategies for the assessment of matrix effect in quantitative bioanalytical methods based on HPLC-MS/MS. Anal Chem. 2003 Jul 1;75(13):3019–30.

Mørck TJ, Sorda G, Bechi N, Rasmussen BS, Nielsen JB, Ietta F, et al. Placental transport and in vitro effects of Bisphenol A. Reproductive Toxicology. 2010 Aug;30(1):131–7.

Ndaw S, Remy A, Jargot D, Robert A. Occupational exposure of cashiers to Bisphenol A via thermal paper: urinary biomonitoring study. International Archives of Occupational and Environmental Health. 2016 Aug;89(6):935–46.

OECD. OECD Existing Chemicals Database - Bisphenol A [Internet]. 2003 [cited 2019 Nov 20]. Available from: https://hpvchemicals.oecd.org/UI/SIDS_Details.aspx?key=6d209d66-9690-4739-8745-ac4732d5f53d&idx=0

OECD. Organisation for Economic Co-operation and Development, Guidelines for the testing of chemicals, Section 4, Test Nº 428: Skin absorption: In Vitro Method [Internet]. 2004a [cited 2019 Sep 11]. Available from: https://www.oecd-ilibrary.org/environment/test-no-428-skin-absorption-in-vitro-method_9789264071087-en

OECD. Organisation for Economic Co-operation and Development, Series on Testing and Assessment Nº 28, Guidance Document for the Conduct of Skin Absorption Studies. [Internet]. OECD; 2004b [cited 2019 Sep 11]. Available from: https://www.oecd-ilibrary.org/environment/guidance-document-for-the-conduct-of-skin-absorption-studies_9789264078796-en

OECD. Organisation for Economic Co-operation and Development, Series on Testing and Assessment Nº. 156, Guidance Notes on Dermal Absorption. [Internet]. 2011. Available from: https://www.oecd.org/chemicalsafety/testing/48532204.pdf

Pinnagoda J, Tupker RA, Agner T, Serup J. Guidelines for transepidermal water loss (TEWL) measurement. A report from the Standardization Group of the European Society of Contact Dermatitis. Contact Derm. 1990 Mar;22(3):164–78.

Reale E, Fustinoni S, Mercadante R, Polledri E, Hopf NB. Simultaneous Quantification of Bisphenol A, Its Glucuronide Metabolite, and Commercial Alternatives by LC-MS/MS for In Vitro Skin Absorption Evaluation. Chem Res Toxicol. 2020 Sep 21;33(9):2390–400.

Selzer D, Abdel-Mottaleb MMA, Hahn T, Schaefer UF, Neumann D. Finite and infinite dosing: Difficulties in measurements, evaluations and predictions. Advanced Drug Delivery Reviews. 2013 Feb 1;65(2):278–94.

Skledar DG, Schmidt J, Fic A, Klopčič I, Trontelj J, Dolenc MS, et al. Influence of metabolism on endocrine activities of bisphenol S. Chemosphere. 2016 Aug;157:152–9.

Thayer KA, Taylor KW, Garantziotis S, Schurman SH, Kissling GE, Hunt D, et al. Bisphenol A, Bisphenol S, and 4-Hydroxyphenyl 4-Isprooxyphenylsulfone (BPSIP) in Urine and Blood of Cashiers. Environ Health Perspect. 2016 Apr;124(4):437–44.

Toner F, Allan G, Dimond SS, Waechter JM, Beyer D. In vitro percutaneous absorption and metabolism of Bisphenol A (BPA) through fresh human skin. Toxicol In Vitro. 2018 Mar;47:147–55.

US EPA. Bisphenol A alternatives in thermal paper, Final report. United States Environmental Protection Agency; 2014.

Vervliet P, Gys C, Caballero-Casero N, Covaci A. Current-use of developers in thermal paper from 14 countries using liquid chromatography coupled to quadrupole time-of-flight mass spectrometry. Toxicology. 2019 Mar 15;416:54–61.

Yang Y, Yang Y, Zhang J, Shao B, Yin J. Assessment of bisphenol A alternatives in paper products from the Chinese market and their dermal exposure in the general population. Environ Pollut. 2019 Jan;244:238–46.

Zalko D, Jacques C, Duplan H, Bruel S, Perdu E. Viable skin efficiently absorbs and metabolizes bisphenol A. Chemosphere. 2011 Jan;82(3):424–30.

Zhu H, Jung E-C, Phuong C, Hui X, Maibach H. Effects of soap–water wash on human epidermal penetration. J Appl Toxicol. 2016 Aug 1;36(8):997–1002.

Annex III

Influence of experimental parameters on in vitro human skin permeation of Bisphenol A

E. Reale[a], A. Berthet[a], P. Wild[a,b], D. Vernez[a], N. B. Hopf[a]

[a] Center for Primary Care and Public Health (Unisanté), affiliated to University of Lausanne, Route de la Corniche 2, 1066 Epalinges-Lausanne, Switzerland.

[b] French Research and Safety Institute (INRS), 1 rue du Morvan, CS 60027, F-54519, Vandœuvre cedex, France.

Corresponding author: Nancy B. Hopf PhD, Center for Primary Care and Public Health (Unisanté), Route de la Corniche 2, 1066 Epalinges-Lausanne, Switzerland. E-mail: Nancy.Hopf@unisante.ch. Ph.: 0041-21-3149558

Abstract

Bisphenol A (BPA) in vitro skin permeation studies have shown inconsistent results, which could be due to experimental conditions. We studied the impact of in vitro parameters on BPA skin permeation using flow-through diffusion cells with ex-vivo human skin (12 donors, 3-12 replicates). We varied skin status (viable or frozen skin) and thickness (200, 400, 800 µm), BPA concentrations (18, 250 mg/l) and vehicle volumes (10, 100 and 1000 µl/cm^2). These conditions led to a wide range of BPA absorption (2%-24% after 24 hour exposure), peak permeation rates (J = 0.02-1.31 µg/cm^2/h), and permeability coefficients (K$_p$ = 1.6-5.2 x 10^{-3} cm/h). This is the first time steady state conditions were reached for BPA aqueous solutions in vitro (1000 µl/cm^2 applied at concentration 250 mg/l). A reduction of the skin thickness from 800 and 400 µm to 200 µm led to a 3-fold increase of J (P < 0.05). A reduction of the vehicle volume from 1000 to 100 led to a 2-fold decrease in J (P > 0.05). Previously frozen skin led to a 3-fold increase in J compared to viable skin (P < 0.001). We found that results from published studies were consistent when adjusting J according to experimental parameters. We propose appropriate J values for different exposure scenarios to calculate BPA internal exposures for use in risk assessment.

Keywords

BPA, percutaneous absorption, human skin, skin thickness, vehicle volume, permeation constant

1. Introduction

Bisphenol A (BPA) is a high production volume chemical (OECD, 2003) with endocrine disruptive effects (Peretz et al., 2014). It is primarily used in polycarbonate plastics such as food and drink containers, as well as in tin cans with epoxy resin lining. Food and drinks in contact with BPA-containing materials are the major source of BPA exposure (EFSA, 2015). In March 2015, the European Food Safety Authority (EFSA) Panel for Food Contact Materials, Enzymes, Flavourings and Processing Aids (CEF) gave a Scientific Opinion on public health risks related to the presence of BPA in foodstuff. It concluded that there is no health concern for any age group from dietary exposure, but noted considerable uncertainty in the exposure estimates for non-dietary sources (EFSA, 2015). Indeed, exposure from food alone cannot explain reported BPA blood and urine concentrations (Mielke and Gundert-Remy, 2009; Völkel et al., 2002). This underestimation of exposure could potentially be due to additional routes of absorption such as skin contact contributing to the overall human exposure to BPA.

The second largest BPA source of exposure is thermal paper used in receipts, labels and tickets, where BPA is used as a color developer (EFSA, 2015). Upon handling, BPA migrates from the thermal paper onto the skin and can be absorbed (Biedermann et al., 2010) or ingested due to hand-to-mouth transfer (Hormann et al., 2014). Skin exposure could contribute significantly to overall BPA body burden. Contrary to ingested BPA, skin absorbed BPA does not undergo first-pass metabolism but goes directly into the systemic circulation (Gundert-Remy et al., 2013). Ndaw et al. (2016) reported that cashiers handling thermal paper receipts daily had higher urinary BPA concentrations compared to non-occupationally exposed workers.

Estimated *in vitro* BPA skin permeation studies have shown inconsistent results, which could be due to experimental conditions (Champmartin et al., 2020; Demierre et al., 2012; Kaddar et al., 2008; Liu and Martin, 2019; Marquet et al., 2011; Mørck et al., 2010; Toner et al., 2018; Zalko et al., 2011). These studies reported different results for total absorbed BPA (epidermis + dermis + receptor fluid) ranging between 18% (Toner et al., 2018) and 87% (Zalko et al., 2011). Skin permeation kinetics were assessed in five of these studies, which report peak permeation rates (J, $\mu g/cm^2/h$) ranging four orders of magnitude between 3.0×10^{-5} and 7.0×10^{-1} $\mu g/cm^2/h$ (see Table 1). These values were obtained in finite dose experiments where the permeation rate, also called flux, was not constant, but increased to a peak (J_{peak}) before progressively decreasing (Kasting, 2001). In infinite dose experiments, the permeant on the skin is not depleted. Infinite dose permeation rates reach a maximum constant value (steady state) described by Fick's first law of diffusion:

$$J_{ss} = K_p \times C$$

where J_{ss} represents the diffusion of a mass per unit time and exposed membrane area, K_p is the permeability coefficient (cm/h), a kinetic parameter unique to the test substance, and C is the concentration of the substance in the solution applied on the membrane.

BPA skin absorption did not reach the steady state in any of these previous studies. Liu and Martin (2019) reported a K_p value for BPA in water; however, a decrease in J after 11 h of exposure suggest that steady state was not reached in their study. Due to these inconsistencies, no overall conclusion can be made concerning BPA's permeation through human skin. Consequently, a range of different skin permeation values has been used in risk assessments (ANSES, 2013; EFSA, 2015) and in toxicokinetic models (Karrer et al., 2018; Mielke and Gundert-Remy, 2012). The CEF Panel is seeking more data on BPA toxicokinetics to reduce the uncertainty regarding skin absorption in BPA hazard assessments (EFSA, 2018).

Table 2 Experimental setup and results of BPA ex vivo human skin permeation kinetics studies in the literature.

Authors	Marquet et al., 2011	Demierre et al., 2012	Toner et al., 2018	Liu and Martin, 2019	Champmartin et al., 2020
Skin parameters					
Skin thickness (µm)	400	200	350-400	120	476 ± 56
Skin status	Frozen	Frozen	Viable	3D model with metabolic activity	Viable
Skin anatomical location	NA	Dorsal part of upper leg	Abdomen	Human skin model	Abdomen
Methods					
System	Static diffusion cells	Flow through-diffusion cells	Flow through-diffusion cells, 12-well plate for metabolism	Static diffusion device in 6-well plates	Static diffusion cells
BPA concentration (mg/l)	4000	194[a]	300, 60, 12, 2.4	5, 1	400
Vehicle	Acetone	Water	Phosphate buffered saline (PBS)	Water	Water, Acetone, Sebum
Vehicle volume (µl/cm^2)	50	9.4	10	1538	50
BPA dose (µg/cm^2)	200	1.82	3, 0.6, 0.12, 0.024	7.7, 1.5	20
Receptor fluid	RPMI[b], 2% BSA[b], 1% penicillin/streptomycin	Physiological saline solution	DMEM[b] + 1% ethanol + UDPGA[b] 2mM + PAPS[b] 40 µM	PBS [b]	RPMI 1640 solution + 0.2% gentamycin + 2.5% penicillin–streptomycin + 2% BSA[b]
Exposure time (h)	24	24	24	25	24
Results					
J (µg/cm^2/h)	0.12	0.022	3.4E-03, 0.48E-03, 0.14E-03, 0.03E-03 [c]	0.163, 0.036 [d]	0.70, 0.0372, 0.0186 [e]
K$_p$ (cm/h)	NA	NA	NA	0.033, 0.036 [d]	NA, 9.3E-05, 4.65E-05 [e]

NA, not available

[a] BPA-$^{13}C_{12}$ concentration, equivalent to 184 mg BPA/l

[b] Acronyms: RPMI Rosewell Park Memorial Institute medium, BSA bovine serum albumin, DMEM Dulbecco's Modified Eagle Medium, UDPGA Uridine 5'-diphosphoglucuronic acid, PAPS 3'-phosphoadenosine-5'-phosphosulfate, PBS Phosphate buffered saline

[c] Values corresponding to the 300, 60, 12, and 2.4 mg/l dosing solutions, respectively.

[d] Values corresponding to the 5 and 1 mg/l dosing solution, respectively

[e] Values corresponding to water, acetone, and sebum vehicle, respectively. For BPA applied in acetone and sebum reported values are J$_{ss}$.

The differences in published BPA skin permeation data are probably due to different experimental parameters. The Organisation for Economic Co-operation and Development (OECD) Test Guideline 428 (OECD, 2004a), Guidance Document 28 (OECD, 2004b) and Guidance Notes 156 (OECD, 2011) allow skin permeation laboratories the flexibility to adapt several experimental parameters to their research purposes. However, this flexibility makes it difficult to compare results across studies.

The aim of this study was to assess the influence of different experimental parameters on BPA skin permeation kinetics based on the hypothesis that the same experimental setups should lead to the same results. The main experimental parameters that can affect skin permeation are skin state (viable and frozen), vehicle volume

(volume of BPA solution applied on the skin), concentration of the dosing solution applied on the skin, and skin thickness. We thus focused our experimental design on these parameters.

2. Methods

2.1 Materials and chemicals

BPA was purchased from Sigma-Aldrich Chemie GmbH, Buchs, Switzerland. HPLC-grade acetonitrile and water were obtained by Sigma-Aldrich Chemie GmbH, Buchs, Switzerland. Physiological saline solution (saline) was prepared dissolving 0.9% (w/v) sodium chloride (purissim. p.a. $\geq$ 99.5%, supplied by Sigma-Aldrich Chemie GmbH, Buchs, Switzerland) in Milli-Q® water (Milli-Q® Advantage ultra-pure water system, Millipore, Milford, MA, USA). BPA test solutions were prepared at different BPA concentrations (18, 164, 250 mg/l) in MilliQ water. The 250 mg/l concentration was based on the reported range of BPA water solubility values (120-300 mg/l, source: US EPA (2014)), 164 mg/l concentration was chosen for comparison with one published article on BPA skin permeation (Demierre et al., 2012), and 18 mg/l was a third value to test the effect of concentration on BPA kinetics. BPA was soluble in both donor and receptor fluids at the tested concentrations as required by the OECD guidelines. The maximum BPA concentration in water was 250 mg/l, which was reached only after sonicating the solution for 1 hour and leaving it for 24 h. This solution was considered saturated and was within the reported water solubility values.

2.2 Skin permeation assays

Skin permeation studies were carried out in agreement with the OECD guideline 428 (OECD, 2004a). Skin permeation was assessed through viable human skin using a 9-cell jacketed flow-through diffusion cell system (PermeGear® obtained from SES Analytical System, Bechenheim, Germany). Saline was pumped (50 µl/min; peristaltic pump from Ismatec IPC-N, IDEX Health and Science GmbH, Wertheim-Mondfeld, Germany) through the receptor chamber. Cells were kept at 32°C by a heated water-bath circulator (Haake SC 100 Digital Immersion Circulator, 100 °C w/cla, Thermo Scientific, Newington, NH, USA). Full thickness human abdominal skin was obtained immediately following surgery from the Plastic and Reconstructive Surgery Department (DAL) at the Centre Hospitalier Universitaire Vaudois (CHUV, Lausanne, Switzerland) (ethical protocol 264/12). Patients' data were kept anonymous except for gender and age. Number of donors and replicates varied considerably from one experiment to the other because it depended on the availability of the skin from the Plastic and Reconstructive Surgery Department on experimental days. Skin was rinsed with saline and dermatomed (Acculan®II, B. Braun/Aesculap, Sempach, Switzerland) at 800, 400 or 200 µm. The skin

thickness used in each experiment is listed in Table 2. Then skin was cut into circular sections to fit the flow-through diffusion cells (11.28 mm diameter, 1 cm^2 area). These skin flaps were mounted onto the flow-through diffusion cells with the stratum corneum facing up and left to stabilize for 30-min. No more than two h elapsed from retrieving to mounting the skin onto the cells. Trans-epidermal water loss (TEWL) (VapoMeter wireless, Delfin Technologies Ltd., Kuopio, Finland) was measured for each skin flap to assess skin sample integrity (Bronaugh and Maibach, 2005). Skin samples with a TEWL greater than 11 g/m^2/h were excluded (Pinnagoda et al., 1990). Skin samples were exposed to different volumes of BPA test preparations at different concentrations for 24 h.

In order to facilitate comparison, several parameters used in our experiments were the same as a previously published article on BPA skin permeation (Demierre et al., 2012): flow-through system, use of aqueous solution as vehicle to apply BPA on the skin, use of saline as receptor fluid, receptor fluid's flow rate, frequency and number of collecting times. Parameters that varied from Demierre et al. (2012) were namely skin state, skin thickness, vehicle volume, and BPA concentration in the test preparation. The different parameters used for each experiment are listed in Table 2. Frozen skin (EXP2 in Table 2) refers to previously frozen skin that had been frozen (- 80°C) immediately after dermatoming, stored for up to six months, and thawed at room temperature before testing. In all experiments, receptor fluid was sampled by a fraction collector (FC 204, Gilson Inc., Middleton, WI, USA) at specific time intervals up to 24 h. Test solution was removed from donor chambers with a pipette and skin surfaces were wiped with cotton swabs and paper tissues at the end of the experiments where 1000 µl were applied. This was not necessary for experiments with volumes smaller than 1000 µL as these skin samples were already dry after 24 h. TEWL was tested again at the end of each experiment to confirm skin integrity throughout the whole experiment. Methods and results of EXP5 in Table 2 have been previously described (Reale et al., 2020). Briefly, experimental conditions were identical to those described for EXP6 in Table 2 except for vehicle volume (100 µl instead of 1000 µl).

Table 3 Summary of BPA skin permeation experiments

Experiment	Concentration [mg BPA/l]	Vehicle volume[µl/cm^2]	Dose [µg/cm^2]	Skin donors [D]	Total skin samples [n]	Skin thickness [µm]	Skin state
EXP0	164	10	1.6	2	6	800	Viable
EXP1	250	100	25	3	10	800	Viable
EXP2	250	100	25	3	9	800	Frozen (-80°C)
EXP3	18	100	1.8	2	6	800	Viable
EXP4	250	1000	250	3	10	800	Viable
EXP5 [a]	250	100	25	3	12	200	Viable
EXP6	250	1000	250	1	3	200	Viable
EXP7	250	1000	250	1	3	400	Viable

[a] EXP5 data are reported here from Reale et al. (2020).

2.3 Sample assays

BPA concentrations in the receptor fluid samples were quantified by high-performance liquid chromatography coupled with fluorescence detection (HPLC-FLD). Samples were filtered with 4-mm syringe filters (PTFE 0.45 µm, BGB Analytik) and then injected into the HPLC. The HPLC was equipped with the following: a pump (Prostar 240, Varian Inc.) pumping HPLC-grade acetonitrile (A) and water (B) in gradient mode at 0.5 ml/min; an auto-sampler (Prostar 410, Varian Inc.) injecting 10 µl sample; a packed column (Accucore™ Phenyl-X column 150 mm x 4.6 mm I.D., 2.6 µm, Thermo Scientific) heated at 30°C; a fluorescence detector (Prostar 363, Varian Inc.) set at an excitation wavelength of 225 nm and an emission wavelength of 306 nm. The gradient program started with 60:40 A:B (v/v) and increased linearly to 98:2 A:B from 0 to 5 min. This condition was held until 8.5 min. From 8.5 to 9 min, the elution program returned to the initial condition and then held for 13 min. Under these conditions, BPA's retention time was 4.55 min. The calibration standards were prepared in saline, over the range 1.95-500 µg/l, where linearity was ensured (mean $R^2 = 0.999$). Calibration curves were calculated by linear regression of the peak area subtracted of the blank peak area, plotted over the nominal concentration for each calibration standard. A value equal to zero was used for each sample concentration under the lower limit of quantification (LLOQ = 1.95 µg/l). Precision (CV %) and accuracy (% deviation from nominal concentration) were calculated for two replicates of three concentrations (7.8, 62.5 and 125 µg/l) on three different days. Precision was 10%, 2% and 2%, and accuracy 104%, 98%, and 99% for the three tested concentrations.

2.4 Permeation rate, lag time, and permeability coefficient

The cumulative amount of BPA in the receptor fluid per unit skin area was plotted over time for each skin sample (permeation curve). For each plot, the peak permeation rate (J_{peak}, µg/cm^2/h) was calculated as the slope of the steepest linear portion of the permeation curve by fitting a piecewise linear model with an initial plateau and subsequent increase using a nonlinear regression model. The linear portion after the initial plateau was identified visually prior to the fitting. K_p was calculated using Fick's first law only for those experiments where J reached a maximum constant value (steady state, J_{ss}). The lag time, or time needed to reach the steady state (t_{lag}), was calculated as the time (x-axis) intercept of the steady state portion of the permeation curve. When the steady state was not reached, the time to reach the peak permeation rate (apparent lag time) was calculated as the time (x-axis) intercept of the steepest linear portion of the permeation curve.

2.5 Statistical data analysis

The by-experiment estimates of J, K_p and t_{lag} were further analyzed as a function of several experimental parameters using a linear mixed-effect model. These parameters were skin state (viable vs. frozen), skin thickness, vehicle volume applied on skin, and BPA concentration applied on skin. Skin donor was used as a random effect. Restricted Maximum Likelihood was used to fit this mixed model. We report estimates and standard errors of J, K_p and t_{lag} obtained as predictions from this model. The difference in J, K_p and t_{lag} values due to the variation on one tested parameter was considered statistically significant when P value was <0.05. Statistical data analysis was done using Stata/IC v. 14.0 (StataCorp LLC, TX, USA).

3. Results

Table 3 summarizes the results by paired comparisons between experiments differing by only one experimental parameter (Table 3, column "Experimental parameter for statistical analysis"): skin state (viable vs. frozen), vehicle concentration, vehicle volume, and skin thickness. The effects of vehicle concentration, vehicle volume and skin thickness were tested with viable skin. The reported results are the mean BPA amount in the receptor fluid (as % of the dose) after 24 h of exposure, as well as model-based estimates of J, t_{lag}, and K_p. These estimates take into account the within-donor correlation, which is highly influential given the uneven number of replicates for each donor. This is the reason why the results for the same experiments varied slightly across the comparisons (e.g. J_{peak} for EXP1 was 0.14 and 0.21 for skin status and vehicle concentration, respectively). The effects that the studied experimental parameters had on BPA mean skin permeation curves are shown in Figures 1 to 4. Mean permeation curves were calculated over total skin samples used for experiments EXP1 to EXP7. EXP0 of Table 2 was not compared statistically because it differed by two or more parameters with any other experiment. The mean (±SD) J_{peak} value for EXP0 was 0.006 (±0.003) (n = 6) (permeation curve not shown). It is worth noting that in the paired comparisons where vehicle volume changed, either the dose or the concentration also needed to change. We opted to keep concentration constant, as it is directly related to J, which is the parameter we compared across experiments.

Mean BPA permeation curves for viable and frozen skin are compared in Figure 1. Human skin frozen at -80°C had 3.4-fold higher J (P < 0.001) compared to viable skin. Mean BPA permeation curves for different BPA concentrations are shown in Figure 2. A 14-fold increase in applied BPA concentration (18 vs. 250 mg/l) led to a 10.5-fold increase in J (P < 0.05), as expected since J is dependent on the permeant's concentration. Mean BPA permeation curves for different vehicle volumes are shown in Figure 3. The curves show that J reached a maximum constant value, i.e. J_{ss}, only in the experiment where 1000 µl of vehicle were applied on the skin.

Table 4 Effect of different experimental parameters on BPA skin permeation kinetics. Model-based estimates (±se) are reported. Human skin was viable in all experiments except in EXP2.

Experiment	Experimental parameter for statistical analysis	Vehicle volume [µl]	Dose [µg/cm²]	Skin thickness [µm]	BPA in receptor fluid at 24 h [% of the dose]	J_{peak} [µg/cm²/h] model-based estimate (±se)	P^a	K_p × 10^{-3} [cm/h] model-based estimate (±se)	P^a	t_{lag} [h] model-based estimate (±se)	P^a
	Skin status										
EXP1	**Viable skin**	100	25	800	13 (±8)	0.14 (±0.08)		NA		8.1[e] (±0.5)	
							<0.001		NA		0.009
EXP2	**Frozen skin**	100	25	800	24 (±8)	0.47 (±0.08)		NA		6.5[e] (±0.5)	
	Vehicle concentration [mg/L]										
EXP1	**250**	100	25	800	13 (±8)	0.21 (±0.06)		NA		8.0[e] (± 2.2)	
							0.041		NA		0.947
EXP3	**18**	100	1.8	800	16 (±8)	0.02 (±0.07)		NA		8.2[e] (± 2.7)	
	Vehicle volume [µl/cm²]										
EXP1	**100**	100	25	800	13 (±8)	0.21 (±0.08)		NA		8.0[e] (±1.0)	
							0.078[g]		NA		0.03[g]
EXP4	**1000**	1000	250	800	2.0 (±1.1)	0.42 (±0.08)[f]		1.66 (±0.33)		11.1 (±1.0)	
EXP5[b]	**100**	100	25	200	32 (±12)	0.72 (±0.18)		NA		3.9[e] (± 0.4)	
							0.119[h]		NA		<0.001[h]
EXP6	**1000**	1000	250	200	8.4 (±1.1)	1.31 (±0.31)[f]		5.25 (±1.32)		8.3 (± 0.8)	
	Skin thickness [µm]										
EXP1	**800**	100	25	800	13 (±8)	0.21 (±0.15)		NA		8.0[e] (±0.5)	
							0.013[i]		NA		<0.001[i]
EXP5[b]	**200**	100	25	200	32 (±12)	0.70 (±0.14)		NA		3.9[e] (± 0.5)	
EXP4	**800**	1000	250	800	2.0 (±1.1)	0.41 (±0.09)[f]	NA	1.63 (±0.36)	NA	11.1 (±1.2)	NA
EXP7	**400**	1000	250	400	3.1 (±1.7)	0.49 (±0.15)[f]	0.614[c]	1.94 (± 0.58)	0.614[c]	7.5 (±1.8)	0.021[c]
EXP6	**200**	1000	250	200	8.4 (±1.1)	1.31 (±0.15)[f]	<0.001[d]	5.23 (± 0.58)	<0.001[d]	7.7 (±1.8)	0.032[d]

NA, not available.

[a] P value calculated from Restricted Maximum Likelihood statistical analysis.
[b] EXP5 data are reported here from Reale et al. (2020).
[c] P values calculated comparing EXP7 with EXP4 (400 versus 800 µm skin thickness).
[d] P values calculated comparing EXP6 with EXP4 (200 versus 800 µm skin thickness).
[e] Apparent lag times.
[f] J_{SS}.
[g] P values calculated comparing EXP1 with EXP4 (100 versus 1000 µl of vehicle volume for 800 µm skin thickness).
[h] P values calculated comparing EXP5 with EXP6 (100 versus 1000 µl of vehicle volume for 200 µm skin thickness).
[i] P values calculated comparing EXP5 with EXP1 (200 versus 800 µm skin thickness for 100 µl of vehicle volume).

A volume increase from 100 to 1000 µl led to a non-significant increase in J both with 800 and 200 µm-thick skin (P = 0.078 and 0.119, respectively). Figure 4 shows the mean skin permeation curves of BPA through human skin dermatomed at 800 µm and at 200 µm, both for 100 and 1000 µl vehicle volume. With 100 µl vehicle volume, a decrease in skin thickness from 800 µm to 200 µm led to a 3.3-fold increase (P = 0.013) of BPA's J. With 1000 µl vehicle volume, a decrease in skin thickness from 800 µm to 200 µm led to a 3.2-fold increase (P < 0.001) of J, while a decrease in skin thickness from 800 to 400 µm led to a non-significant increase

in J (0.614). The amount of BPA detected in the receptor fluid after 24 h was more than double for the 200 µm-thick skin exposure, compared to the 400 and 800 µm-thick skin.
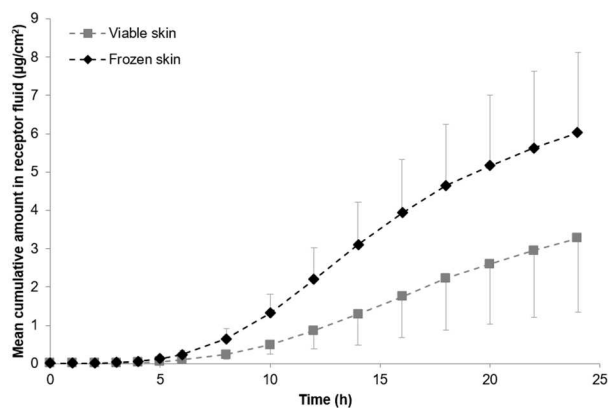

Fig. 1 Effect of freezing skin on BPA skin permeation: comparison of BPA mean skin permeation curves for 800 µm-thick viable (EXP1) and frozen (EXP2) skin during 24 hours of exposure to 25 µg/cm² of BPA. One-sided error bars (SD) are shown in the figure for clarity purposes.
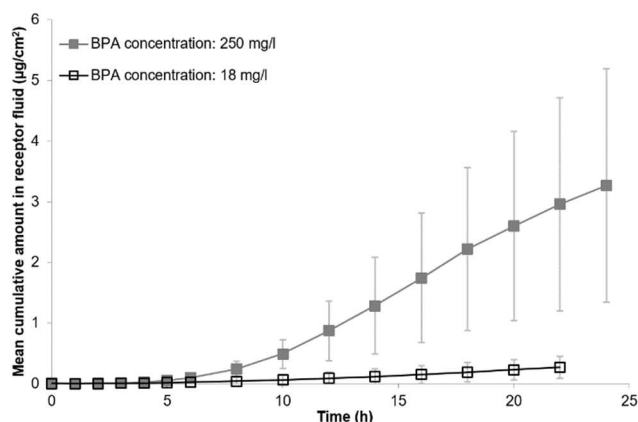
Fig. 2 Effect of BPA concentration in the vehicle applied on the skin on BPA skin permeation: comparison of BPA mean (± SD) skin permeation curves for 250 mg/l (EXP1) vs. 18 mg/l (EXP3) during 24 hours of exposure. Vehicle volume added on the skin was 100 µl/cm².
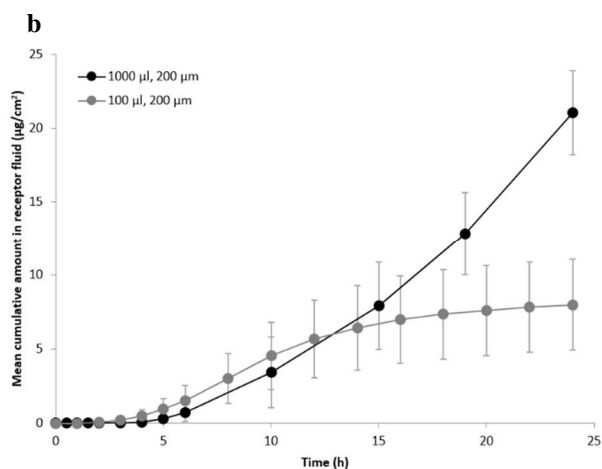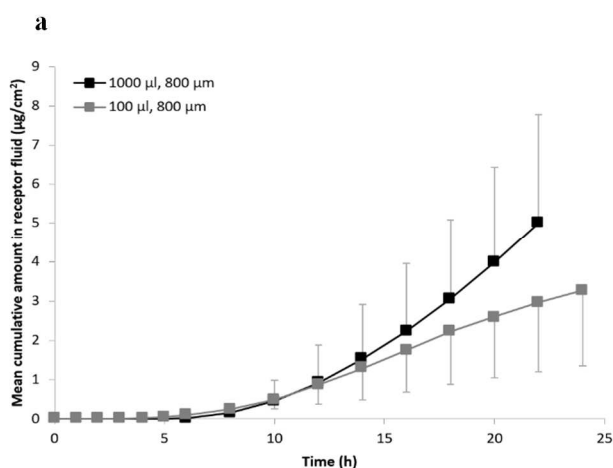
Fig. 3 Effect of vehicle volume applied on viable skin on mean BPA skin permeation curves of 800-µm (a) (EXP1, EXP4) and 200-µm-thick skin (b) (EXP5, EXP6) during 24 h of exposure. One-sided error bars (SD) are shown on figure A for clarity purposes. EXP5 data were extracted from Reale et al. (2020). Note the different scale on the y-axes.
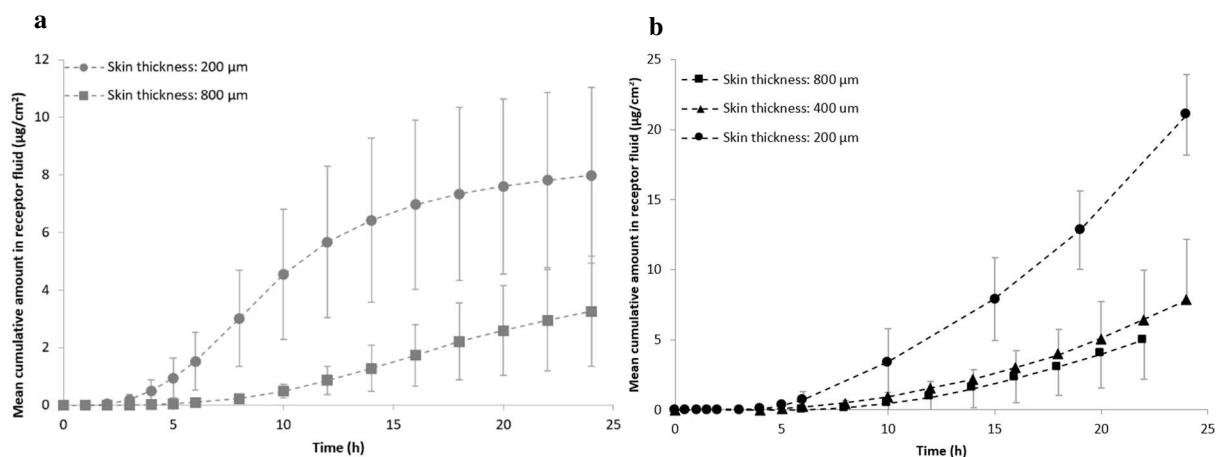
Fig. 4 Effect of skin thickness on BPA mean (± SD) permeation curves during 24 h of exposure to 100 µl (a) (EXP1, EXP5) and 1000 µl (b) (EXP 4, EXP6, EXP7) vehicle volume. EXP5 data were extracted from Reale et al. (2020)

4. Discussion

We studied the effect that different experimental parameters have on BPA skin permeation kinetics. Our results show that a skin thickness increase from 200 to 400/800 µm and viable/frozen skin state had the greatest significant effect on J. Neither a volume increase from 100 to 1000 µl nor a skin thickness increase from 400 to 800 µm significantly affected J. Applying 1000 µl of BPA test solution on the skin resulted in an infinite dose that led to the steady state after 7-11 h (t_{lag}) depending on the skin thickness. As for J, K_p decreased significantly with a skin thickness increase from 200 to 400/800 µm.

As expected, significant differences in J were found between experiments with different concentrations (EXP1 and EXP3). This difference was also observed between viable and frozen skin (EXP1 and EXP2). Numerous studies have addressed the effect of skin storage, showing that storing human skin at -20°C does not have any effects on its barrier function (Dennerlein et al., 2013; Harrison et al., 1984; Moody et al., 2009; Williams, 2003). In our study, the skin was stored at -80°C. The increased permeability of skin frozen at -80°C is in contrast with some literature data (Barbero and Frasch, 2016) and in line with other studies (Hawkins and Reifenrath, 1984; Nielsen et al., 2011). Therefore, it is likely that freezing at -80°C is harsher on barrier function compared to -20°C.

J and K_p decreased significantly (3.3-fold) when the skin thickness increased from 200 µm to 400 and 800 µm. Although, the number of replicates (n=3) is below the recommended value (n=4) by OECD (OECD, 2004a) for

EXP6 and EXP7, which is a clear limitation of this study, the permeation curves of skin samples with different skin thicknesses (200, 400, and 800 μm) from the same skin donor were similar to Figure 4B (data not shown). Several explanations for the observed decrease in J and K_p for thicker skin are possible. K_p is inversely proportional to the path length across the skin, thus the thicker the skin, the longer the path length and the smaller the K_p. In addition, the stratum corneum is a lipid-rich environment compared to the watery viable epidermis and dermis. For lipophilic substances such as BPA ($\log K_{OW} = 3.4$ (EC IHCP, 2010)), the epidermis and dermis may act as rate-limiting layers in the diffusion through the skin (Moss et al., 2015; Wilkinson et al., 2006). The main clearance of substances absorbed in the skin occurs where the majority of the skin's vasculature resides, in the dermis at its junction with the epidermis (Moss et al., 2015). In human abdominal skin, this junction is at approximately 70 μm from the skin surface (Rees and Robertson, 2010). Therefore, the use of thicker skin samples (400-800 μm) may lead to an underestimation of BPA skin permeation kinetics, but it may also allow the quantification of the BPA stored in the skin. BPA skin storage has been reported by several authors (13-15% of applied dose (Kaddar et al., 2008; Liu and Martin, 2019; Reale et al., 2020; Toner et al., 2018); 25% by Mørck et al. (2010); 42% by Zalko et al. (2011)). This storage could potentially lead to BPA post-exposure release.

EXP0 shared the experimental setup with Demierre et al. (2012) with the exception of skin thickness (800 μm in EXP0 vs. 200 μm in Demierre et al. (2012)), skin state (viable vs. frozen at -20°C), and a slightly higher BPA concentration in the dosing solution. Calculating a J for 200 μm by taking into account our result of a 3.3-fold increase in J with a skin thickness reduction from 800 to 200 μm, resulted in a J of 0.020, which is very similar to Demierre et al. (2012)'s results. Applying the 3.4-fold difference for skin state yielded 0.067 μg/cm²/h, which is 3-fold higher than in Demierre et al. (2012). This may suggest that this factor applies only for skin frozen at -80°C, which was our freezing condition, but not for skin frozen at -20°C as in Demierre et al. (2012)'s study. Our results showed that J did not vary significantly between 400 and 800 μm skin thickness. J values obtained in the EXP0 experiment (800 μm skin thickness) and the *in vitro* flow-through diffusion cell study of Toner et al. (2018) (350 - 400 μm skin thickness) were in the same order of magnitude (0.006 μg/cm²/h in EXP0, 0.0034 in Toner et al. (2018)), despite differences in vehicle and receptor fluid (Toner et al. used phosphate buffered saline solution as vehicle and receptor fluid).

A volume increase from 100 to 1000 μl did not significantly change J for the 200- nor the 800-μm thick skin, despite the 10-fold difference in applied dose (25 vs. 250 μg/cm²). This suggests that once the skin is sufficiently hydrated, increasing the volume of water on the skin does not affect the skin permeation further. However, the skin permeation curve for the 100 μl vehicle volume experiment (EXP1 in figure 3A, and EXP5 in

figure 3B for 800 µm and 200 µm-thick skin, respectively) showed a decrease after 12 h of exposure. Before 12 h, the curves were similar irrespective of volume applied and skin thickness. The decrease observed in the 100 µl skin permeation curve's slope after 12 h of exposure could be due to effects arising from finite dosing and from total evaporation of the 100 µl vehicle from the skin (EFSA, 2015), which resulted in dryer, hence less permeable skin (Bunge et al., 2012; Frasch et al., 2014; Zhu et al., 2016).

A comparison of EXP5 and Demierre et al. (2012) suggests that the vehicle evaporation effect might be more important when comparing 100 µl with 10 µl of vehicle volume. EXP5 and Demierre et al. (2012)'s study shared the same experimental setup except for vehicle volume (100 µl vs. 10 µl), skin state (viable vs. frozen at -20°C), and a higher BPA concentration in the dosing solution (250 vs. 184 mg/l). Despite the fact that Demierre et al. (2012)'s skin was frozen, their J value (0.022 µg/cm^2/h) was 30-fold smaller than that of EXP5 (0.72 µg/cm^2/h). This difference in J values was likely to be due to the difference in vehicle volume, rather than the slight difference in concentration. In experiments where 10 µl/cm^2 of water vehicle are used, the vehicle volume is so small that it is barely visible on the skin; when 100 µl/cm^2 of water vehicle are used, the skin is completely covered by the vehicle for several hours. Water increases skin hydration, which is known to increase skin permeability of other compounds. When comparing the application of 10 µl/cm^2 and 100 µl/cm^2, our J values for BPA were 30-fold greater for the larger vehicle volume.

The role of vehicle volume on BPA skin permeation kinetics is probably more important for water than for other commonly used vehicles, as BPA permeates more readily through the skin when applied in aqueous vehicle, compared to acetone or sebum (Champmartin et al. 2020). Champmartin et al. (2020) studied the effects of vehicle type on BPA skin permeation, and observed that BPA permeated human viable skin faster when vehicle was water > acetone > sebum. Furthermore, the BPA dose (20 µg/cm^2 in 50 µl of 400 mg/l BPA solutions) through 476 µm-thick skin was infinite in acetone and sebum vehicles, and finite in water vehicle. As BPA readily permeates the skin when vehicle is water, dose conditions (100 µg/cm^2 of a saturated solution) ten-fold higher than the ones recommended by the (OECD, 2004a) were not enough to reach the steady-state in our study. This difficulty in maintaining infinite dose conditions has been observed also for other lipophilic substances (Selzer et al., 2013). In our study, steady state conditions were achieved and BPA's K_p could be calculated but only for EXP 4, 6, and 7 when 1000 µl vehicle volume was applied. The higher J_{ss} and K_p values were observed for the thinner skin samples (200 µm, EXP6), which was expected as previously discussed.

No direct comparison of our J values with those of Marquet et al. (2011), Champmartin et al. (2020), and Liu and Martin (2019) was possible because too many parameters were different: vehicle volume and type, diffusion system, BPA concentration, skin thickness, and receptor fluid. Moreover, Liu and Martin (2019) used an *in vitro*

3D-skin model (120 μm) with custom permeation devices and approximately 1500 μl/cm^2 of low concentration dosing solutions (1 and 5 mg/l). These particular conditions led to a plateau in BPA permeation curve indicating finite dose conditions.

In risk assessment and in toxicokinetic modelling, a substance's absorbed amount (expressed as percent of the applied dose) is often used to calculate the internal dose. However, the dependence of BPA's absorbed amount on the experimental set up is unclear. Here, we propose to use J values that correspond to different exposure scenarios. A cashier touching thermal paper receipts several times per day has a fairly constant amount of BPA on the skin all day long (Biedermann et al., 2010). BPA migrates onto the cashier's skin in solid phase, and, to be absorbed must be dissolved in sebum, sweat or other liquids. Average sweat output is approximately 2 μl/cm^2 (Misra et al., 2010), and average BPA migrated on the skin from thermal paper is 1.1 μg/cm^2 (Biedermann et al., 2010). BPA migration onto humid or greasy skin can be ten times higher than on dry/normal skin (Biedermann et al., 2010). Therefore, a J value for 10 μl vehicle volume, 200 μm-thick, viable skin (approximately 0.02 cm/h) could represent a scenario where the person touching the receipts has dry hands. K_p and J values for 1000 μl water vehicle volume, 200 μm-thick, viable skin (5.2 x 10^{-3} cm/h and 1.31 μg/cm^2/h, respectively), could represent the worst-case scenario of a person with wet hands.

5. Conclusions

Overall, comparison among a few studies shows that the different results of different experimental set ups agree with each other. The difference in the results depends on some experimental parameters, such as skin thickness and the vehicle volume. The use of thinner skin (200 μm) may be appropriate for *in vitro* skin permeation kinetic studies of BPA, and the use of thicker skin (400-800 μm) for *in vitro* mass balance studies to account for possible storage effect in the skin. Different vehicle volumes could represent different exposure scenarios with dry and wet hands' skin. For dry (normal) skin, Demierre et al. (2012)'s J value of 0.022 μg/cm^2/h may be used. For exposure scenarios where hands are wet, the worst-case scenario is represented by the steady state J_{ss} and K_p values of 1.31 μg/cm^2/h and 5.23 x 10^{-3} cm/h, respectively.

References

ANSES, 2013. Anses 2013 - Evaluation des risques du bisphenol A pour la sante humaine.

Barbero, A.M., Frasch, H.F., 2016. Effect of Frozen Human Epidermis Storage Duration and Cryoprotectant on Barrier Function Using Two Model Compounds. Skin Pharmacol Physiol 29, 31–40. https://doi.org/10.1159/000441038

Biedermann, S., Tschudin, P., Grob, K., 2010. Transfer of bisphenol A from thermal printer paper to the skin. Analytical and Bioanalytical Chemistry 398, 571–576. https://doi.org/10.1007/s00216-010-3936-9

Bronaugh, R., Maibach, H., 2005. Percutaneous Absorption: Drugs, Cosmetics, Mechanisms, Methodology. https://doi.org/10.1201/9780849359033

Bunge, A.L., Persichetti, J.M., Payan, J.P., 2012. Explaining skin permeation of 2-butoxyethanol from neat and aqueous solutions. Int J Pharm 435, 50–62. https://doi.org/10.1016/j.ijpharm.2012.01.058

Champmartin, C., Marquet, F., Chedik, L., Décret, M.-J., Aubertin, M., Ferrari, E., Grandclaude, M.-C., Cosnier, F., 2020. Human in vitro percutaneous absorption of bisphenol S and bisphenol A: A comparative study. Chemosphere 252, 126525. https://doi.org/10.1016/j.chemosphere.2020.126525

Demierre, A.-L., Peter, R., Oberli, A., Bourqui-Pittet, M., 2012. Dermal penetration of bisphenol A in human skin contributes marginally to total exposure. Toxicology Letters 213, 305–308. https://doi.org/10.1016/j.toxlet.2012.07.001

Dennerlein, K., Schneider, D., Göen, T., Schaller, K.H., Drexler, H., Korinth, G., 2013. Studies on percutaneous penetration of chemicals - Impact of storage conditions for excised human skin. Toxicol In Vitro 27, 708–713. https://doi.org/10.1016/j.tiv.2012.11.016

EFSA, 2018. Call for data relevant to the hazard assessment of Bisphenol A (BPA) [WWW Document]. URL https://www.efsa.europa.eu/sites/default/files/engage/180309.pdf (accessed 9.30.19).

EFSA, 2015. Scientific Opinion on the risks to public health related to the presence of bisphenol A (BPA) in foodstuffs. EFSA Journal 13, 3978. https://doi.org/10.2903/j.efsa.2015.3978

European Commission, Joint Research Centre, Institute for Health and Consumer Protection, 2010. European Union Risk Assessment Report - Environment Addendum of April 2008 - 4,4'-ISOPROPYLIDENEDIPHENOL (BISPHENOL-A) - Part 1 Environment, EU RAR.

Frasch, H.F., Barbero, A.M., Dotson, G.S., Bunge, A.L., 2014. Dermal permeation of 2-hydroxypropyl acrylate, a model water-miscible compound: Effects of concentration, thermodynamic activity and skin hydration. International Journal of Pharmaceutics 460, 240–247. https://doi.org/10.1016/j.ijpharm.2013.11.007

Gundert-Remy, U., Mielke, H., Bernauer, U., 2013. Commentary: Dermal penetration of bisphenol A—Consequences for risk assessment. Toxicology Letters 217, 159–161. https://doi.org/10.1016/j.toxlet.2012.12.009

Harrison, S.M., Barry, B.W., Dugard, P.H., 1984. Effects of freezing on human skin permeability. J. Pharm. Pharmacol. 36, 261–262. https://doi.org/10.1111/j.2042-7158.1984.tb04363.x

Hawkins, G.S., Reifenrath, W.G., 1984. Development of an in vitro model for determining the fate of chemicals applied to skin. Fundam Appl Toxicol 4, S133-144. https://doi.org/10.1016/0272-0590(84)90145-3

Hormann, A.M., vom Saal, F.S., Nagel, S.C., Stahlhut, R.W., Moyer, C.L., Ellersieck, M.R., Welshons, W.V., Toutain, P.-L., Taylor, J.A., 2014. Holding Thermal Receipt Paper and Eating Food after Using Hand Sanitizer Results in High Serum Bioactive and Urine Total Levels of Bisphenol A (BPA). PLoS One 9. https://doi.org/10.1371/journal.pone.0110509

Kaddar, N., Harthé, C., Déchaud, H., Mappus, E., Pugeat, M., 2008. Cutaneous Penetration of Bisphenol A in Pig Skin. Journal of Toxicology and Environmental Health, Part A 71, 471–473. https://doi.org/10.1080/15287390801906824

Karrer, C., Roiss, T., von Goetz, N., Gramec Skledar, D., Peterlin Mašič, L., Hungerbühler, K., 2018. Physiologically Based Pharmacokinetic (PBPK) Modeling of the Bisphenols BPA, BPS, BPF, and BPAF with New Experimental Metabolic Parameters: Comparing the Pharmacokinetic Behavior of BPA with Its Substitutes. Environ Health Perspect 126, 077002. https://doi.org/10.1289/EHP2739

Kasting, G.B., 2001. Kinetics of finite dose absorption through skin 1. Vanillylnonanamide. Journal of Pharmaceutical Sciences 90, 202–212. https://doi.org/10.1002/1520-6017(200102)90:2<202::aid-jps11>3.0.co;2-e

Liu, J., Martin, J.W., 2019. Comparison of Bisphenol A and Bisphenol S Percutaneous Absorption and Biotransformation. Environ. Health Perspect. 127, 67008. https://doi.org/10.1289/EHP5044

Marquet, F., Payan, J.-P., Beydon, D., Wathier, L., Grandclaude, M.-C., Ferrari, E., 2011. In vivo and ex vivo percutaneous absorption of [14C]-bisphenol A in rats: a possible extrapolation to human absorption? Archives of Toxicology 85, 1035–1043. https://doi.org/10.1007/s00204-011-0651-z

Mielke, H., Gundert-Remy, U., 2012. Physiologically Based Toxicokinetic Modelling as a Tool to Support Risk Assessment: Three Case Studies. Journal of Toxicology 2012, 1–11. https://doi.org/10.1155/2012/359471

Mielke, H., Gundert-Remy, U., 2009. Bisphenol A levels in blood depend on age and exposure. Toxicology Letters 190, 32–40. https://doi.org/10.1016/j.toxlet.2009.06.861

Misra, Uk, M., Al, E., 2010. Clinical Neurophysiology (2Nd Edition). Elsevier India.

Moody, R.P., Yip, A., Chu, I., 2009. Effect of Cold Storage on In Vitro Human Skin Absorption of Six 14C-Radiolabeled Environmental Contaminants: Benzo[a]Pyrene, Ethylene Glycol, Methyl Parathion, Naphthalene, Nonyl Phenol, and Toluene. Journal of Toxicology and Environmental Health, Part A 72, 505–517. https://doi.org/10.1080/15287390802328713

Mørck, T.J., Sorda, G., Bechi, N., Rasmussen, B.S., Nielsen, J.B., Ietta, F., Rytting, E., Mathiesen, L., Paulesu, L., Knudsen, L.E., 2010. Placental transport and in vitro effects of Bisphenol A. Reproductive Toxicology 30, 131–137. https://doi.org/10.1016/j.reprotox.2010.02.007

Moss, G., Gullick, D., Wilkinson, S., 2015. Predictive Methods in Percutaneous Absorption. Springer-Verlag, Berlin Heidelberg. https://doi.org/10.1007/978-3-662-47371-9

Ndaw, S., Remy, A., Jargot, D., Robert, A., 2016. Occupational exposure of cashiers to Bisphenol A via thermal paper: urinary biomonitoring study. International Archives of Occupational and Environmental Health 89, 935–946. https://doi.org/10.1007/s00420-016-1132-8

Nielsen, J.B., Plasencia, I., Sørensen, J.A., Bagatolli, L.A., 2011. Storage conditions of skin affect tissue structure and subsequent in vitro percutaneous penetration. Skin Pharmacol Physiol 24, 93–102. https://doi.org/10.1159/000322304

OECD, 2011. Organisation for Economic Co-operation and Development, Series on Testing and Assessment Nº. 156, Guidance Notes on Dermal Absorption.

OECD, 2004a. Organisation for Economic Co-operation and Development, Guidelines for the testing of chemicals, Section 4, Test Nº 428: Skin absorption: In Vitro Method.

OECD, 2004b. Organisation for Economic Co-operation and Development, Series on Testing and Assessment Nº 28, Guidance Document for the Conduct of Skin Absorption Studies. OECD. https://doi.org/10.1787/9789264078796-en

OECD, 2003. OECD Existing Chemicals Database - Bisphenol A [WWW Document]. URL https://hpvchemicals.oecd.org/UI/SIDS_Details.aspx?key=6d209d66-9690-4739-8745-ac4732d5f53d&idx=0 (accessed 11.20.19).

Peretz, J., Vrooman, L., Ricke, W.A., Hunt, P.A., Ehrlich, S., Hauser, R., Padmanabhan, V., Taylor, H.S., Swan, S.H., VandeVoort, C.A., Flaws, J.A., 2014. Bisphenol A and Reproductive Health: Update of Experimental and Human Evidence, 2007–2013. Environmental Health Perspectives 122, 775–786. https://doi.org/10.1289/ehp.1307728

Pinnagoda, J., Tupker, R.A., Agner, T., Serup, J., 1990. Guidelines for transepidermal water loss (TEWL) measurement. A report from the Standardization Group of the European Society of Contact Dermatitis. Contact Derm. 22, 164–178. https://doi.org/10.1111/j.1600-0536.1990.tb01553.x

Reale, E., Vernez, D., Hopf, N.B., 2020. Skin Absorption of Bisphenol A and Its Alternatives in Thermal Paper. Ann Work Expo Health. https://doi.org/10.1093/annweh/wxaa095

Rees, J., Robertson, K., 2010. Variation in Epidermal Morphology in Human Skin at Different Body Sites as Measured by Reflectance Confocal Microscopy. Acta Derm Venerol 90, 368–373. https://doi.org/10.2340/00015555-0875

Selzer, D., Abdel-Mottaleb, M.M.A., Hahn, T., Schaefer, U.F., Neumann, D., 2013. Finite and infinite dosing: Difficulties in measurements, evaluations and predictions. Advanced Drug Delivery Reviews, Modeling the human skin barrier - Towards a better understanding of dermal absorption 65, 278–294. https://doi.org/10.1016/j.addr.2012.06.010

Toner, F., Allan, G., Dimond, S.S., Waechter, J.M., Beyer, D., 2018. In vitro percutaneous absorption and metabolism of Bisphenol A (BPA) through fresh human skin. Toxicol In Vitro 47, 147–155. https://doi.org/10.1016/j.tiv.2017.11.002

US EPA, 2014. Bisphenol A alternatives in thermal paper, Final report. United States Environmental Protection Agency.

Völkel, W., Colnot, T., Csanády, G.A., Filser, J.G., Dekant, W., 2002. Metabolism and kinetics of bisphenol a in humans at low doses following oral administration. Chem. Res. Toxicol. 15, 1281–1287.

Wilkinson, S.C., Maas, W.J.M., Nielsen, J.B., Greaves, L.C., van de Sandt, J.J.M., Williams, F.M., 2006. Interactions of skin thickness and physicochemical properties of test compounds in percutaneous penetration studies. Int Arch Occup Environ Health 79, 405–413. https://doi.org/10.1007/s00420-005-0056-5

Williams, A., 2003. Transdermal and Topical Drug Delivery from Theory to Clinical Practice. Pharmaceutical Press.

Zalko, D., Jacques, C., Duplan, H., Bruel, S., Perdu, E., 2011. Viable skin efficiently absorbs and metabolizes bisphenol A. Chemosphere 82, 424–430. https://doi.org/10.1016/j.chemosphere.2010.09.058

Zhu, H., Jung, E.-C., Hui, X., Maibach, H., 2016. Proposed human stratum corneum water domain in chemical absorption. J. Appl. Toxicol. 36, 991–996. https://doi.org/10.1002/jat.3208